Universitat Politècnica de Catalunya

Departament d'Enginyeria Elèctrica

PhD Thesis

Power conditioner based fuel cell and backup power system with supercapacitor

Autor: **Juan Carlos Trujillo Caballero**

Directors: **Oriol Gomis Bellmunt**
Daniel Montesinos i Miracle

Barcelona, February 2012

Universitat Politècnica de Catalunya
Departament d'Enginyeria Elèctrica
Centre d'Innovació Tecnològica en Convertidors Estàtics i Accionament
Av. Diagonal, 647. Pl. 2
08028 Barcelona

Primera impressió, February 2012

Oficina de Doctorat
UNIVERSITAT POLITÈCNICA DE CATALUNYA

Acta de qualificació de tesi doctoral

Curs acadèmic:

Nom i cognoms
Juan Carlos Trujillo Caballero

DNI / NIE / Passaport
X9431466V

Programa de doctorat
Ingeniería Eléctrica

Unitat estructural responsable del programa
Luis Sainz Sapera

Resolució del Tribunal

Reunit el Tribunal designat a l'efecte, el doctorand / la doctoranda exposa el tema de la seva tesi doctoral titulada

Power conditioner based fuel cell and backup power system with supercapacitor

Acabada la lectura i després de donar resposta a les qüestions formulades pels membres titulars del tribunal, aquest atorga la qualificació:

☐ APTA/E ☐ NO APTA/E

(Nom, cognoms i signatura)	(Nom, cognoms i signatura)	
President/a	Secretari/ària	
(Nom, cognoms i signatura)	(Nom, cognoms i signatura)	(Nom, cognoms i signatura)
Vocal	Vocal	Vocal

_____, _____ d'/de _____ de _____

El resultat de l'escrutini dels vots emesos pels membres titulars del tribunal, efectuat per l'Oficina de Doctorat, a instància de la Comissió de Doctorat de la UPC, atorga la MENCIÓ CUM LAUDE:

☐ SI ☐ NO

(Nom, cognoms i signatura)	(Nom, cognoms i signatura)	(Nom, cognoms i signatura)
Vicerectora de Recerca Presidenta de la Comissió de Doctorat	Cap de l'Oficina de Doctorat Secretària de la Comissió de Doctorat	Secretari/ària del tribunal (o membre del tribunal de la UPC)

Barcelona, _____ d'/de _____ de _____

Diligència "Internacional del títol de doctor o doctora"

Com a secretari/ària del tribunal faig constar que la tesi s'ha defensat en part, i com a mínim pel que fa al resum i les conclusions, en una de les llengües habituals per a la comunicació científica en el seu camp de coneixement i diferent de les que són oficials a Espanya. Aquesta norma no s'aplica si l'estada, els informes i els experts externs provenen d'un país de parla hispana.

(Nom, cognoms i signatura)
Secretari/ària del tribunal

Acknowledgements

I would like to thank God for giving me health, patience, wisdom and strength during my training.

My advisors, Dr. Oriol Gomis Bellmunt, for his great patience, availability and help during the development of this thesis and Dr. Daniel Montesinos i Miracle, for his advice and useful observations.

Special thanks to Dr. Antoni Sudrià i Andreu, for giving me the opportunity and confidence in the continuity of my studies. His great teaching has helped me a lot.

My friend Dr. Ricardo López García, for helping me to continue my studies and guide me always in the right direction.

I greatly appreciate the full support my parents, Jose Oscar Trujillo Calderón and Rosalina Caballero Gonzalez and my brothers, José Oscar, Jesús Enrique, Mario Arturo and Marco Antonio, have given me. Undoubtedly I would not have been able to finish this work without their help. Thank you for trusting and always believing in me.

My girlfriend, Gabriela Alcalde, for motivating and supporting me in my learning process, thank you for your patience. To my friends, for their pleasant company and advice in the development of my thesis: Adrià, Agusti, Paola P., Rodrigo, Martha R., Sergi C., Sergi F., Maria M. Luis S., Andreas S. Roberto V. and in general, to all the friends from CITCEA-UPC that helped me personally and professionally, thank you all.

Finally I would like to thank the Universidad Politécnica de Cataluña for their financial support and CITCEA-UPC for giving me support at any time.

Resumen

Las PEMFCs son el tipo más popular de celdas de combustible (FCs) y tradicionalmente usan hidrógeno como combustible. Uno de los problemas de la FC es su dinámica relativamente lenta a causa de la constante de tiempo de suministro de hidrógeno y oxígeno, que varía en un rango de varios segundos. En este sentido, un supercondensador (SC) responde más rápido que una FC cuando existe un cambio en la demanda de energía hacia la carga. Al usar un banco de SCs junto a la FC, se logra tener mejor desempeño y mayor tiempo de vida de la FC debido a la rápida absorción y suministro de energía de los supercapacitores ante dichos cambios de carga, dando entonces un mayor tiempo de respuesta a la FC. Por tanto, se hace necesario el estudio de estructuras que permitan el acondicionamiento de la potencia con sus respectivos sistemas de control, que puedan mitigar las desventajas mencionadas de la misma FC. Varias investigaciones han estudiado las diferentes propuestas de topologías con sus respectivos controles para operar a FC y SC. En esta tesis se propone un esquema de control, implementado digitalmente para operar un módulo PEMFC de 1,2 kW y un SC a través de un convertidor DC/DC híbrido. Se ha propuesto una FC como fuente de energía primaria y un SC se ha propuesto como fuente auxiliar de energía. Así mismo se proporciona una validación experimental del sistema implementado en el laboratorio. Se han realizado varias pruebas para verificar que el sistema alcanza una excelente regulación de la tensión de salida (V_0) y tensión de supercapacitor (V_{SC}) bajo perturbaciones de potencia de FC (P_{FC}) y potencia de salida (P_0) así como otras pertubaciones descritas en el análisis de resultados.

Abstract

PEMFCs are the most popular type of Fuel Cells (FCs) and traditionally use hydrogen as the fuel. One FC problem is its relative slow dynamics caused by the time constant of the hydrogen and oxygen supply systems that can be in the range of several seconds. In this sense, supercapacitors (SCs) respond faster than FC to a fast increase or decrease in power demand. Thus, using SCs together with FCs improves FC life and performance by absorbing faster load changes and preventing fuel starvation of the FC. Therefore, it becomes necessary to study structures of power conditioners with their respective control systems that can mitigate the disadvantages mentioned of the FC itself. Several researches have studied the different topologies with their respective control proposals to operate FC and SC. This thesis proposes a digital control scheme to operate a PEMFC module of 1.2 kW and a SC through a DC/DC hybrid converter. A FC has been proposed as a primary source of energy and a SC has been proposed as an auxiliary source of energy. An experimental validation of the system implemented in the laboratory is provided. Several tests have been performed to verify that the system achieves an excellent output voltage (V_0) regulation and SC Voltage (V_{SC}) control, under disturbances from FC power (P_{FC}) and output power (P_0) as well as other perturbations described in analysis results.

Thesis Outline

The structure of this thesis consists of seven Chapters. In Chapter one, a conceptual framework of the fuel cell and the supercapacitor are presented. In Chapter two the power conditioners and their respective controls to operate fuel cells and supercapacitors are presented. Chapter three describes the analysis and design of a power conditioner. Chapter four, presents the system modeling, as well as a control structure to operate a hybrid converter and its transfer funtions. Chapter five describes the simulation results performed using the software "$MATLAB - Simulink$". Chapter six shows the experimental results obtained in the laboratory, giving a description of the behavior of the system to different operating conditions. Finally, Chapter seven shows the general conclusions of this thesis, as well as possible future work in the development of the same.

Contents

List of Figures

List of Tables

Nomenclature

Roman symbols

ΔI_{L_1} Inductor current increase L_1 $[A]$

ΔI_{L_2} Inductor current increase L_2 $[A]$

ΔV_0 Ripple output voltage $[V]$

ΔV_{SC} Supercapacitor voltage increase V_{SC} $[V]$

C_0 Output capacitance $[F]$

C_{IN} Input capacitance $[F]$

C_{SC} Supercapacitor capacitance $[F]$

$D_{1,2,3,4}$ Diodes [-]

f_s Switching frequency $[Hz]$

$G_1(s)$ Plant of FC converter [-]

$G_2(s)$ Plant of SC converter [-]

H_2 Hydrogen [-]

I_0 Output current $[A]$

I_{FC_fd} Feedback of I_{FC} $[A]$

I_{FC} Fuel Cell current $[A]$

$I_{FC}*$ Reference of I_{FC} $[A]$

I_{SC_fd} Feedback of I_{SC} $[A]$

I_{SC} Supercapacitor current $[A]$

$I_{SC}*$ Reference of I_{SC} $[A]$

$K_{ADC\_I_{FC}}$ Gain of Analog to Digital converter of I_{FC} [-]

$K_{ADC\_I_{SC}}$ Gain of Analog to Digital converter of I_{SC} [-]

$K_{ADC\_V_0}$ Gain of Analog to Digital converter of V_0 [-]

$K_{ADC\_V_{SC}}$ Gain of Analog to Digital converter of V_{SC} [-]

$K_{i\_I_{FC}}$ Integral gain of I_{FC} [-]

$K_{i\_I_{SC}}$ Integral gain of I_{SC} [-]

$K_{i\_V_0}$ Integral gain of V_0 [-]

$K_{i\_V_{SC}}$ Integral gain of V_{SC} [-]

K_I Integral gain [-]

$K_{P\_I_{FC}}$ Proportional gain of I_{FC} [-]

$K_{P\_I_{SC}}$ Proportional gain of I_{SC} [-]

$K_{P\_V_0}$ Proportional gain of V_0 [-]

$K_{P\_V_{SC}}$ Proportional gain of V_{SC} [-]

K_P Proportional gain[-]

L_0 Output inductance $[H]$

L_1 Fuel cel inductance $[H]$

L_2 Supercapacitor inductance $[H]$

P_0 Output power $[W]$

P_{FC} Fuel cell power $[W]$

P_{SC} Supercapacitor power $[W]$

PI_I_{FC} Current controller of Fuel Cell

PI_I_{SC} Current controller of Supercapacitor

PI_V_{FC} Voltage controller of Fuel Cell

PI_V_{SC} Voltage controller of Supercapacitor

$Q_{1,2,3,4}$ Transistors [-]

$R_{1,2,3,4,5,6,7,8}$ Load Resistences [Ω]

R_{C_0} Output resistance of bus capacitor [Ω]

R_{L_1} Resistence of Fuel Cell inductance [Ω]

R_{L_2} Resistence of Supercapacitor inductance [Ω]

R_{LOAD} Load resistance [α]

R_{SC} Resistence of Supercapacitor [Ω]

$S_{W_{1,2,3}}$ Switches

T_{OFF} Turn off period [s]

T_{ON} Turn on period [s]

V_{0_fd} Feedback output voltage [V]

V_0 Output Voltage [V]

V_0* Reference output voltage [V]

V_{FC} Fuel Cell Voltage [V]

V_{SC_fd} Feedback supercapacitor voltage [V]

V_{SC} Supercapacitor Voltaje [V]

$V_{SC}*$ Reference of supercapacitor voltage [V]

Z Impedance [Ω]

0 Oxygen [-]

C Capacitance of a capacitor [F]

M Gain [-]

Q Electric charge [F]

Greek symbols

α_{FC} Duty cycle of Fuel Cell [-]

α_{SC} Duty cycle of Supercapacitor [-]

α Duty cycle [-]

Acronyms

DC/DC Direct current to direct current

AC Alternating Current

ADC Analog to Digital Converter

AFC Alkaline Fuel Cell

AMR Automated Meter Reading

CCM Continuous Conduction Mode

CITCEA Centre d'Innovació Tecnològica en Convertidors Estàtics i Accionaments

DC Direct Current

DMFC Direct Methanol Fuel Cell

DSP Digital Signal Processing

EMI Electromagnetic Interference

ESR Equivalent Series Resistor

FC Fuel Cell

IGBT Insulated Gate Bipolar Transistor

JTAG Joint Test Action Group

MCFC Molten Carbonate Fuel Cell

MOSFET Metal Oxide Semiconductor Field Effect Transistor

PAFC Phosphoric Acid Fuel cell

PEMFC Proton Exchange Membrane Fuel Cell

PFC Power Factor Correction

PI Proportional Integral

Nomenclature

PWM	Pulse Width Modulation
RMS	Root Mean Square
SC	Supercapacitor
SOFC	Solid Oxide Fuel Cell
UPC	Universitat Politècnica de Catalunya
UPS	Uninterrupted Power Supply
ZCS	Zero Current Switching
ZVS	Zero Voltage Switching

Chapter 1

Introduction

1.1 Introduction

Fuel cells (FCs) tend to be an important source of energy in the future [2]. Nowadays, there is a great interest in its use, as fossil fuels are increasingly affecting the environment [3], with the climate change, acid rain, ice melting, greenhouse effect, air pollution, oil spills, damage to the agriculture, sea level raising, etc. For this reason, FCs modules that meet a wide range of powers are being developed covering the worldwide energy demand [4]. At present, the development of renewable sources of energy has an important role to protect the environment and the energy crisis around the world. The fuel cell can be a very valid substitute for conventional fossil energies [5]. However, the fuel cell still has a slow dynamic which is limited by the supply of hydrogen and oxygen to the system, so therefore, its response to changes in load demand is still slow. Accordingly, the fuel cell requires an auxiliary energy storage whose function is to help mitigate the inconvenience presented by the slow dynamic of a fuel cell.

The SC is a very attractive storage device to operate as an auxiliary source of power fuel cell it. It presents very fast dynamics and can store more energy than a conventional capacitor. Hybrid converters are usually used as a primary energy source such as fuel cell and a secondary source such as the SC offering many advantages as it allows the FC to operate for longer integrating both technologies. Some applications of hybrid systems with fuel cells are the uninterruptible power supply (UPS) and the hybrid electrical vehicles (HEV) [6].

Based on the reviewed literature, it can be determined that the most used topologies of power systems based on FCs are the non-isolated DC-DC converters and the isolated DC-DC converters. The non-isolated converters are boost and cuk with their respective variants, the isolated ones are: forward,

push pull, half bridge and full bridge converters with their respective variants [7, 8].

This Section summarizes the study of topologies used in FC/SC application and since the intention is to achieve high performance at all times, there are also some basic dynamic requirements of the DC-DC converter like high efficiency, high reliability and good output regulation. Figure 1.1 shows the block diagram of a typical power system based on FCs. In the reviewed literature, it shows a tendency to improve properties such as efficiency, volume, weight, equipment reliability and cost [9, 10].

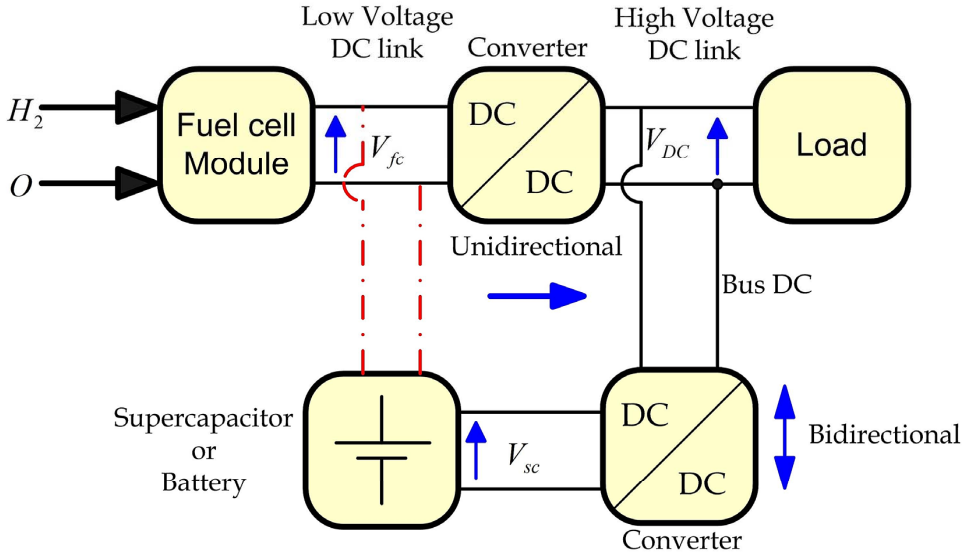

Figure 1.1: FC power conditioning for electric power application scheme.

Another important point seen in the proposed systems of power conditioners is the need for an energy storage mechanism (SCs), not only to give support or provide additional power to the system, but also to support the peak current demanded by the load. In the power conditioners, the energy used in SCs must be restored. This requires additional features to the system, such as the ability to recharge. This depends directly on the topology of the power converters.

1.1.1 Literature review in hybrid systems

Thoungthon et al.[11] studied the control strategy of the FC/SC hybrid power source for electric vehicles. The hybrid converter presents a control principle to use FC as a main power source which operates with a boost converter and SC as auxiliary power source which operates with a bidirectional converter. The conception proposes the hybrid system control as a regulation to the DC bus voltage with a fast auxiliary source as only power delivery.

Sánchez-Squella et al.[12] studied energy management in electrical systems fed by multiple sources. They proposed a topology that is used in some electric vehicles. To ensure energy exchange, the interconnection of the storage and load devices is performed by using power converters. In this sense, the power converters are electronically switched to a circuit capable to adapt the port voltage or current magnitudes to decisive values. The current and voltage are tracked with control loops, usually proportional integrals (PIs).

Cervantes Isle et al.[13] studied supplied hybrid control technique in FC/SC electric vehicle platforms developing a control scheme to operate a FC/SC hybrid converter. Some tests certify that the control was able to have an excellent output voltage regulation with disturbances in the load and its input voltage.

Gebre T. et al.[14] studied the control of converters to operate the FC and SC. The control was designed with proportional-integral controllers PI where the objective was to regulate the DC bus voltage. Some measured variables were the fuel cell current and the output DC voltage. The design had two control loops; the inner loop regulates the FC current and the outer loop regulates the output voltage.

Bernard Davat et al.[15] studied a multiphase interleaved step-up converter for high power FC applications. The purpose of this system consisted in parallel connections of three boost converters in order to operate at high powers. The proposed control system has been used to measure the input current of each converter and close the current loops. As well it connects three current loops converters in parallel.

T. Azib et al. [16] studied a control strategy for a parallel FC/SC hybrid converter proposing a power conditioner that can operate with two converters (FC and SC). These are used to integrate a power conditioner, where this

integration is connected in parallel on the DC output voltage. The control scheme has been proposed with the intention of manipulating the energy transfer of FC as the primary source and SC as the secondary source to the demands of the output power load.

A. Kirubakaran et al. [17] studied fuel cell technologies and power electronic interface. The study shows that it is possible to improve the efficiency of the power converters used for the operation of FCs, getting a better system performance. Therefore, some techniques have been studied that can help to significantly reduce the switching losses of the converters and increase the efficiency of them. The techniques usually employed were crossing zero voltage (ZVS) and zero current crossing (ZCS).

Oleksandr Krykuno et al. [18] studied the DC/DC converters for FC applications. Some converters like boost, push pull and extended forward were mathematically analyzed as the main purpose to find the most efficient converter for the boost converter to present a better efficiency. Therefore, boost converter is a good option to operate the FC system.

Farzad Abdous et al. [19] studied a DC/DC converter control by the sliding mode method. The sliding mode method has been employed to operate the FC to control the output voltage through the outer close loop and FC current regulation through the inner close loop. The sliding mode method is used to operate in discontinue forms.

1.2 General objective

The main objective of this research is to design a methodology for a power conditioner applied to a hybrid system of a fuel cell and a supercapacitor, as well as to implement a control structure that allows the governing of the whole system.

1.3 Particular objectives

The particular objectives of the thesis are the following:

- To study the fuel cell technology (structure, operation, types, applications).

- To study the supercapacitor technology (structure, operation, electrical characteristics, applications).
- To study the power conditioners systems and their control structures based on FCs/SCs.

1.4 Contributions

Tha main contributions of this thesis focuses on the following:

- To proposed a configuration of the power conditioner to operate fuel cell as primary source and backup power system with supercapacitor as a auxiliary source.
- To proposed a control structure to operate the power conditioner.
- To simulated in Matlab-Simulink software of the proposed system operating in closed loop.
- Implementation of the power conditioner and DSP programming of the control structure proposed by software code composer estudio.
- Validation of experimental results in the laboratory.

1.5 Fuel cell

1.5.1 Definition

A Fuel cell is an electrochemical device that through a series of electrochemical reactions converts energy from fuel (typically hydrogen) into electrical energy. In addition to generating electricity and heat, fuel cells generate water. FCs are similar in operation, to the batteries that produce direct current (DC), but unlike them, a FC does not get exhausted and it cannot be recharged [20].

1.5.2 Principle of operation

The PEMFC (Proton exchange membrane fuel cell) has two electrodes which are separated by two electrolytes. Oxygen passes through one electrode and hydrogen over the other. When hydrogen gets ionized it loses an electron. When this happens, both particles (hydrogen and electrons) take different paths towards the second electrode. The hydrogen migrates to the other

electrode while the electron makes it through a conductive material[21]. Figure1.2 shows a schematic of a fuel cell.

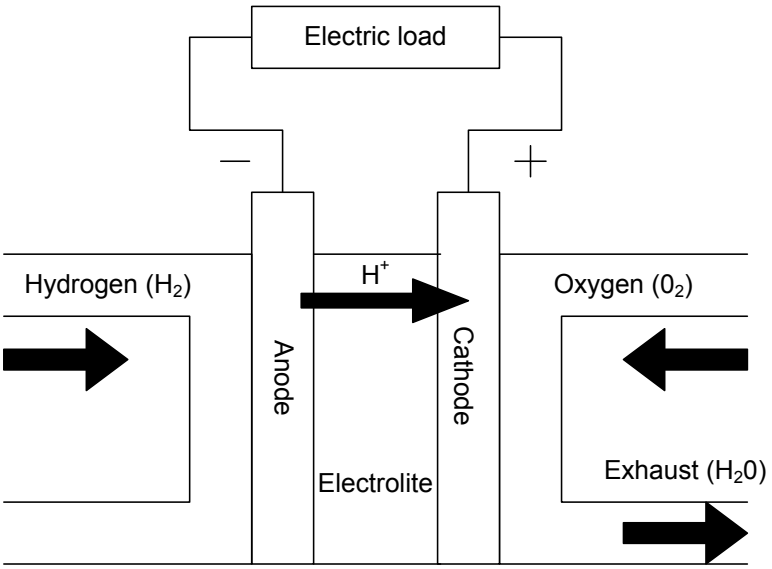

Figure 1.2: Fuel cell.

The PEMFC operates very much like to a battery. The difference being that the PEMFC produces electricity from an external source of fuel and oxygen as opposed to the limited capacity of energy storage that the battery has. The reactives typically used in a fuel cell are hydrogen on the anode side and oxygen on the cathode side. Moreover conventional batteries consume solid reactive, and once depleted, must be eliminated or charged with electricity.

1.5.3 Electrical characteristics

The ideal voltage of a single cell of FC is 1.23 V at 25 ^oC, 1 atmosphere and to obtain high levels of tension, it would be necessary to have a large number of cells. Therefore, to reduce complexity and assembly costs, the low voltage electric loads are preferred. Usually it is necessary to accommodate the voltage level at high levels to liaise with other stages of the supply system. Figure 1.3 shows the different losses of regions of operation in fuel cell at steady state.

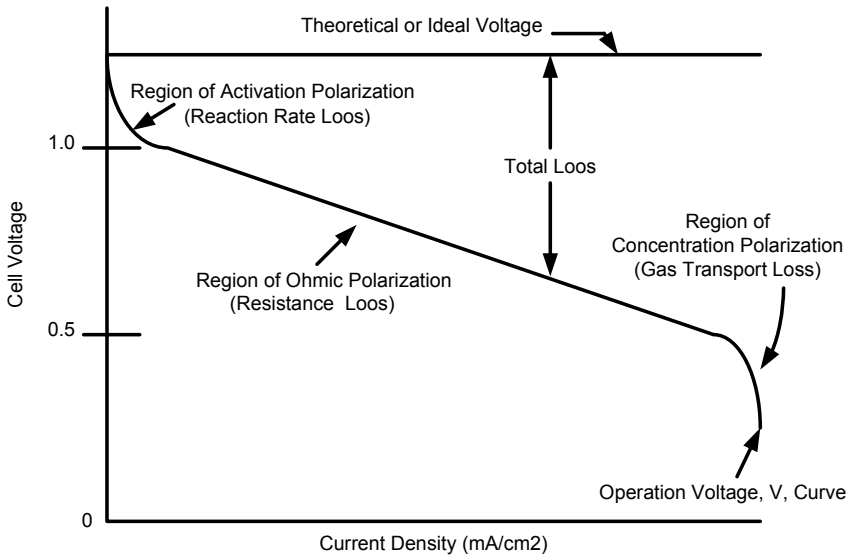

Figure 1.3: Cell Voltage−Current Density curve of an ideal fuel cell [1].

The three types of losses are shown below:

- **Activation region**: occurs when the operation of charge transfer at the electrode-electrolyte interface is slow.
- **Ohmic Polarization**: results from the electrical resistances of the fuel cell.
- **Concentration polarization region**: occurs when the availability of reactants is limited by diffusion, thus resulting concentration gradients reduce the activity of the electrode leading to losses in the output voltage.

1.5.4 FC types

In general the different types of fuel cells are designed in a similar form although they vary depending on their construction of the electrolyte. There are six main types which are shown below [22]:

- **Alkaline fuel cells (AFC)**, this type of FC is very old, its cost is very high and it is not very commercialized. The AFC operates at temperatures between 65 and 220 ^{o}C with a pressure of 1 atmosphere and each cell can deliver up to 1.2 V.

- **Proton-exchange membrane fuel cells (PEMFCs)** are the most common fuel cell used in light transports. They operate at relatively low temperatures (in the order of 80 ^{o}C). The PEMFCs have an electrical efficiency between 40 and 60 percent and its main advantages are high power density and longer lifetime in comparison to other fuel cells. Automotive manufacturers use this in their applications for light vehicles.

- **Phosphoric acid fuel cells (PAFCs)**, PAFCs have had a greater impact on a commercial level than any other fuel cell. These PAFCs generate electricity from over 40 to 80 percent of its efficiency. They operate at temperatures from 180 to 210 ^{o}C and they are very appropriate for use in stationary generation as hotels, hospitals and buildings. Also the PAFCs are used in mobile applications such as trucks, boats or trains. They are in commercial production units of approximately 200 kW.

- **Molten carbonate fuel cells (MCFCs)** operate at temperatures of 600 and 700 ^{o}C, so they heat in gas turbines and vapor is used to have an increase in efficiency. Among its advantages are the following: they do not require noble metals, they can use for operation natural gas, synthesis gas, biogas, etc. Its main disadvantage is the high cost.

- **Solid oxide fuel cells (SOFCs)** the SOFCs operate at high temperatures in the order of 1000 ^{o}C so it is not necessary to use noble metal electrodes, therefore it is possible to reduce its cost. SOFC has its high efficiency between 80 and 85 percent. The SOFCs are attractive as an energy source because they do not pollute and are usually very reliable. Its main application is in industrial applications and where high power is required.

- **Direct methanol fuel cells (DMFCs)** this type of fuel cell uses methanol as fuel; its operation is very similar to the PEMFC. The DMFC works at low temperatures in the order of $50 - 100\ ^oC$. The DMFC is very useful in portable applications such as mobile phones and laptops and it is considered in the transportation industry.

1.5.5 Applications

Fuel cells operate in a wide range of powers being used in four areas such as the residential, stationary, transportation, and portable [23].

- **Residential** is where fuel cells can be connected to the network and supply electrical power when required or they can even be used in rural areas where there is no electricity. Because fuel cells produce heat, they are good for heating a house.

- **Stationary** is used mainly in hotels, universities, clinics, buildings and industry being significantly less costly than fossil fuels.

- **Transportation**, many automobile companies are doing studies and tests on their new car models with the fuel cell with the idea of implementing them in cars. Some manufacturers include Ford, Daimler-Chrysler, Volkswagen, etc. Other applications are in ships, trains and planes.

- **Portable** has been a large niche for fuel cell applications because portable devices can be operated from very low powers. Among its main applications are: mobile phones, laptops, palms, video cameras, alarms, battery chargers, etc. Normally the type of fuel cell that is used for low power is DMFC where its main fuel is methanol.

An important aspect to consider is the fact that fuel cells are a source of clean energy which brings many benefits to the environment. As the technology continues advancing, prices of fuel cells will get cheaper so they will be more commonly used in our homes.

1.5.6 Advantages and disadvantages

In general FCs offer many advantages when compared to fossil energy sources. Although some of the FCs attributes are only valid for some applications, most advantages are more general. However, there are some disadvantages facing developers and the commercialization of fuel cells [24].

Advantages

- Fuel Cells do not need conventional fuels such as oil or gas and can therefore eliminate economic dependence on politically unstable countries. Since hydrogen can be produced anywhere where there is water and electricity, production of potential fuel can be distributed widely.
- Low temperature fuel cells (PEM-DMFC) have low heat transmission which makes them ideal for military applications.
- They are a great alternative in energy planning in short, medium and long term.
- Fuel cells represent a great alternative for clean and efficient energy.
- They can be easily transportable, which makes them much more flexible.
- It is a technology that promises much in the future, as petroleum starts getting finished, there will be a need to use non-conventional sources of electricity.
- It is a source of energy which does not produce noise, and they can be used in cogeneration processes.
- It has great flexibility to operate with other systems of electricity generation to increase the efficiency of the system.

Disadvantages

- The technology is not yet fully developed and there are only a few prototypes available right now.
- Incapacity to accept regenerative energy.
- Slow load response.

- It is still a high cost technology, due to its recent entry to the market and they are not very well known worldwide.
- They are far from having ideal characteristics of a voltage source. The operator delivers a non-regulated power making it necessary to use power converters.
- It presents a slow response in the start-up and to changes in demand for power in the load.
- Inability to accept regenerative energy.

1.6 Supercapacitor

1.6.1 Definition

A supercapactor is defined as an electrochemical device capable of storing electrical energy and of releasing energy. They are also known as double-layer capacitors. Among its main features outstands its high energy density [25].

1.6.2 Principle of operation

The SC is constructed similarly to a conventional capacitor which consists of two electrodes separated by an electrolyte. One way to increase the capacitance lies in the fact of decreasing the distance between the two plates and increasing the surface. Figure 1.4 shows a schematic view of a SC.

When a voltage or potential difference is applied to the capacitor, one of the electrodes has positive charges and the other one negative charges. The opposite charges attract and in this way energy is stored in the supercapacitor.

The charge Q stored in a capacitor of capacity C Farads a voltage U expressed by

$$Q = CU \tag{1.1}$$

The capacitors can be used to store energy. The energy stored in a capacitor is given by the expression.

$$E = \frac{1}{2}CU^2 \tag{1.2}$$

where E is the stored energy in Joules. The capacity of a capacitor C in farads is given by

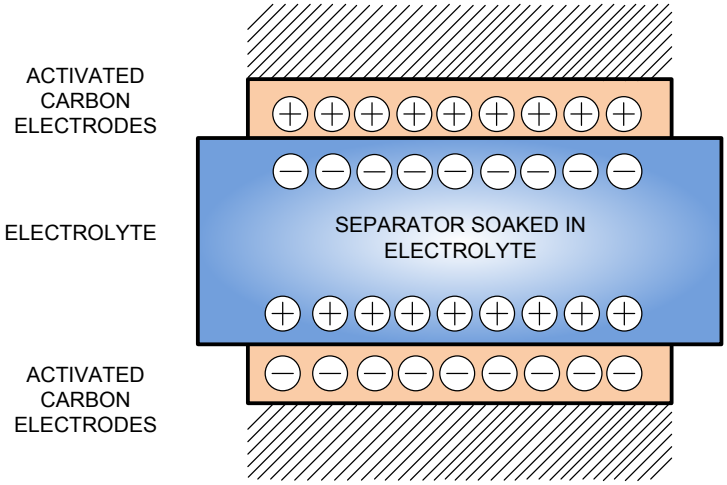

Figure 1.4: Working principle of a supercapacitor.

$$C = \epsilon \frac{A}{d} \tag{1.3}$$

where ϵ is the permitivity dielectric material between the plates, A is the surface of the plates and d is the distance that separates them. Thus, the SC technology to achieve high capacity is to reduce the gap between the electrodes. On the surface of each electrode there is a layer of electrolytic ions, hence the name double-layer. However the disadvantage of this technology is the maximum voltage that the capacitor can support which presents low values in the order of 2.5 V. This limits severely the amount of energy that can be stored, as shown in [13].

1.6.3 Applications

Due to these properties of life and management of voltage and current the SCs have been used in various applications:

- **Consumer**: Digital cameras, laptop computers, PDAs, GPS, hand held devices, toys, flashlights and restaurant paging devices.
- **Automotive**: The SCs represent a very promising development more particularly in the automobile transport systems, they represent a high

efficiency in this application, it is important to mention that the SCs reach their maximum utilization in the discharge energy during the acceleration of the vehicle.

- **Industrial**: The SCs have increased their applications. Technology continues to progress and they play an important role in the industry. To mention a few of them are: telecommunications, security doors, backup power systems, cranes, devices used in power electronics.

1.6.4 Advantages and disadvantages

Recently, the SCs have emerged as an important new alternative to other devices in production and storage of electricity as fuel cells or batteries. The main advantage compared to fuel cells and batteries is the power, it is capable of injecting. Other features of the SCs are fast charge and discharge, they can provide high load currents, which damage the battery, the number of life cycles of the same order of millions of times, there do not require maintenance, working conditions most adverse temperature. Here are the relevant advantages and disadvantages.

Advantages

- They have a longer lifetime than a battery or fuel cell due to their higher number of charge and discharge cycle.
- Low cost per cycle.
- Good reversibility.
- High output power.
- Non-corrosive electrolyte and low toxicity of materials.
- Great range to operate at high temperature.
- High electrical efficiency 95 percent.

Disadvantages

- The main disadvantage of SCs are their limited ability to store energy, and today, it is highly expensive.
- The voltage varies with stored energy, therefore it is necessary to use sophisticated electronic control systems and make use of the power converters to storage and recover more effectively electrical power.
- SCs have low voltages so serial connections are needed to obtain higher voltages. Because as this it is necessary to interconnect a large number of units to build devices with the propose to increase their voltage.

1.7 Conclusions

This first Chapter has presented the general and specific objectives of this thesis. A conceptual framework of the supercapacitor and fuel cell, showing their definitions, principles of operation, electrical characteristics, applications, advantages and disadvantages. The SC and FC technology has been studied in this Chapter as well as the great importance that both technologies are having once marketed, in a range of applications for both low and high power. One of the most important is in the automotive market due to its non-environmental pollution. It is necessary to know all the virtues and benefits offered by these technologies to make the most of their performance, not forgeting that, they require the use of power electronics to mitigate the inherent disadvantages.

Chapter 2

Power converters for FC and SC

2.1 Topologies of the DC/DC converters applied to FC

The DC/DC converter for FC applications must be fit into the requierements: high step-up conversion ratio, high stability of the output voltage during the variations of the output current and the input voltage, DC/DC converter operating with unidirectional current, high efficiency and low cost.

Below are shown the different converters that can operate the fuel cell.

2.1.1 Boost converter

Figure 2.1 shows the electrical circuit of the boost converter. The boost converter is a simple topology where research has been done to improve its optimization. In a FC application, the converter has the following features [26]:

1.-Switch referred to ground.
2.-Output voltage with reference signal is equal to the input voltage.
3.-It is not possible to disconnect the input of the output (difficult protection).

The transfer function of this converter is:

$$M = \frac{V_0}{V_{FC}} = \frac{1}{1-\alpha} \tag{2.1}$$

where:

M= Transfer function
V_0= Output voltage $[V]$.

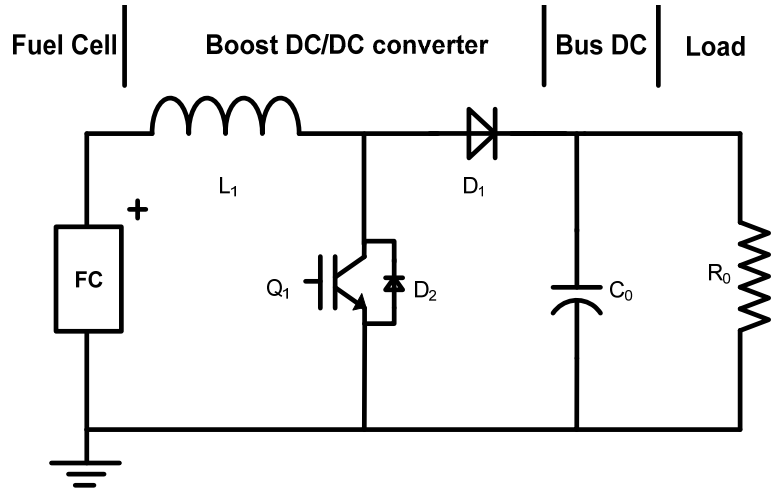

Figure 2.1: Boost converter.

V_{FC}= Fuel cell voltage $[V]$.
α= Duty cycle[-].

The main advantages and disadvantages [27] offered by the boost converter in a power system based on FCs are:

Main advantages

1.-High efficiency.
2.-The power structure of the converter makes the input current a non-pulsating type, which is ideal for feeding a FC.
3.-Simple design of the inductor.
4.-Low cost, simple control and design.

Main disadvantages

1.-Overcurrent in the startup.
2.-High stresses voltage on the switch if there is a large variation in magnitude between the input and output.

Single-phase isolated boost converter

Figure 2.2 shows the circuit of the isolated boost fullbridge topology. The switch-on ratios of the transistors are 0.5, by which the upper Q_1, Q_2 and the lower transistors Q_3, Q_4 are clocked synchronously but in antiphase [28]. The inductor L_1 allows a low current ripple.

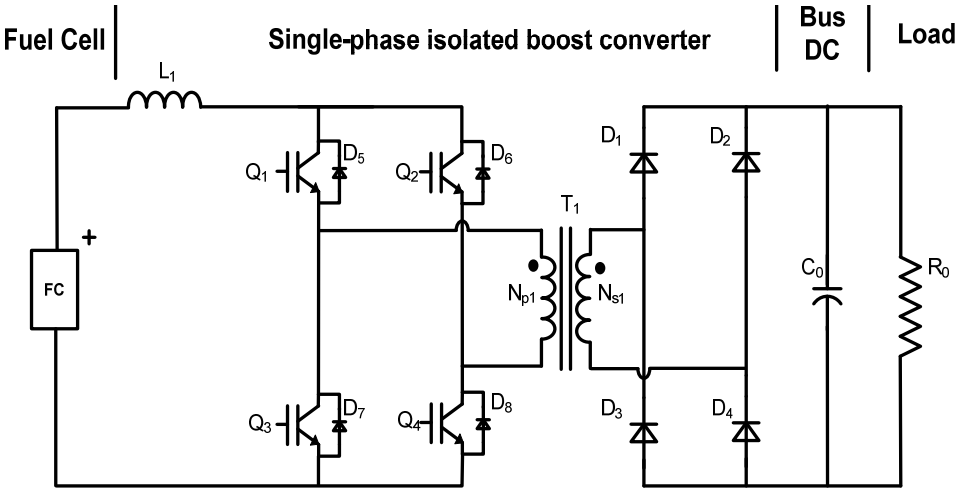

Figure 2.2: Schematic circuit of a single-phase boost converter.

Multi-phase isolated boost converter

Figure 2.3 shows a circuit schematic of a multi-phase isolated boost converter. The circuit consists of twelve controlled switches with antiparallel diodes ($Q_1 - Q_{12}, D_7 - D_{18}$) and six diodes ($D_1 - D_6$) to generate a DC voltage output. Because the current is shared by three-phases, the current stress on each device is reduced. As a result, the problems of diode recovery and higher switch and diode losses are substantially alleviated. Also, because the topology is a buck-derived type of converter, the controller implementation is simplified [29].

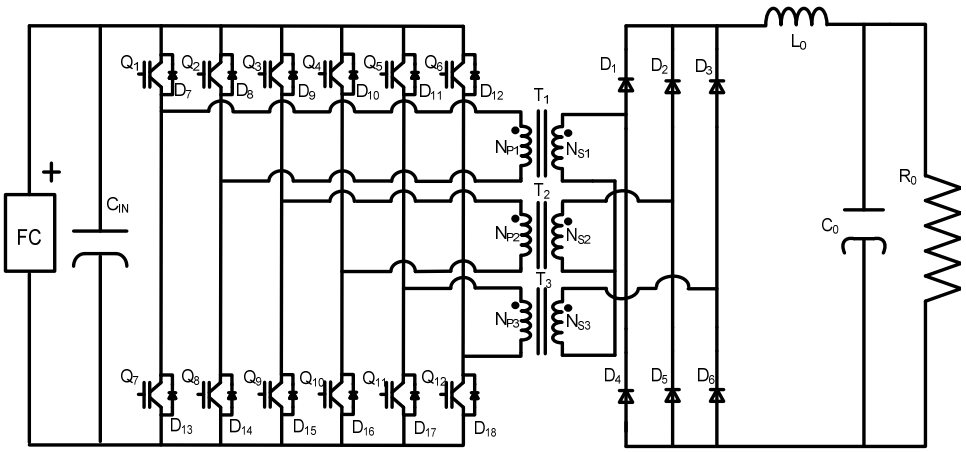

Figure 2.3: Schematic circuit of a multi-phase boost converter.

2.1.2 Buck-boost converter

Figure 2.4 shows the electrical circuit of the converter, where the output voltage is always reversed in polarity with respect to the input [30].

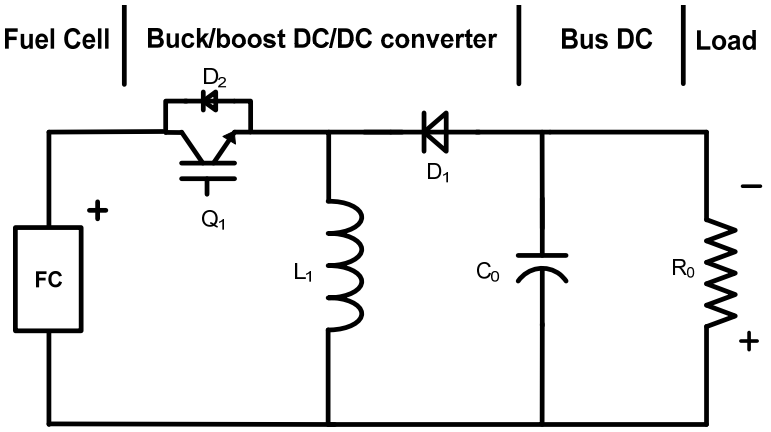

Figure 2.4: Buck/boost converter.

The transfer function of this converter is:

$$M = \frac{V_0}{V_{FC}} = \frac{\alpha}{1-\alpha} \tag{2.2}$$

Where:

M= Transfer function.
V_0= Output voltage [V].
V_{FC}= Fuel cell voltage [V].
α= Duty cycle [-].

In this case, the output voltage can be greater than the input, if the duty cycle is greater than 0.5, the output voltage increases with respect to the input voltage, and if the duty cycle is less than 0.5, the output voltage decreases with respect to its input.

Main features of buck-boost converter are:

1.-Output voltage with different reference to input voltage.
2.-Input current pulse.
3.-Buck-boost converter is possible to disconnect the input/output (protection).
4.-Buck-boost does not require galvanic isolation.

The main advantages and disadvantages offered by the buck-boost converter in a power system based on FCs are:

Main advantages

1.-Simple design of the inductor.
2.-Buck-boost converter can be very efficient.
3.-Buck-boost converter does not need a transformer, only an inductor.
4.-Very compact packaging.
5.-Competitive price.
6.-Used for charge and discharge backup storage energy (SC).

Main disadvantages

1.-Input current pulse (non protection with the FC).
2.-It does not have galvanic isolation.
3.-High stresses of semiconductor device.
4.-The duty cycle is limited.

2.1.3 Cuk converter

It is possible to obtain the Cuk converter if you use the principle of duality in the buck-boost converter. This converter provides a negative polarity regulated output voltage with respect to the common terminal of the input voltage. Figure 2.5 shows the circuit of a cuk converter [31].

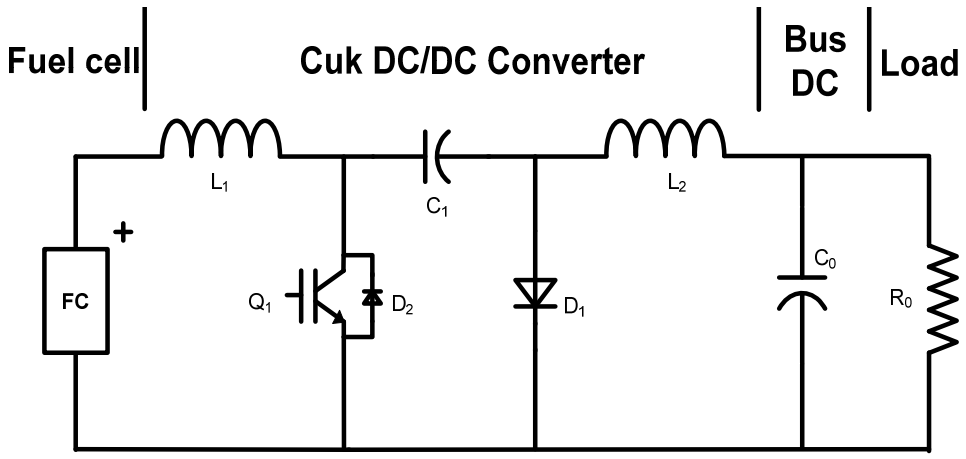

Figure 2.5: Cuk converter.

The transfer function of this converter is:

$$M = -\frac{V_0}{V_{FC}} = \frac{\alpha}{1-\alpha} \tag{2.3}$$

Where:

M= Transfer function.
V_0= Output voltage $[V]$.
V_{FC}= Fuel cell voltage $[V]$.
α= Duty cycle [-].

The cuk converter has the characteristic that its output voltage can be higher or lower than the input voltage [31].

Main features of cuk converter are:

1.-Switch referred to ground.
2.-Output voltage with different reference to input voltage.
3.-Non pulsating input current.
4.-In cuk converter is possible to disconnect the input of the output.

The main advantages and disadvantages offered by the cuk converter in a power system based on FCs are:

Main advantages

1.-In the cuk converter the energy transfer is made by a capacitor which protects the FC from the output.
2.-Its input and output are non-pulsating.
3.-Cuk converter can offer very low levels of current ripple on the FC.

Main Disadvantages

1.-High RMS current in the capacitors.
2.-Cuk converter does not have galvanic isolation.
3.-More expensive than boost and buck-boost converts.
4.-More devices.
5.-The duty cycle is limited.

Isolated cuk converter

Figure 2.6 shows the schematic of the isolated cuk converter, which steps-up the input voltage to a high DC voltage and provides galvanic isolation as well. The isolated cuk converter attains fewer components, enables integrated magnetics, leading to low input and output current ripples and lower electromagnetic interference EMI as compared to other conventional isolated step-up converters.

The magnetic integration yields significant savings in weight and volume as well. However, because the current through the transformer sees an almost instantaneous change due to the switching of Q_1, the leakage inductance in the cuk converter has to be really low; otherwise, the voltage spikes across Q_1 and Q_2 could potentially destroy the device.

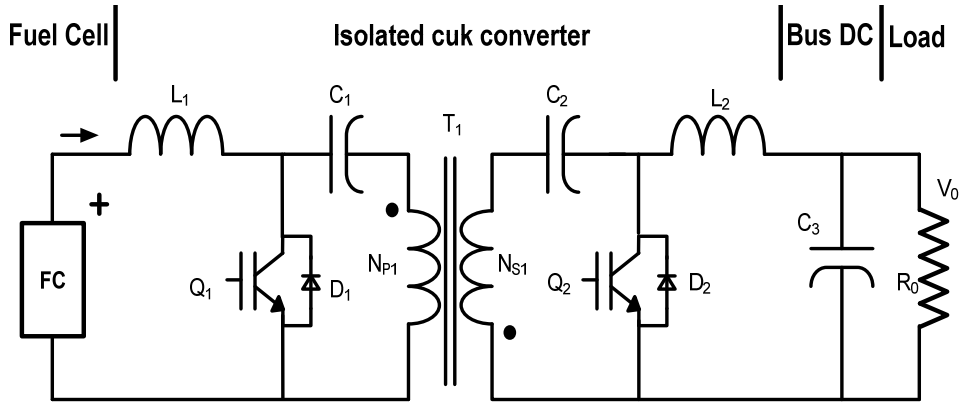

Figure 2.6: Isolated cuk converter.

2.1.4 Forward converter

The Figure 2.7 shows the conventional forward converter, the transfer function is similar to the buck converter, but now the inductor is multiplied by the turns ratio transformer.

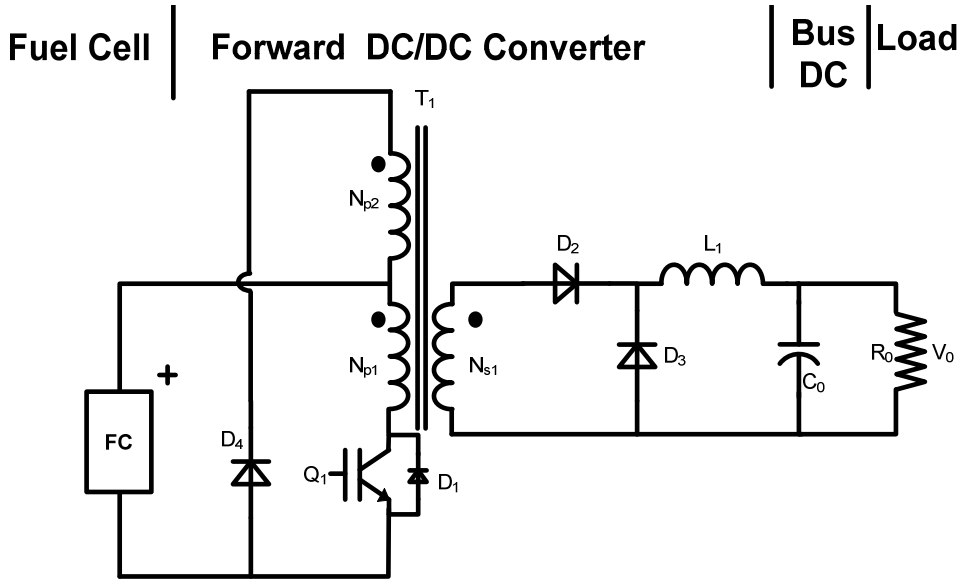

Figure 2.7: Electric circuit forward converter.

$$M = -\frac{V_0}{V_{FC}} = \frac{N_{S1}}{N_{P1}} = N\alpha \tag{2.4}$$

Where:

M= Transfer function.
V_0= Output voltage $[V]$.
V_{FC}= Fuel cell voltage $[V]$.
N_{S1}= Secondary winding [-].
N_{P1}= Primary winding [-].
N= Transformation ratio [-].
α= Duty cycle [-].

The main features of converter forward are:

1.-The forward converter requires single transistor.
2.-Non-pulsating output current.
3.-Forward converter requires an auxiliary winding to demagnetize the transformer.

The main advantages and disadvantages offered by the forward converter in a power system based on FCs are:

Main advantages

1.-High efficiency.
2.-Forward converter has galvanic isolation.
3.-Protection with the FC.
4.-Less devices comparated with isolated topologies.
5.-Non-pulsating output current.

Main disadvantages

1.-Forward converter does not work with high power applications.
2.-The duty cycle is limited.
3.-Pulsanting input, which forward converter is not limited with inductor device.
4.-High stress in voltage from semiconductor devices.

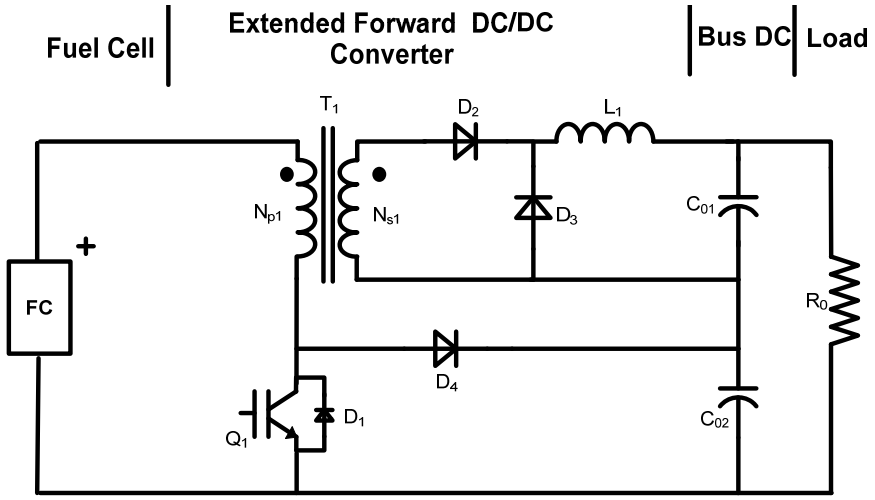

Figure 2.8: Electric circuit extended forward converter.

A variant of the forward converter is the extended forward converter [8] (shown in Figure 2.8). This topology has the characteristic of adding a capacitor C_{02} in series with a capacitor C_{01} both connected in the DC bus, the capacitor C_{02} is connected with the diode D_4 and this one with the switch Q_1. Thus it is possible to transfer energy to output, besides this topolgy allows reduction to the voltage stress on switching in Q_1.

2.1.5 Push Pull converter

The Figure 2.9 shows the electrical circuit of the push pull converter. Note that the switches conduct the output inductor current reflected to the primary and also must support at least twice the supply voltage [32].

The transfer function of this converter is:

$$M = -\frac{V_0}{V_{FC}} = 2\alpha\frac{N_{S1}}{N_{P1}} = 2\alpha N \tag{2.5}$$

Where:

M= Transfer function.
V_0= Output voltage $[V]$.
V_{FC}= Fuel cell voltage $[V]$.

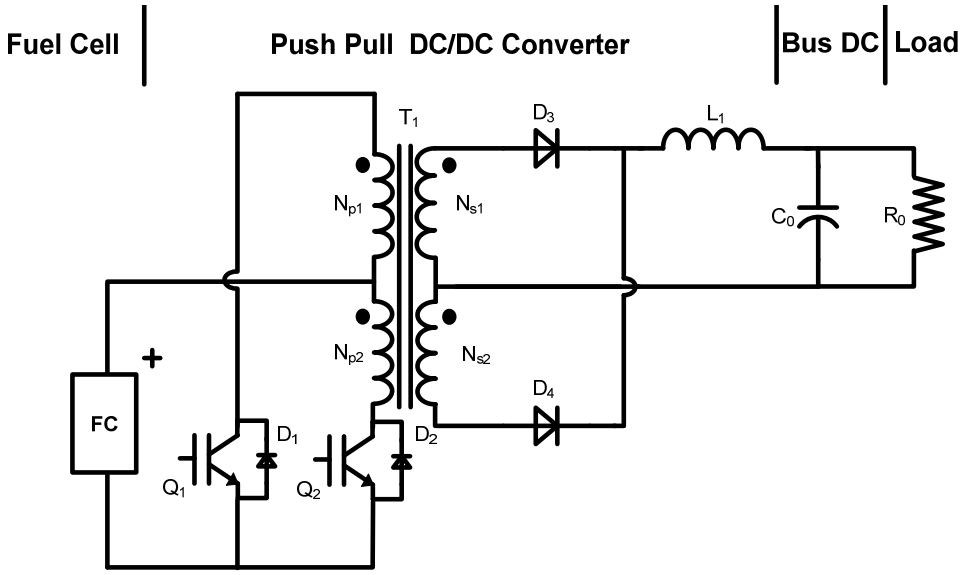

Figure 2.9: Electric circuit push pull converter.

α= Duty cycle [-].
N_{P1}= Primary winding [-].
N_{S1}= Secondary winding [-].
N= Transformation ratio [-].

Main features of push pull converter are:

1.-Two transistors referenced to ground.
2.-Stress voltage in the transistor double the input voltage.
3.-Precise timing to avoid saturation.

The advantages and disadvantages offered by the push-pull converter in a power system based on FCs are:

Main advantages

1.-Provides isolation between FC power supply and load.

Main disadvantages

1.-Pulsating input current. Due to the structure of the power converter, the input current is pulsating and this is an inconvenient to operate with FC applications.
2.-Forward converters and push-pull do not have good performance in high power applications.

The efficiency of a push-pull converter is limited by the leakage inductance of the transformer. This is because, during turn off, the switches induce a voltage peak due to leakge inductance. The push-pull efficiency is better, compared with boost converter.

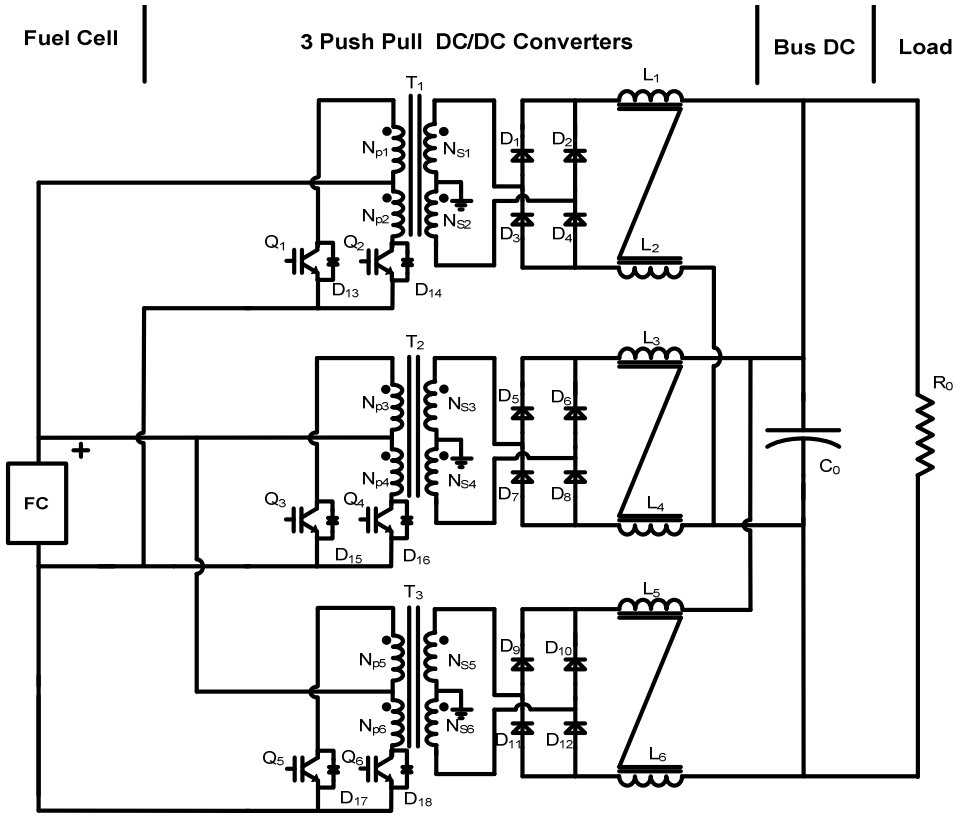

Figure 2.10: Electric circuit for 3 parallel output push-pull converters in application to FC.

Figure 2.10 shows a proposed power conditioning design to operate at 5 kW.

Figure 2.10 shows a topology of application for FC using a connection tree push pull converter whose outputs are in parallel to suitably boost the FC voltage from a range of $22 - 41\ V$ to $400\ V$ and $5\ kW$.

Figure 2.11 shows a push-pull converter, which has a high frequency transformer with double winding in primary side and secondary respectively. The push-pull converter can operate at high power, since the high frequency transformer can raise the input voltage to a higher voltage output. However, a bad winding coupling in the transformer could cause a saturation in the transformer core and therefore, a bad operation of the push-pull converter.

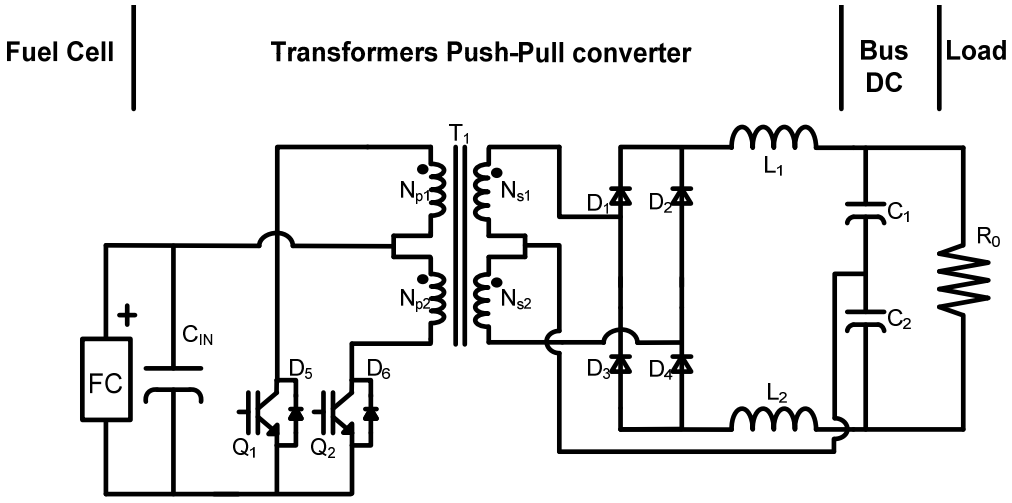

Figure 2.11: Step-up high frequency transformer push-pull topology.

2.1.6 Half bridge converter

Figure 2.12 shows the electrical circuit of the half bridge converter. There are essentially two transistors, one referenced ground and another floating one [33].

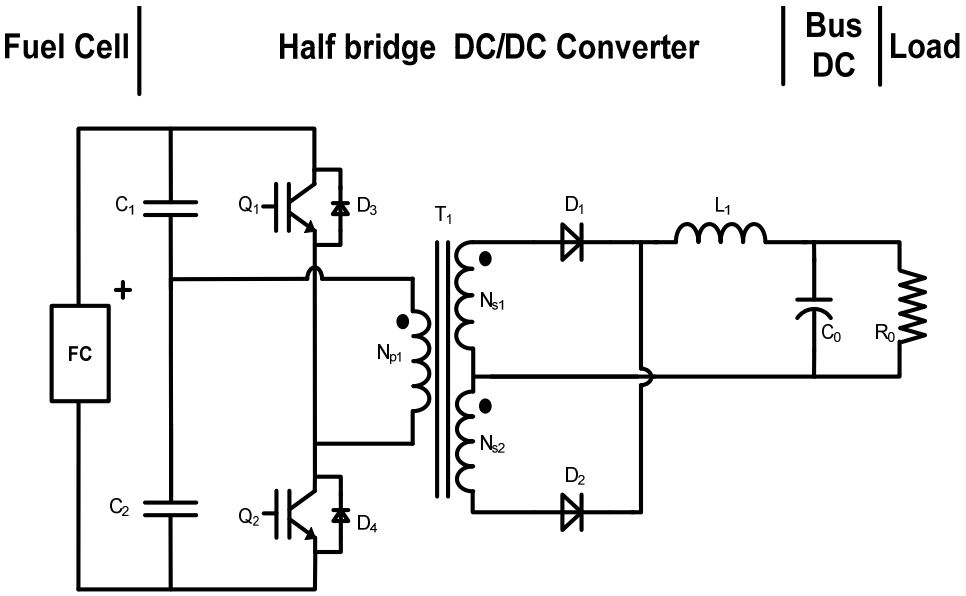

Figure 2.12: Electric circuit of half bridge in FC applications.

The transfer function of this converter is:

$$M = -\frac{V_0}{V_{FC}} = \alpha \frac{N_{S1}}{N_{P1}} = \alpha N \tag{2.6}$$

Where:

M= Transfer function.
V_0= Output voltage $[V]$.
V_{FC}= Fuel cell voltage $[V]$.
α= Duty cycle [-].
N_{S1}= Number of turns of secundary winding [-].
N_{P1}= Number of turns of primary winding [-].
N = Transformation ratio [-].

The advantages and disadvantages offered by the half bridge converter in a power system based on FCs are:

Main advantages

1.-Protection with the FC (half bridge converter has galvanic isolation).
2.-Soft switching structures.
3.-The half bridge configuration needs only two transistors.

Main disadvantages

1.-The output voltage is reduced by a factor of 0.5 (the factor of 0.5 can be compensated by doubling the transformer turns ratio n, causing the transistor currents to double).
2.-The half bridge configuration finds application at middle power levels.

2.1.7 Weinberg converter

Figure 2.13 shows the weinberg converter which has two switches like the push pull converter where the switch forms are the same. The weinberg converter does not have output inductance and the main disadvantage is in the peak voltage switches by Q_1 and Q_2 respectively, due to the leakage inductance of the transformers [34].

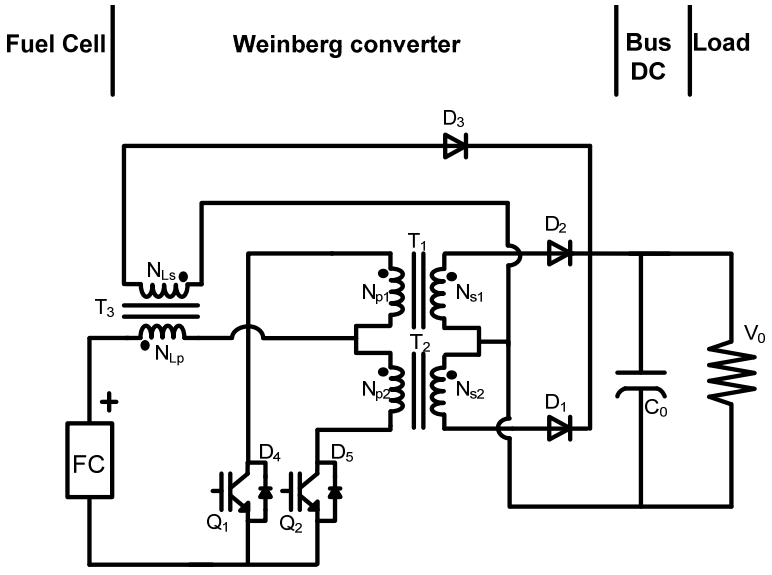

Figure 2.13: Topology of the Weinberg converter.

2.1.8 Full bridge converter

Figure 2.14 shows the electrical circuit of the full bridge converter. They are essentially four transistors, two referenced ground and the others floating ones [35].

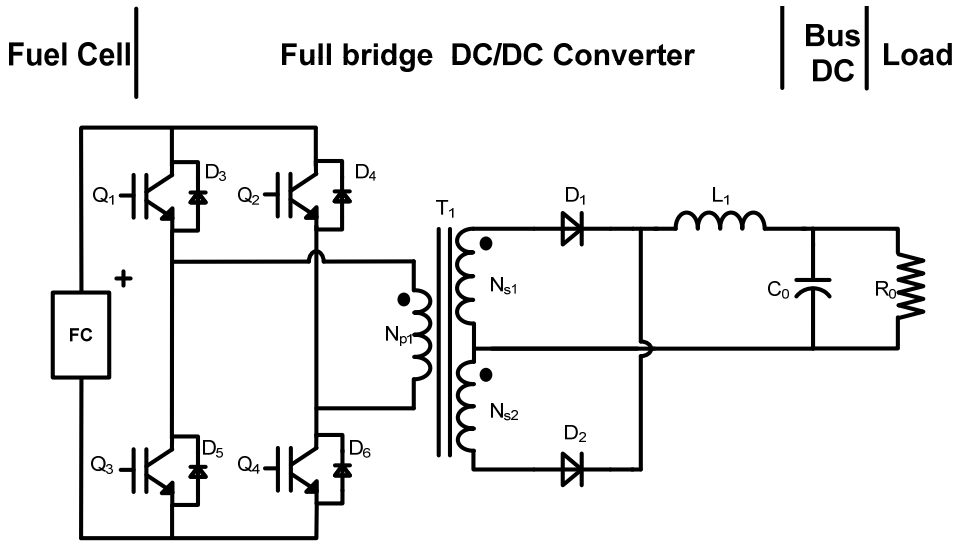

Figure 2.14: Electric circuit of full bridge in FC applications.

The transfer function of this converter is:

$$M = -\frac{V_0}{V_{FC}} = 2\alpha\frac{N_{S1}}{N_{P1}} = 2\alpha N \tag{2.7}$$

Where:

M= Transfer function.
V_0= Output voltage $[V]$.
V_{FC}= Fuel cell voltage $[V]$.
α= Duty cycle [-].
N_{S1}= Number of turns of secundary winding [-].
N_{P1}= Number of turns of primary winding [-].
N= Transformation ratio [-].

The M of the full-bridge converter is equal to the M of the push pull converter. The advantages and disadvantages offered by the full-bridge converter in a power system based on FCs are:

Main advantages

1.-Voltage and current stress in each transistor is equal to the input voltage.

2.-Ideal for high and medium power.

3.-The galvanic insulation between the FC and the load is obtained with a high frequency transformer of reduced size and weight [36].

4.-The full bridge achieves ZVS and ZCS, proposed for power conditioning in FC applications.

5.-The soft switching operation can increase the overall converter efficiency but depends on how much the switching frequency is increased.

6.-Full bridge does not have problems with being limited by the minimal duty cycle.

7.-Galvanic isolation from FC with load (protection against circuit damage).

Main disadvantages

1.-The full bridge efficiency is lower than the other power converters. This maybe because of the transformer losses, including copper loss and the higher switching losses due to number of switches, more expensive than other topologies of power converters.

2.2 Topologies of the DC/DC converter applied to SC

Within the requirements of the SCs to operate a backup power system there are two things:

a) SC requires a DC/DC converter, because of it is necesary to regulate its output voltage. The SC needs a bidirectional converter in current mode, due to the charge and discharge of the SC.

b) Increase of the SC input voltage by DC/DC converter to output voltage where it is connected in DC bus.

Below are the converters that perform this action.

2.2.1 Half bridge

This converter has been found in the literature and connects the storage power system at the output DC bus V_0, which is the high side. The configuration of bidirectional converter is shown in Figure 2.15. The SC bank offers a higher energy density than conventional capacitors and batteries [37].

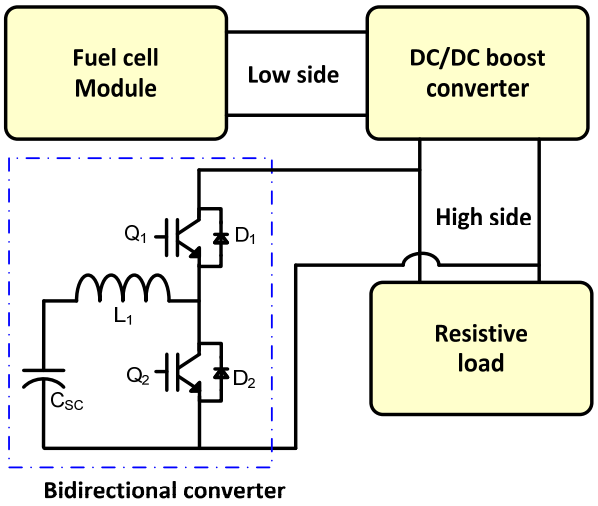

Figure 2.15: Bidirectional half-bridge converter used in storage energy systems.

For the correct operation of the half-bridge converter, it requires switching Q_1 and Q_2 alternately, because if switching Q_1 and Q_2 simultaneously, it would cause a short circuit in the branch of switches Q_1 and Q_2 respectively. The half-bridge converter operates in bidirectional current, also called in two quadrants, therefore the SCs can charge when the current is positive and discharge when the current is negative.

2.2.2 Full bridge

Figure 2.16 shows a block diagram where the bidirectional full-bridge converter operates with the SC. This system consists of two converters, the first is a unidirectional full-bridge DC/DC converter for the FC operation and the second is a bidirectional full-bridge DC/DC converter for SC operation. The block of Unidirectional full-bridge DC/DC power converter seen in Figure 2.16 is able to supply the power flow from FC to load in one direction [38]. On the other hand, the bidirectional full-bridge DC/DC converter allows both directional power flow for SC charge and discharge.

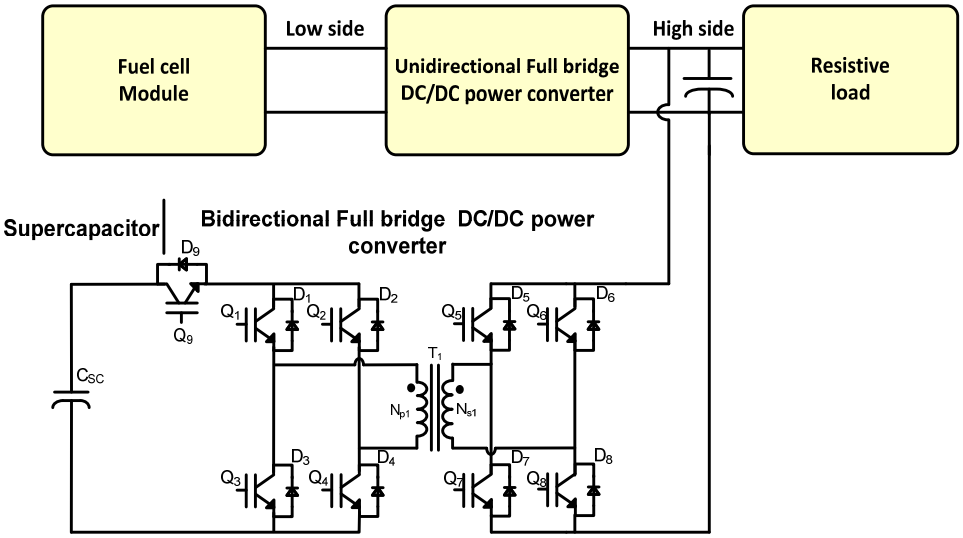

Figure 2.16: Full-bridge bidirectional current.

The response of the bidirectional full-bridge DC/DC converter should also be fast enough to compensate for the slow dynamics of the FC during start-up or sudden load changes.

2.3 Hybrid topologies of the DC/DC converters applied to FC/SC

2.3.1 Scheme with low frequency isolation

The Figure 2.17 shows a diagram of a system based on a low frequency transformer (50 Hz). The system consists of three stages of conversion to

allow proper management of the FC, but is not included isolation between the FC and SC [39].

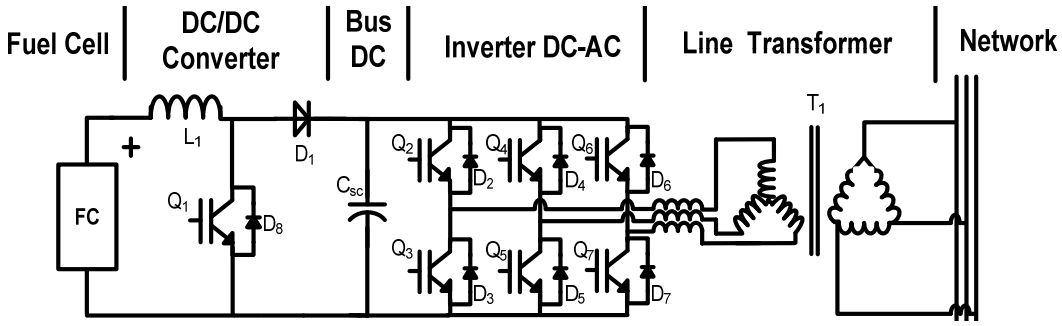

Figure 2.17: FC power converter topology with a line frequency isolation transformer.

The conditioning system is based on a boost converter powered by a FC, the output of the converter is connected to a battery bank, which is the DC bus. Subsequently, the DC bus is converted to AC by an inverter DC-AC. Due to these characteristics, the conditioning system needs to use a low frequency transformer that will raise the voltage at the same time providing insulation to the load. The system is simple and robust. However, there is a low power density associated with the transformer. Furthermore, due to the use of traditional technologies of conversion (hard switching), the current and voltage efforts undergoing the semiconductor devices are high.

2.3.2 Scheme with high frequency isolation

One of the trends to resolve the low power density is the use of switched converters which provide high frequency isolation [40]. Figure 2.18 shows the circuit topology, where the high frequency is obtained between isolation of the FC and the load through a DC-DC converter, in this case, working with a push pull converter. The power conditioner works with two boost converters connected in cascade.

The selected push pull topology exhibits high efficiency capability. The main feature of a push pull DC-DC converter is that it uses a high frequency transformer and the SC backup system is connected to high voltage DC bus.

Figure 2.19 shows the DC-DC conversion stage, that consists of two FCs and two boost converters. A bidirectional half-bridge converter has been

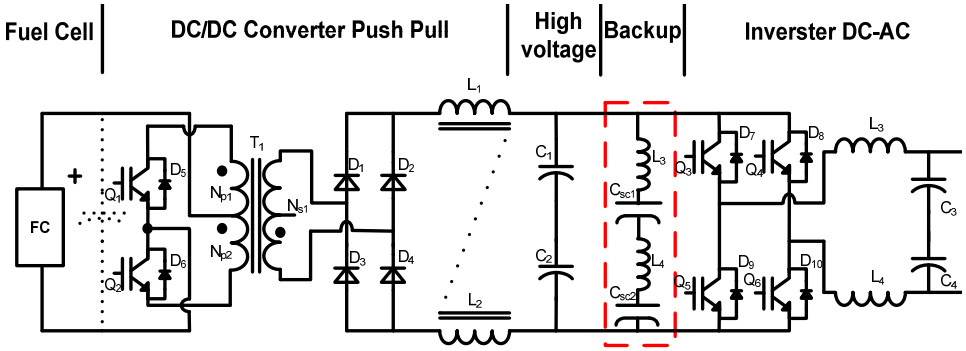

Figure 2.18: Push pull converter with high frequency isolation.

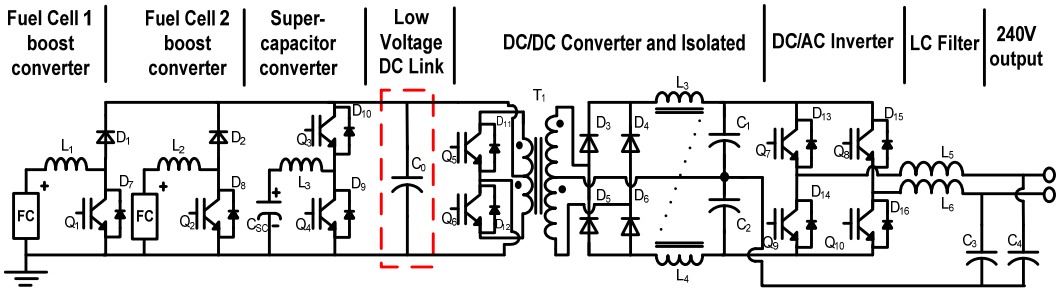

Figure 2.19: Two boost converter conected in cascade for operate FC/SC system.

employed to operate a SC. One of the advantages presented by this circuit is the elimination of pulse current seen by the FC using a boost converter (inductor at the input) [41]. In addition, providing a regulated voltage bus allows an optimal design for the isolated converter of the second stage. However, these advantages are penalized with increased conversion stages.

Both schemes would result in advantages and disadvantages to the system that are not clarified until a thorough study of both alternatives. Ideally, from the point of view of the battery, the system power conditioner can provide isolation from the FC and the load, which fully protects the battery and increases its lifetime, but it would add complexity and cost to the power conditioner system.

Another trend of power conditioners is to reduce the number of stages in order to increase efficiency and reduce system complexity.

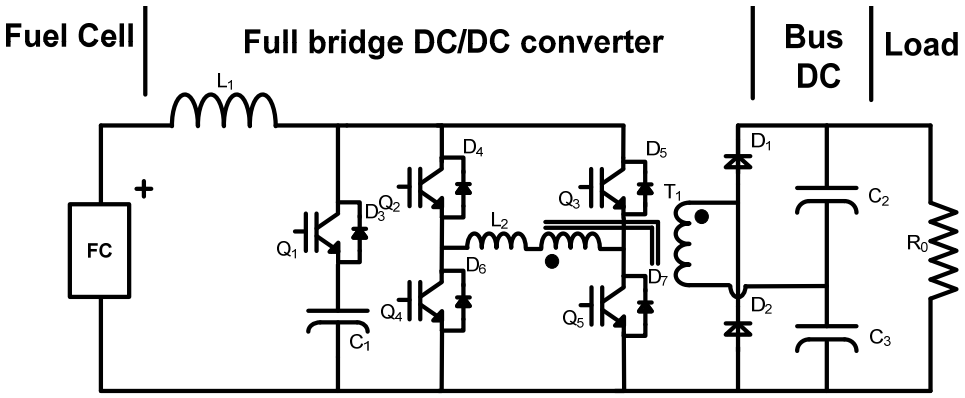

Figure 2.20: Boost isolated current-fed full-bridge converter.

One alternative to reduce losses associated with the operation of the converter DC/DC at high frequency is the use of soft switching techniques. Figure 2.20 shows a boost isolated current-fed full-brigde converter [42], which has added an auxiliary circuit comprising a switch to recover the energy stored in the parasitic inductance of the transformer. This circuit also allows ZVS in the main switches.

2.4 Control systems to operate FC/SC converters

Several researchers have studied the different topologies with their respective control proposals to operate FC and SC. Thoungthon et al. [43] present a control strategy used to control power from the FC power to the motor, and state of charge of the battery. The Figure 2.21 shows the FC hybrid power source for a distributed generation system. For the control algorithm, the Figure 2.22 shows how to manage energy exchanges between the DC bus V_0.

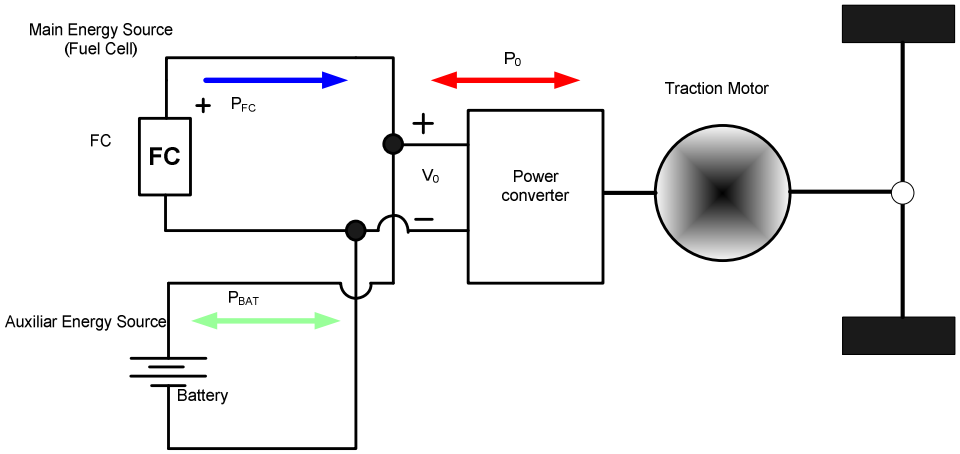

Figure 2.21: Diagram block of the proposed system.

The control strategy is a cascade control structure composed of three loops looking at Figure 2.23. The outer loop is a battery state of charge (SBC) control loop composed of SBC^* as a reference of SBC. The middle loop is the baterry current control composed of $I_{BAT}{}^*$ as a battery current reference coming from the outer loop and $I_{FC}{}^*$ as a FC current reference.

Another hybrid control is seen in Figure 2.24. The FC in the hybrid system is only operating in a nearly steady state condition and SCs are functioning during transitory energy delivery or transitory energy recovery. The main purpose of the control system is to regulate DC bus voltage V_0. Taking into account the FC dynamics. With a FC as the main source, Thounthong et al. [44] have tried hybrid sources built with a PEMFC as main source and SCs as secondary source to regulate the DC bus voltage V_0 through a power control (P_O=P_{FC}+P_{SC}). The conception is that the hybrid system control proposes a regulation of the DC bus voltage V_0 through the power

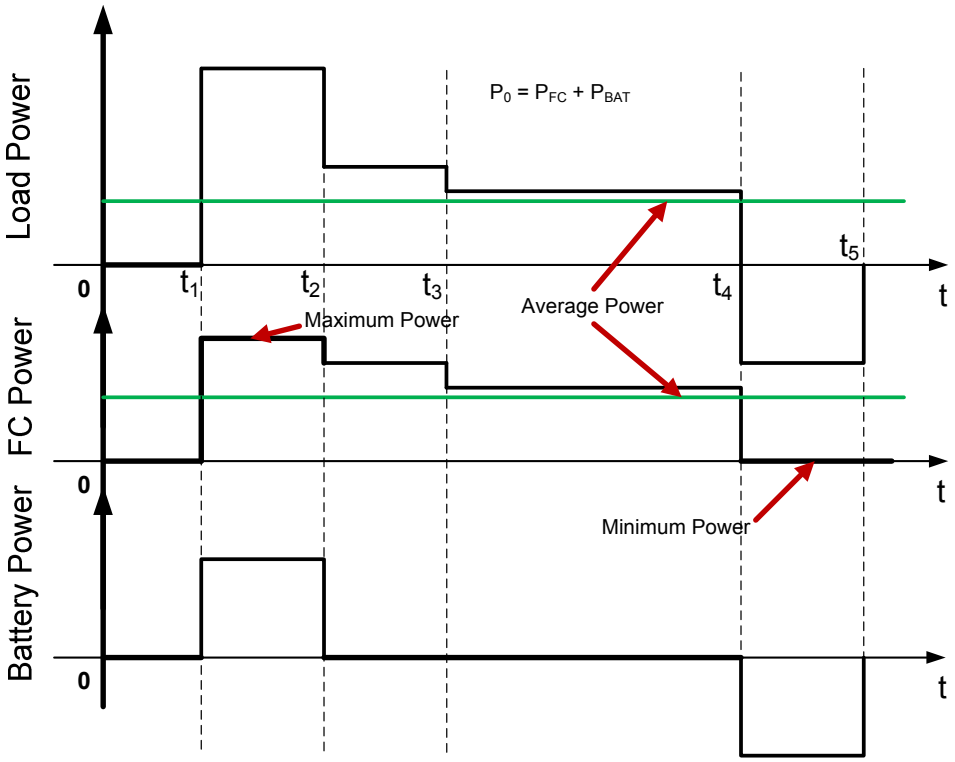

Figure 2.22: Power profile of a structure to operate FC and auxiliary energy source.

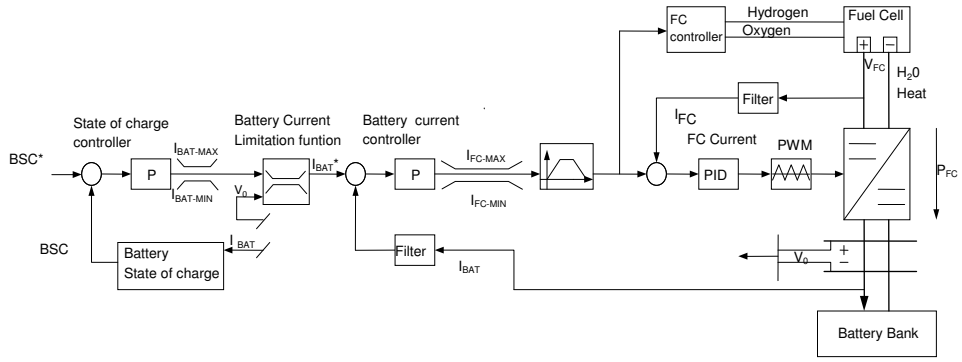

Figure 2.23: Control structure of a FC/battery hybrid power source.

only delivered by the fast auxiliary source. And SC voltage V_{SC} is regulated through the slow main source, the FC.

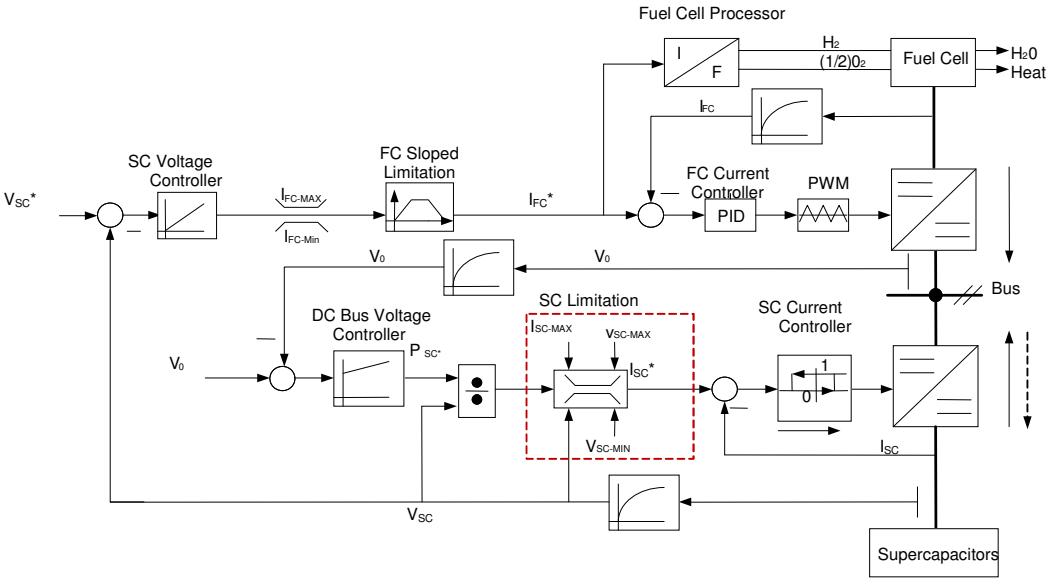

Figure 2.24: Block diagram of a structure Control to operate FC and SC.

2.5 Conclusions

Some DC/DC converters have been studied for the integration of a power conditioner to operate FC and SC. Within DC/DC, different types of converters like boost, cuk, forward, push-pull, half-bridge and full-bridge have been found. However, the boost converter has a greater efficiency than any other converter mentioned here, therefore, this converter is very commonly used to operate FC. The Boost converter is a topology with few components, low cost, simple design and control. On the other hand, in the operation of the SC, it requires a bidirectional half-bridge converter in current (for the charge and discharge of the SC).

A common structure used in the power conditioner is the fact that both

FC converter as SC converter, are connected in the same output DC bus, independent of the type of the DC/DC converter used. Control structures used in power conditioner to operate FC and SC usually require 5 closed-loop control to control the variables I_{FC}, I_{SC}, V_{FC}, V_{SC} and V_0. In some cases, the hysteresis control method is used and in others only controllers PIs.

Chapter 3

Proposed configuration

3.1 Analysis of the power conditioner

Figure 3.1 shows the proposed power conditioner. This system consists of two modules: FCs and SCs, therefore it is required two power converters. The main converter operates the FC which corresponds to a unidirectional boost converter called, in this thesis, the FC converter and the second converter operates the SC which corresponds to a bidirectional current half bridge called SC converter.

It is important to describe the principle of operation and analysis of FC and SC converters. To describe the operation of the system it is necessary to describe each of the modules: FC module, FC converter, SC module and SC converter.

3.1.1 FC module

The fuel cell used in this thesis corresponds to a $Nexa^{TM}$ module which has the ability to supply 1.2 kW in DC. It is important to mention that the power supplied by the FC is unregulated, the nominal voltage in operating the Nexa module is 26 V_{DC}. However it may vary depending on the power demanded by the load, so their values are in the range of 43 to 26 V operation. The Nexa module has a control system which allows monitoring of the variables measured and their own security and if there was any fault, the same control system is capable of sending the stop command to the user to check the system failure.

The control system is responsible for constantly monitoring the number listed below:

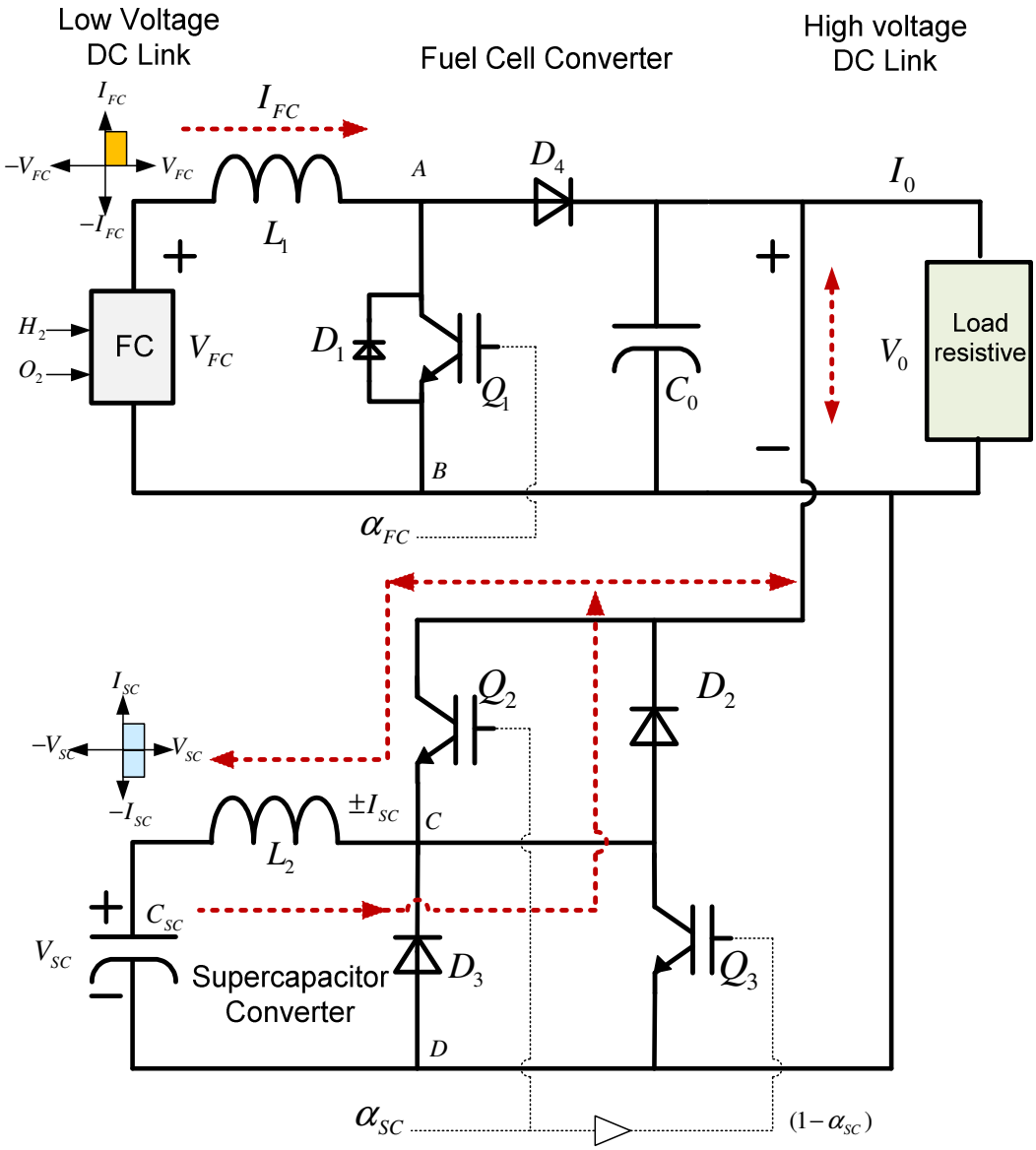

Figure 3.1: Proposed power conditioner.

Figure 3.2: The Nexa power module.

- Stack temperature.
- Stack voltage.
- Current stack.
- Hydrogen pressure.
- Air mass flow.
- Stack power, etc.

The module of the Ballard Nexa fuel cell employed on this thesis is shown in the following Figure 3.2. To manipulate the system operation it is necessary to operate the analog signals and digital form which is controlled by a control board.

The control system is responsible for operating the solenoid valves and hydrogen purge $Nexa^{TM}$ module. Furthermore, the control system operates a relay, with the system protection function as if there were a fault in the

load, that automatically controls the signal and sends to the relay to open, in normal operating conditions the relay is closed.

3.1.2 FC converter

The scheme of the FC converter is shown in Figure 3.3 which corresponds to a boost converter which output voltage is always higher than the FC voltage. To reduce the voltage ripple at the output of the converter, a capacitor is added. FC converter has been analysed in continuous conduction mode [45].

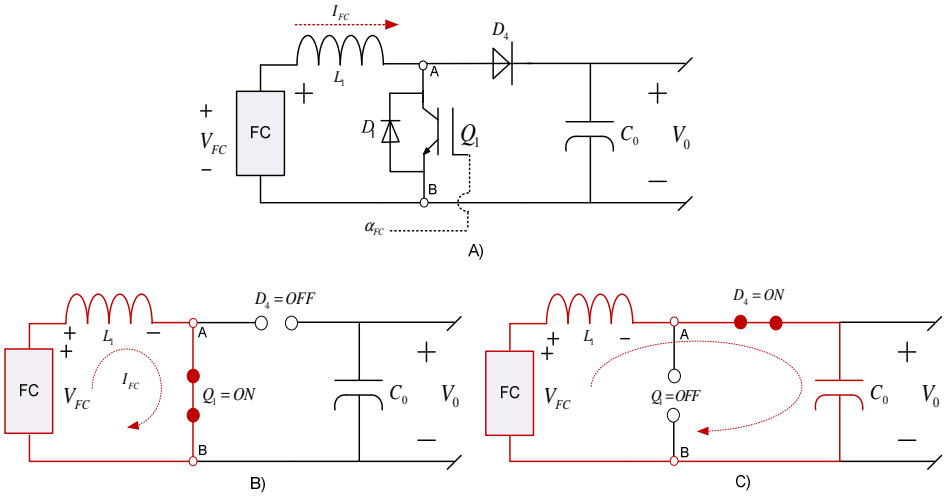

Figure 3.3: A) Fuel cell converter. B) Equivalent circuit in mode Turn on. C) Equivalent circuit in mode Turn off.

The basic principle of a FC converter consists of two distinct states (see Figure 3.3 B) and C), turn on and turn off.

During turn on

When the switch Q_1 is turned on, the diode D_4 is reversed biased, thus isolating the output stage. During this sequence, the inductance stores energy while the capacitor keeps the output voltage.

During turn off

When the switch Q_1 is turned off, the output stage receives energy from the inductor as well as from the input V_{FC}.

Continuous conduction mode

Figure 3.4 shows the steady state waveforms for this mode of conduction where the inductor current flows through the inductor L_1 and never falls to zero.

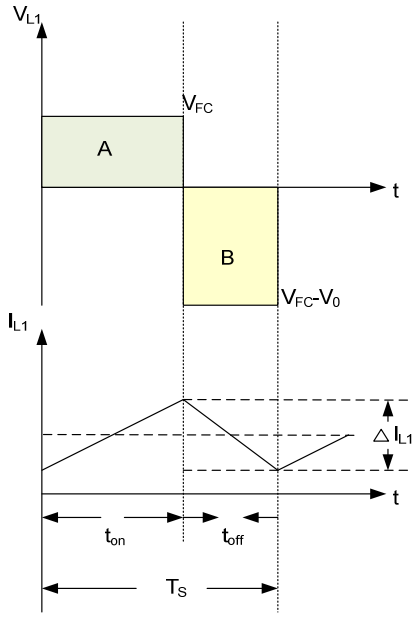

Figure 3.4: Continuos conduction mode.

In a steady state, the time integral of the inductor voltage over a time period should be zero, it is represented by.

$$V_{FC} \cdot t_{on} + (V_{FC} - V_0) \cdot t_{off} = 0 \tag{3.1}$$

Developing the Equation (3.1) is obtained

$$\frac{V_0}{V_{FC}} = \frac{1}{1 - \alpha_{FC}} \tag{3.2}$$

Inductor value

When observing the Figure 3.4 it is possible to find the inductor value, analyzing the turn on state.

$$\Delta I_{L_1} = \frac{V_{FC}}{L_1} \cdot t_{on} \tag{3.3}$$

Developing and substituting t_{on} in Equation(3.3) it is possible to find the inductor value L_1.

$$L_1 = \frac{V_{FC}\alpha_{FC}}{\Delta I_{L_1} f_s} \tag{3.4}$$

Where:

ΔI_{L_1}= Inductor current increase L_1.
α_{FC}= Duty cycle of FC.

Capacitor value

Observing at Figure 3.5 it is possible to calculate the ripple of the output voltage.

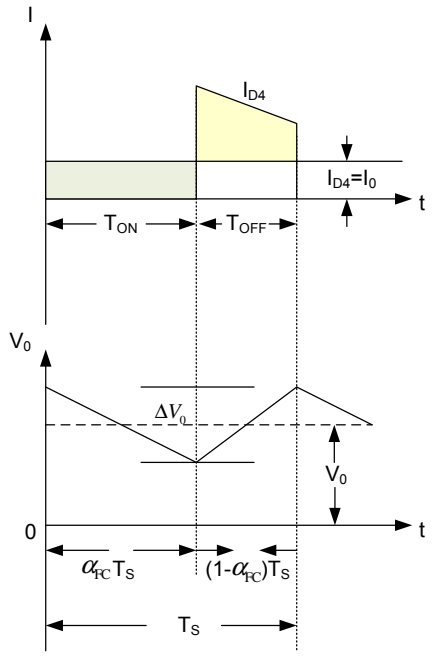

Figure 3.5: Output voltage ripple.

Table 3.1: Specifications to operate the FC converter.

Symbol	value	Units
V_{FC}	$43-26$	V
ΔI_{L_1}	0.8	A
f_S	20	kHz
α_{FC}	0.5	[-]
I_0	6.25	A
ΔV_0	0.2	V

Figure 3.5 shows the area shaded which represents charge ΔQ therefore, I_{D4}=I_0. In this sense, the voltage ripple is given by

$$\Delta V_0 = \frac{\Delta Q}{C} = \frac{I_0 \alpha_{FC}}{C_0 f_s} \tag{3.5}$$

In this way, the capacitor value is obtained by

$$C_0 = \frac{I_0 \alpha_{FC}}{\Delta V_0 f_s} \tag{3.6}$$

Substituting values of Table 3.1 for the inductor value in Equation (3.4) gives the result 1.3 mH, in this case it has proposed a value of $L_1 = 1$ mH. The capacitor values are calculated by Equation (3.6) and give $C_0 = 781$ μF, however it has a proposed value of 1000 μF. The chosen values L_1 and C_0 allow it to operate with the converter in Continuous Conduction Mode (MCC).

3.1.3 Supercapacitor module

In this bench, the supercapacitors shown in Figure 3.6 are the element responsible for the storage of energy. Below are the characteristics of the bank of supercondensadores used. Two commercial modules BPAK0058 E015 Maxwell Technologies are used. Each of these modules has an equivalent capacity of 58 F and 15 V rated voltage.

The characteristics of SCs bank are listed in Table 3.2.

The sizing of the SCs can be made according to parameters of stored energy as well as power or discharge current. The stored energy in a SC responds

Figure 3.6: SCs bank.

Table 3.2: Supercapacitors bank features.

Description	symbol	value	Units
Equivalent capacity	C_{eq}	29	F
Nominal voltage	$U_{-SC,MAX}$	30	V
Minimum Voltage	$U_{-SC,MIN}$	15	V
Current peak maximum	$I_{-SC,PEAK,MAX}$	1500	A
Maximum leakage current	$I_{-LEAKGE,MAX}$	1.0	mA

to the Equation (1.2). According to this, and considering that the SCs bank works in a range of voltages limited by V_{MAX} and V_{MIN}, the available energy is expressed in (3.7)

$$E_{available} = \frac{1}{2}C \cdot \left(V_{MAX}^2 - V_{MIN}^2\right) \tag{3.7}$$

Where C is the equivalent capacity and $\Delta V = V_{MAX}$ - V_{MIN} is the increase of voltage in the load. Following the recommendations of the manufacturer, it is established that $V_{MAX} = V_{NOM}$ and $V_{MIN} = \frac{1}{2}V_{NOM}$.

The capacitive component can be represented by the following Equation;

$$i = C \cdot \frac{dV}{dt} \tag{3.8}$$

where:
i= Current.
C= Capacitance.
dV= Change in voltage.
dt= Change in time (time of discharge).

Manipulating the Equation (3.8) and solving for dV;

$$dV = i \cdot \frac{dt}{C} \tag{3.9}$$

The resistive component can be represented by the following Equation;

$$V = i \cdot R_{SC} \tag{3.10}$$

where:

V= Voltage drop across the resistor.
i= Current.
R_{SC}= Equivalent series resistance.

Equating Equations (3.9) and (3.10):

$$dV = i \cdot \frac{dt}{C} + i \cdot R_{SC} \tag{3.11}$$

where:

Table 3.3: Design parameters of the SCs bank.

Symbol	value	Units
$P_{available}$	10	kW
$U_{-SC,MAX}$	30	V
$U_{-SC,MIN}$	15	V
$I_{-SC,MAX}$	7	A
Δt_{min}	60	s

dV= Change in voltage during the discharge (or charge) of the capacitor.
i= Current during discharge (or charge) of the capacitor.
dt= Discharge duration.
C= SCs module capacity.

Design parameters for the calculation of the equivalent capacity reflected in Table 3.3.

3.1.4 SC converter

Considering the FC's slow response, an auxiliary converter is often needed to help maintain bus voltage during start-up and transient in the load as shown in Figure 3.7, which corresponds to a half-bridge converter. The main characteristic of this topology is the current I_{L_2} because it can flow from the bus voltage V_0 to the V_{SC} and vice-versa. However, the bus voltage V_0 must always be greater than the V_{SC}.

Figure 3.7 also shows the waveforms for the continuous conduction mode of operation where the inductor current I_{L_2} flows continuously. When the switch Q_2 is on for a time duration t_{on}, the switch Q_2 conducts the inductor current and the diode D_3 becomes reverse biased. This results in a positive voltage across inductor $V_{L_2} = V_0 - V_{SC}$. When the switch is turned off, the current decreases and flows through the diode D_2 and $V_{L_2} = -V_0$.

In Figure 3.7, the foregoing Equation (3.12) implies that the areas A and B must be equal. Therefore

$$(V_0 - V_{SC})t_{on} = V_{SC}(T_S - t_{on}) \tag{3.12}$$

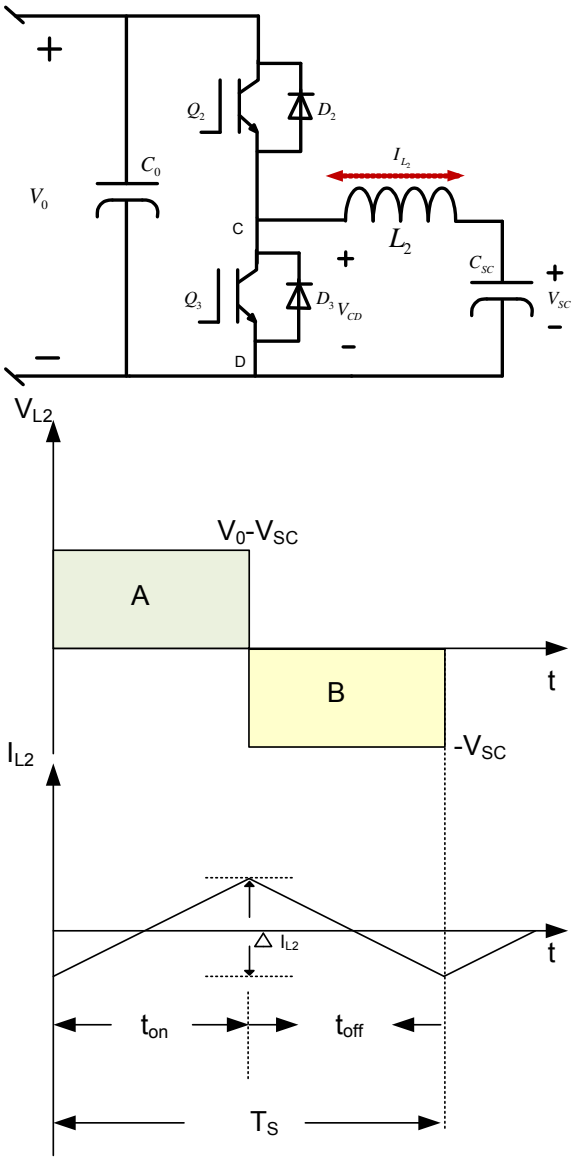

Figure 3.7: Current bidirectional converter to operates the SC.

Table 3.4: Specifications to operate the SC converter.

Symbol	value	Units
V_{SC}	25	V
L_2	3.4	mH
ΔI_{L_2}	0.4	A
f_S	20	kHz
C_{SC}	29	F
V_0	80	V
ΔV_{SC}	0.2	V
P_0	500	W
α_{SC}	0.5	[-]

Simplifying

$$\frac{V_{SC}}{V_0} = \frac{t_{on}}{T_S} \tag{3.13}$$

Therefore, the transfer function of this half-bridge converter is given by

$$V_{SC} = \alpha_{SC} \cdot V_0 \tag{3.14}$$

Where:

α_{SC} = Duty cycle of SC converter.

In Table 3.4 shows the parameter of half-bridge converter. For the inductor value has proposed a $L_2 = 3.4\ mH$ for decrease in the current in SC inductor and because this value is in the interval of continuos conduction mode. For the SC value has proposed $C_{SC} = 29\ F$ allowing a greater capacity for electrical storage energy and therefore longer SC discharge and less current ripple in SC.

3.1.5 Waveforms of FC and SC converter

Waveforms of FC converter

Figure 3.8 shows the typical waveforms of currents and voltage in a FC converter. When a FC converter operates in a continuos mode, the current

through the inductor (I_{L_1}) never falls to zero and the output voltage is always higher than the input voltage.

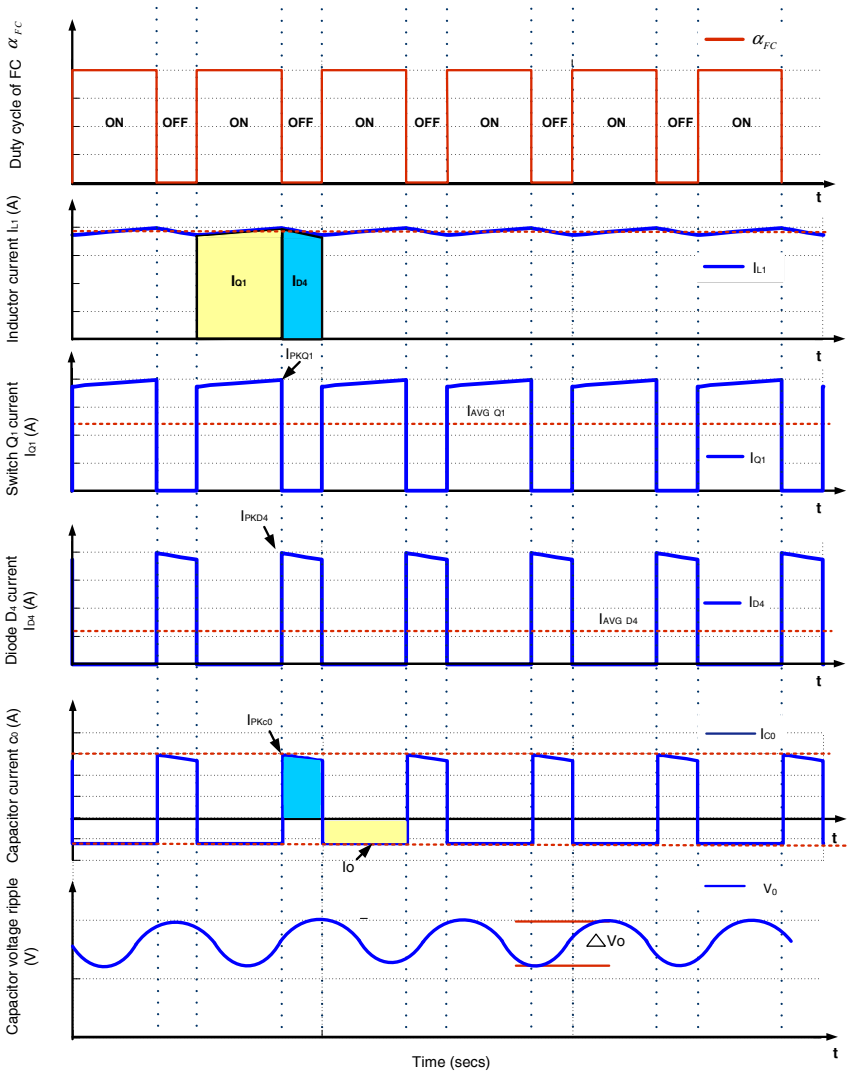

Figure 3.8: Waveforms FC converter.

Waveforms of SC converter

Figure 3.9 shows the current flows of I_{L_2} and Figure 3.10 shows the waveforms of SC converter.

1) Interval $0 \leq t \leq t_1$: On turning off Q_3, the energy stored in L_2 drives current through diode D_2 (free-wheels) and it is releasing to V_0, in this time interval the $V_{AB} = V_0$.
2) Interval $t_1 \leq t \leq t_{on}$: When Q_2 is turned on, the energy from V_0 is stored in L_2 where the I_{L_2} is positive, in this interval the V_{AB} is equal to V_0, and the SC receives power from the V_0.
3) Interval $t_{on} \leq t \leq t_2$: When Q_2 is turned off, the energy stored in inductance L_2 forces current to flow through the diode D_3 (free-wheels) and the V_{AB} is equal to zero, I_{L_2} continues to flow in positive direction and it is fully released.
4) Interval $t_2 \leq t \leq T_s$: When Q_3 is triggered, the V_{SC} forces I_{L_2} to flow in oppositive direction through L_2 and Q_3 therefore, the energy from V_{SC} is stored in L_2. In this time interval V_{AB} is equal to zero.

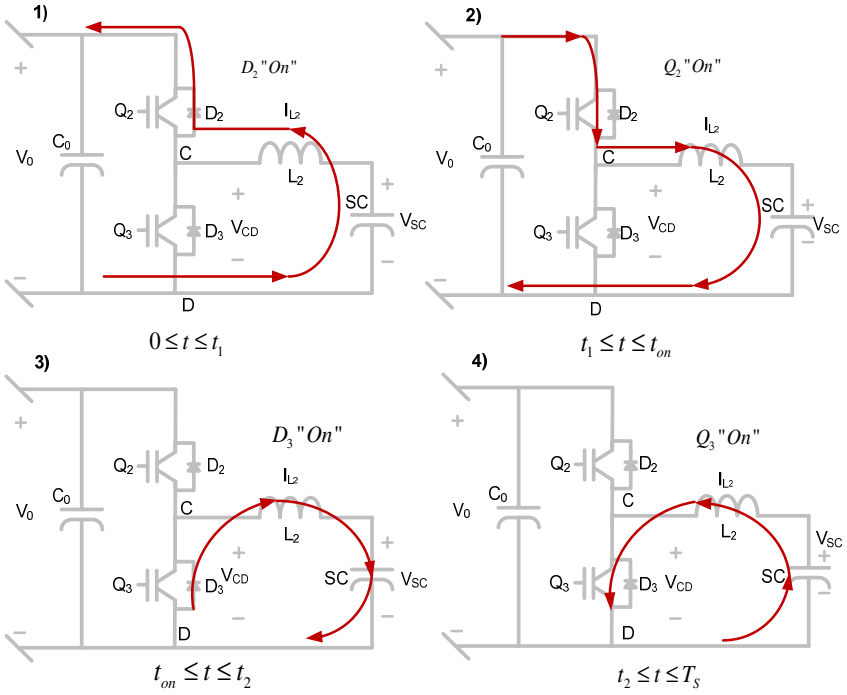

Figure 3.9: Current flows of SC converter.

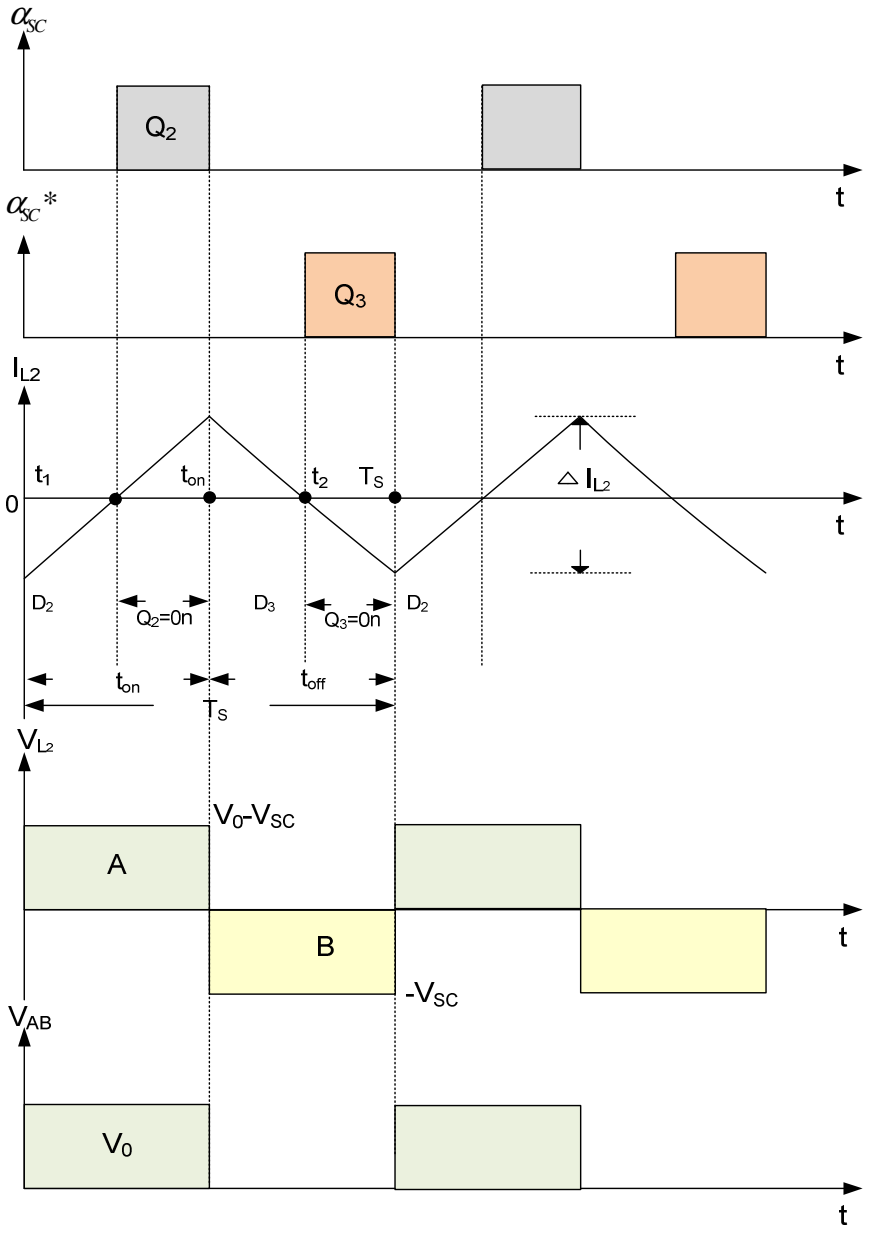

Figure 3.10: Waveforms SC converter.

3.2 Conclusions

A classical boost converter is selected for the FC because this converter can be operated in unidirectional form and it always operates in continuous condition mode. A bidirectional converter (half bridge) is used to operate the SC. Through the analysis of the open-loop of the power conditioner, it has found the values L_1, L_2, C_{SC} and C_0.

Chapter 4

Modeling and control design

4.1 Electric system model

Figure 4.1 shows the proposed power conditioner and the control structure of the system. The hybrid converter has two power supplies: FCs and SCs. The primary converter which is in this case a boost converter operates with the FC.

The second converter is a bidirectional converter used to operate with the SC. When it operates in two modes, the first is used while the SC charges. Then the SC converter acts as a boost converter delivering energy to the resistive load and when the SC is charged then the SC converter acts as a buck converter delivering energy to SC. These two converters are connected in parallel through a DC bus.

The proposed control for the FC converter is shown in Figure 4.1 whose function is controlling the SC voltage V_{SC} and FC current I_{FC} through Proportional-Integral PI controllers that are connected in cascade, in this case PI_V_{SC} and PI_I_{FC}.

The structure of control for the SC converter has the function of controlling the V_0 and current of the SC I_{SC} through the cascaded PI controllers PI_V_0 and PI_I_{SC}. For managing the control system four measurements are required, two for the currents I_{FC} and I_{SC} and two more for V_0 and V_{SC}.

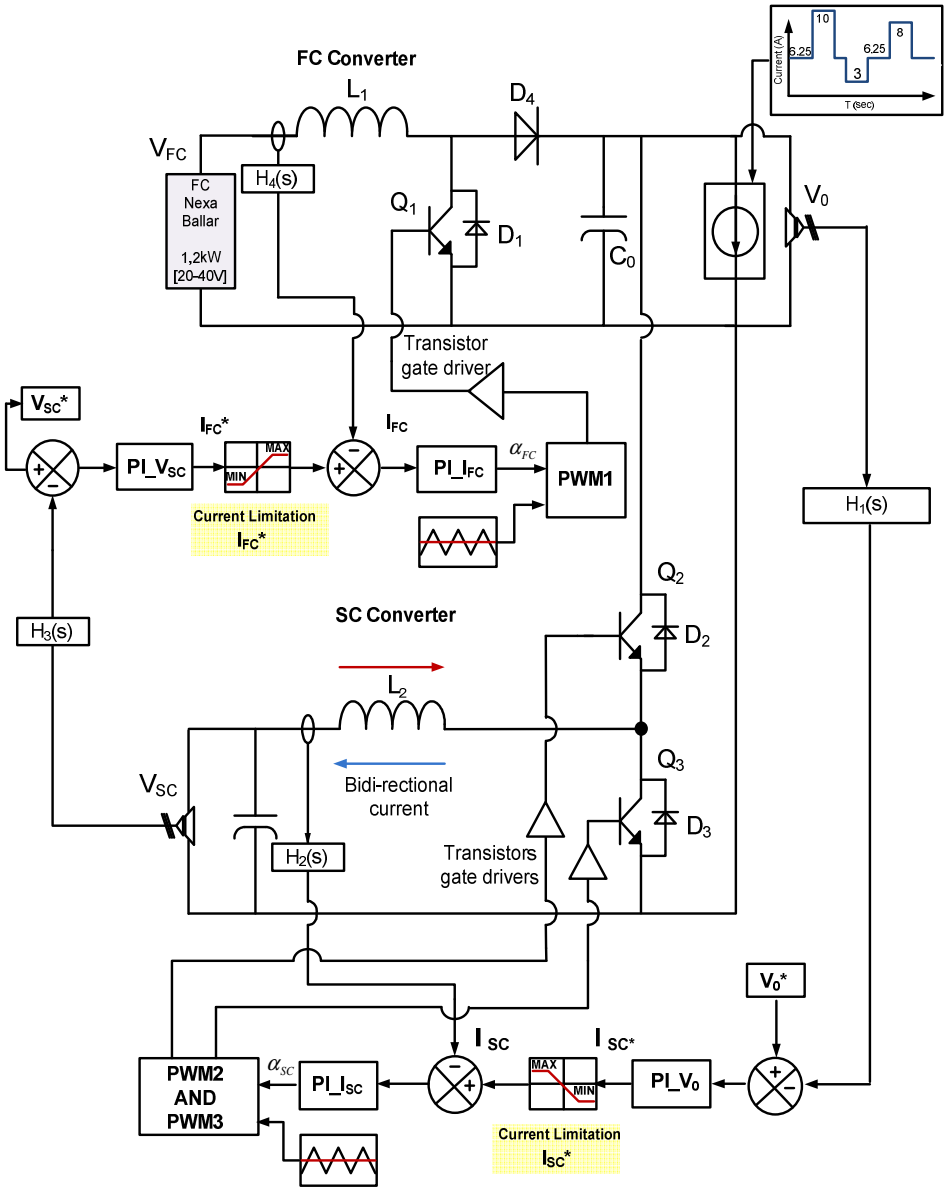

Figure 4.1: Hybrid FC/SC power system.

4.1.1 FC model

A simplified model of FC has been developed to operate the electrical characteristics and dynamics of a fuel cell Ballard Nexa at 1.2 kW seen in Figure 4.2. There are different ways to represent a fuel cell electric circuit, but here is the simplest way to obtain its equivalent circuit taking into account the nominal operating conditions of the fuel cell.

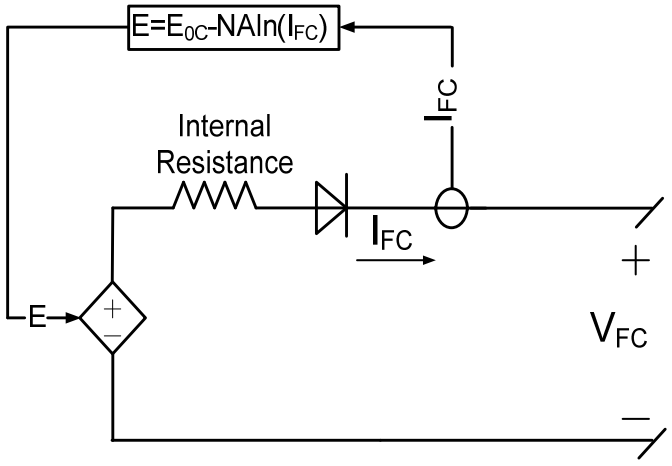

Figure 4.2: Simplified model.

Some equations are usign to represent the FC equivalent,

$$E_{0C} = N\left(E_N - Aln\left(i_0\right)\right) \tag{4.1}$$

$$A = \frac{RT}{Z\alpha F} \tag{4.2}$$

where:

$R = 8.3145\ J/(molK)$.
$F = 96485\ A\ s/mol$.
T= Temperature of operation of FC.
Z= Number of moving electrons.
α = Charge transfer coefficient.
E_N = Nerns voltage.
I_0 = Current exchange.
N = Cell numbers.

4.1.2 SC module

Like a conventional capacitor, the characteristic parameter of a SC is its capacity. Besides the capacity, other parameters make up the electrical circuit equivalent of a SC. The simplest model incorporates an equivalent series resistance as shown in Figure 4.3 [46].

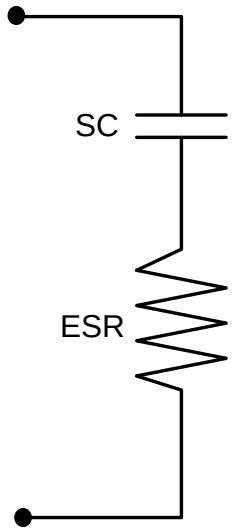

Figure 4.3: Equivalent circuit of a SC.

The equivalent series resistance (ESR) is very small with values in the order of 1-10 $m\Omega$. This modelling does not consider the leakage current, corresponding to the losses of parasitic when the supercapacitor is charged. However, these current values are usually very small in the order of a few $1 - 10\ mA$.

Charge and discharge

The SC charge and discharge cycles are similar to a conventional capacitor [47]. The SC current-voltage relationship is defined by

$$U(t) = \frac{q(t)}{C} = \frac{1}{C}\int_{t}^{t_0} i(\tau)\, dt + V(t_0) \tag{4.3}$$

The previous expression can be made as well by

$$i(t) = \frac{dq(t)}{dt} = C\frac{dU(t)}{dt} \tag{4.4}$$

However, if the charge or discharge occurs at a constant voltage U_0, the voltage responds to a first order system where the constant time τ corresponds to the product $R \cdot C$, as shown in the Equations (4.5) (4.6).

$$U_0 = R \cdot i(t) + \frac{1}{C}\int_0^t i(\tau)dt \tag{4.5}$$

$$U(t) = U_0 \cdot \left(1 - e^{-t/R \cdot C}\right) \tag{4.6}$$

$$i(t) = \frac{U_0}{R} \cdot e^{-t/RC} \tag{4.7}$$

4.2 Control system analysis in closed loop

4.2.1 Description of the control system

Figure 4.4 shows the proposed control scheme to operate two converters of FC and SC respectively. The control for the fuel cell converter structure consists of two Proportional Integral PI´s controllers.

One is located in the inner loop of current PI_I_{FC} which is connected in cascade with the external loop through the controller PI_V_{SC}. On the other hand, the control structure for the SC converter also consists of two PI controllers. One is located in the inner loop current PI_I_{SC}, which is connected in cascade with the outer loop by the controller PI_V_0.

4.2.2 Transfer funtions for the FC converter

Figure 4.5 shows the linear model of FC converter analyzed through dependent voltage and current sources. It is important to mention that FC has been assumed as a voltage source.
Applying voltage Kirchhoff's law in Fig 4.5

$$V_{AB}(t) = L_1\frac{dI_{FC}}{dt} + R_{L_1} \cdot I_{FC}\,(t) + V_{FC}\,(t) \tag{4.8}$$

Substituting $V_{AB}\,(t)$ in Equation 4.8

$$V_0(1 - \alpha_{FC})(t) - V_{FC}(t) = L_1\frac{dI_{FC}}{dt} + R_{L_1} \cdot I_{FC}\,(t) \tag{4.9}$$

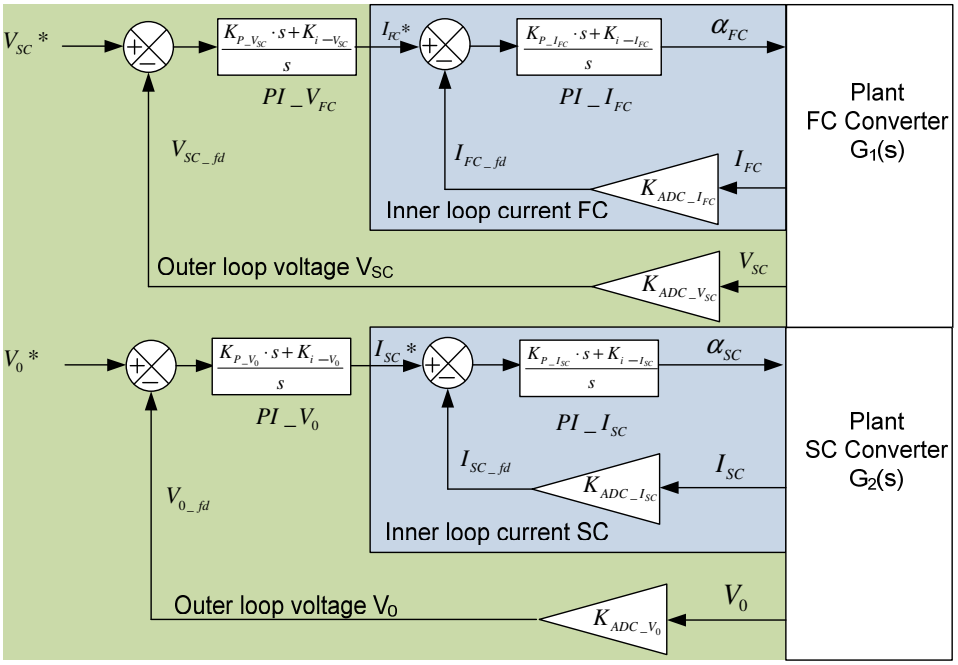

Figure 4.4: Schematic control system.

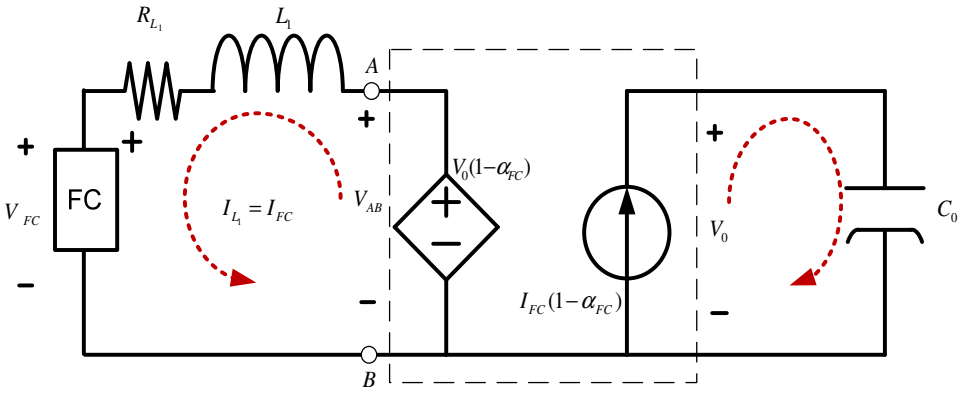

Figure 4.5: Simplified model of the FC converter.

Applying the Laplace transformation,

$$V_0(1-\alpha_{FC})(s) - V_{FC}(s) = I_{FC}(s)(L_1 s + R_{L_1}) \tag{4.10}$$

it can be rewritten as,

$$G_1(s) = \frac{V_0(1-\alpha_{FC})(s) - V_{FC}(s)}{I_{FC}(s)} = L_1 s + R_{L_1} \tag{4.11}$$

In this case, the plant can be seen as a system of first order. it could be expressed by

$$G_1(s) = \frac{K_{pta1}}{\tau_1 s + 1} \tag{4.12}$$

Transfer Function of Inner Loop Current FC

Figure 4.6 shows a representation of the closed loop current, the controller $C_1(s)$ used for this control is a proporcional-integral PI, $K_{ADC\_I_{FC}}$ represents the gain of the current reading to do analog to digital conversion, this number value is compared with the current I_{FC^*}.

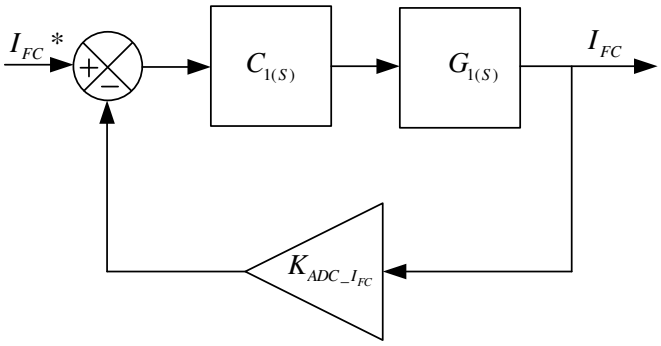

Figure 4.6: Representation of the current loop.

Considering the controller

$$C_1(s) = \frac{K_{P\_I_{FC}} \cdot s + K_{i\_I_{FC}}}{s} \tag{4.13}$$

the transfer function of inner current loop I_{FC} can be obtained, as

$$T_1(s) = \frac{C_1(s) \cdot G_1(s)}{1 + K_{ADC\_I_{FC}} \cdot C_1(s) \cdot G_1(s)} \tag{4.14}$$

Table 4.1: Parameters for the inner control loop of the current FC.

Description	Symbol	Value
Inductance	L_1	1 mH
Resistance	R_{L_1}	0.5 Ω
Output voltage V_0	V_0	50 V
The ADC gain	$K_{ADC\_I_{FC}}$	3.2×10^{-6} [-]
The plant time constant	$\tau_1 = \frac{L_1}{R_{L_1}}$	2×10^{-3} s
Gain from the open loop tranfer function	$Kpta_1 = \frac{V_0}{R_{L_1}}$	100 [-]

Substituting Equations (4.11) and (4.13) in Equation (4.14)

$$T_1(s) = \frac{\frac{Kpta_1 \cdot K_{P\_I_{FC}}}{\tau_1} \cdot s + \frac{Kpta_1 \cdot K_{i\_I_{FC}}}{\tau_1}}{s^2 + \frac{K_{ADC\_I_{FC}} \cdot Kpta_1 \cdot K_{P\_I_{FC}+1}}{\tau_1} + \frac{K_{ADC\_I_{FC}} \cdot Kpta_1 \cdot K_{i\_I_{FC}}}{\tau_1}} \tag{4.15}$$

Transfer Function of Outer Loop Voltage SC

Using the controller;

$$C_2(s) = \frac{K_{P\_V_{SC}} \cdot s + K_{i\_V_{SC}}}{s} \tag{4.16}$$

Considering the inner current loop Equation (4.14) and using the PI controller Equation (4.16), it is possible to find the representation of the transfer function of outer loop voltage SC in Equation (4.17).

$$T_2(s) = \frac{C_2(s) \cdot T_1(s)}{1 + K_{ADC\_V_{SC}} \cdot C_2(s) \cdot T_1(s)} \tag{4.17}$$

4.2.3 Transfer funtions of the SC converter

Figure 4.7 represents the equivalent circuit of half-bridge bidirectional converter. This representation would help facilitate the analysis and find the transfer function of the plant.

Applying Kirchhoff law of voltage to equivalent circuit SC converter, it has been obtained the following Equation:

$$V_{CD}(t) = L_2 \frac{dI_{SC}}{dt} + R_{L_2} \cdot I_{SC}(t) + V_{SC}(t) \tag{4.18}$$

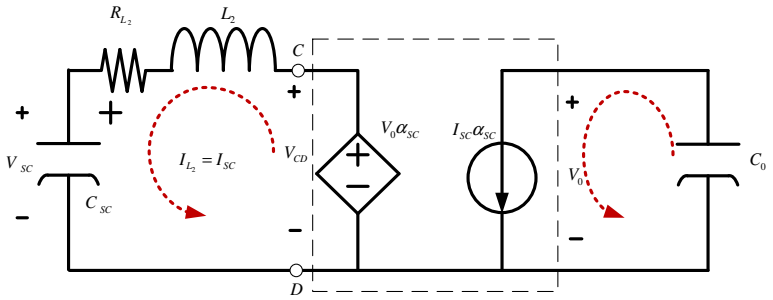

Figure 4.7: Simplified model of the SC converter.

Replacing $V_{CD}(t)$ in Equation 4.18 and manipulating it is given:

$$V_0\alpha_{SC}(t) - V_{SC}(t) = L_2\frac{dI_{SC}}{dt} + R_{L_2}\cdot I_{SC}(t) \tag{4.19}$$

In this sense, the Equation of the system, in the Laplace domain, is shown below:

$$V_0\alpha_{SC}(s) - V_{SC}(s) = I_{SC}(s)\cdot(L_2 s + R_{L_2}) \tag{4.20}$$

Manipulating the Equation (4.20), it has been obtained the transfer function of the plant, using the following expression (4.21):

$$G_2(s) = \frac{V_0\alpha_{SC}(s) - V_{SC}(s)}{I_{SC}(s)} = L_2 s + R_{L_2} \tag{4.21}$$

The plant can be seen as a system of first order. It could be expressed by

$$G_2(s) = \frac{K_{pta2}}{\tau_2\cdot s + 1} \tag{4.22}$$

Transfer Function of Inner Loop Current SC

Figure 4.8 shows a representation of the closed loop current, the controller $C_3(s)$ used for this control is a proportional-integral PI, $K_{ADC\_I_{SC}}$ represents the gain of the current reading to analog to digital conversion, this number value is compared with the current I_{SC^*}.
Considering the controller C_3,

$$C_3(s) = \frac{K_{P\_I_{SC}}\cdot s + K_{i\_I_{SC}}}{s} \tag{4.23}$$

the transfer function of inner current loop I_{FC} can be obtained,

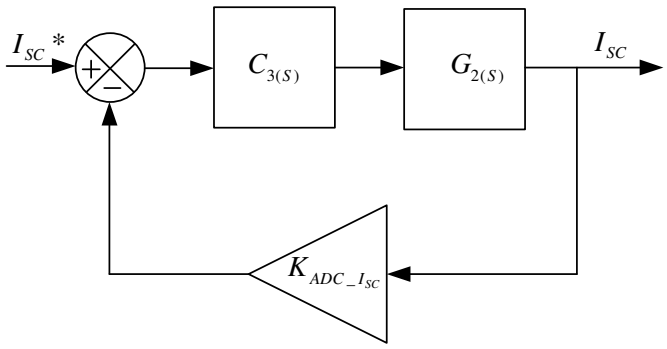

Figure 4.8: Representation of the current loop.

Table 4.2: Parameters for the inner control loop of the current SC.

Description	Symbol	Value
Inductance	L_2	3.4 mH
Resistance	R_{L_2}	0.8 Ω
Output voltage V_0	V_0	50 V
The ADC gain	$K_{ADC\_I_{SC}}$	1.5×10^{-6} [-]
The plant time constant	$\tau_2 = \frac{L_2}{R_{L_2}}$	4.25×10^{-3} s
Gain from the open loop tranfer function	$Kpta_1 = \frac{V_0}{R_{L_2}}$	62.5 [-]
Bus capacity	C_0	1000×10^{-6} F
Mini charge cycle	α_{SC}	0.1 [-]

$$T_3(s) = \frac{C_3(s) \cdot G_2(s)}{1 + K_{ADC\_I_{SC}} \cdot C_3(s) \cdot G_2(s)} \tag{4.24}$$

substituting (4.21) and (4.23) in Equation 4.24, it is given:

$$T_3(s) = \frac{\frac{Kpta_2 \cdot K_{P\_I_{SC}}}{\tau_2} \cdot s + \frac{Kpta_2 \cdot K_{i\_I_{SC}}}{\tau_2}}{s^2 + \frac{K_{ADC\_I_{SC}} \cdot Kpta_2 \cdot K_{P\_I_{SC}+1}}{\tau_2} + \frac{K_{ADC\_I_{SC}} \cdot Kpta_2 \cdot K_{i\_I_{SC}}}{\tau_2}} \tag{4.25}$$

Transfer Function of Outer Loop Voltage V_0

Observing the figure **??**, the DC bus voltage is related to the current of the SC according to the following expressions:

$$I_{bus}(t) = I_{SC}(t)\alpha_{sc} \tag{4.26}$$

$$I_{bus}(t) = C_{SC}\frac{dV_0}{dt} \tag{4.27}$$

Resolving Equationklolijj is obtained the follow expression

$$G_3 = \frac{V_0(s)}{I_{SC}(s)} = \frac{\alpha_{SC}}{C_{SC} \cdot s} \tag{4.28}$$

The controller to be used is expressed in the following Equation:

$$C_4(s) = \frac{Kp_{\_V_0} \cdot s + Ki_{\_V_0}}{s} \tag{4.29}$$

$$T_4(s) = \frac{C_4(s) \cdot G_3(s)}{1 + K_{ADC\_V_0} \cdot C_4(s) \cdot G_3(s)} \tag{4.30}$$

4.3 Pole assignment method for the power conditioner FC/SC

There are several methods to tune a PI controller. One method is an assignment of this method consisting in imposing poles to the system by means of conjugate complex and a negative real part with angle of 45 degrees each one of them on the real axis.

4.3.1 Coefficients values of the FC converter

Considering the I_{FC} transfer function in Equations (4.31) and (4.32), two poles are imposed as in the following expression:

$$P_1 = -\frac{K_1}{\tau_1} + j \cdot \frac{K_1}{\tau_1} \tag{4.31}$$

$$P_2 = -\frac{K_1}{\tau_1} - j \cdot \frac{K_1}{\tau_1} \tag{4.32}$$

which leads to

$$K_{P\_I_{FC}} = \frac{2 \cdot K_1 - 1}{K_{ADC\_I_{FC}} \cdot Kpta1} \tag{4.33}$$

$$K_{i\_I_{FC}} = 2 \cdot \frac{K_1^2}{\tau_1 \cdot K_{ADC\_I_{FC}} \cdot Kpta1} \tag{4.34}$$

According to the values in Table 4.1, coefficients of gain in FC are shown in Table 4.3. The condition to guarantee a stable control system is getting the inner loop of I_{FC}, which will be faster than the outer loop V_{SC}.

Table 4.3: Gain values for the inner loop current of the FC converter.

$K_{P\_I_{FC}}$	$K_{i\_I_{FC}}$
$9.5 * 10^{-8}$	0.0005

Once obtained the values of the coefficients of the inner current loop of the FC converter, it is possible to find the values of the coefficients of the outer loop with iterative methods, assigning values to verify that the control system will reach the value of its consign, under this fact the values obtained from $K_{P\_V_{SC}}$ and $K_{i\_V_{SC}}$.

Table 4.4: Gain values for outer loop of the FC converter.

$K_{P\_V_{SC}}$	$K_{i\_V_{SC}}$
150	0.00001

4.3.2 Coefficients values of the SC converter

Considering the I_{SC} transfer function in Equation (4.25) two poles are imposed as in the following expression:

$$P_3 = -\frac{K_2}{\tau_2} + j \cdot \frac{K_2}{\tau_2} \tag{4.35}$$

$$P_4 = -\frac{K_2}{\tau_2} - j \cdot \frac{K_2}{\tau_2} \tag{4.36}$$

Operating the above Equations have been obtained the Equations (4.37) and (4.38):

$$Kp\_I_{SC} = \frac{2 \cdot K_2 - 1}{K_{ADC\_I_{SC}} \cdot Kpta2} \tag{4.37}$$

$$Ki\_I_{SC} = 2 \cdot \frac{K_2^2}{\tau_2 \cdot K_{ADC\_I_{SC}} \cdot Kpta2} \tag{4.38}$$

The controller gains are found in Table 4.5. The condition to guarantee a stable control system, is getting the inner loop of I_{SC} which will be faster than the outer loop V_0.

Table 4.5: Gain values for inner loop of the SC converter.

$K_{P\_I_{SC}}$	$K_{i\_I_{SC}}$
$3.8 * 10^{-9}$	$2 * 10^{-5}$

Once obtained the values of the coefficients of the inner current loop of the SC converter, it is possible to find the values of the coefficients of the outer loop with iterative methods considering that the external loop controller should be faster than the inner current loop. Under this fact the values obtained from $K_{P\_V_0}$ and $K_{i\_V_0}$ are shown in Table 4.6.

Table 4.6: Gain values for outer loop of the SC converter.

$K_{P\_V_0}$	$K_{i\_V_0}$
200	0.0005

4.3.3 Bode FC and SC converters

Bode FC converter

Plotting the bode of closed loop through the Equation (4.17), it has seen in Figure 4.9, it appears that there is a phase margin of 93 degrees to zero crossing of magnitude. Therefore there is a good phase margin to assure the system stability.

Bode SC converter

Plotting the bode of gain loop through Equation (4.30), it has seen in Figure 4.10, it appears that there is a phase margin of 79 degrees to zero crossing of magnitude.
It is possible to see in the Figure 4.10, high gain in low frequency, wide bandwidth, and a good margin of phase, desirable in half-bridge converter to assure the system stability.

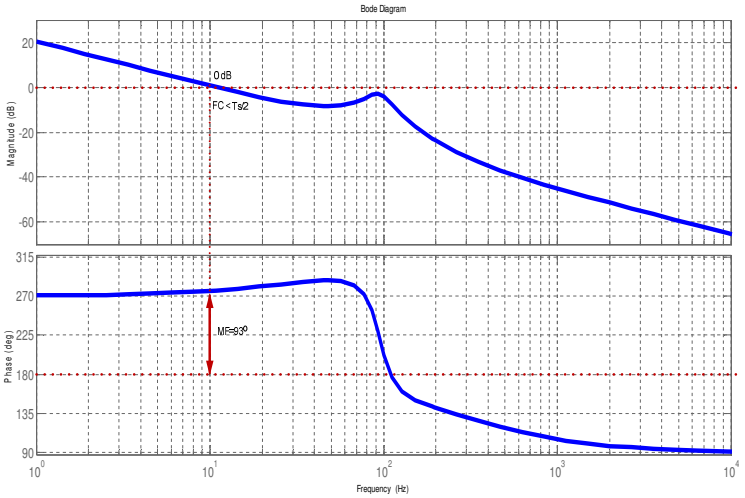

Figure 4.9: Bode response to FC converter

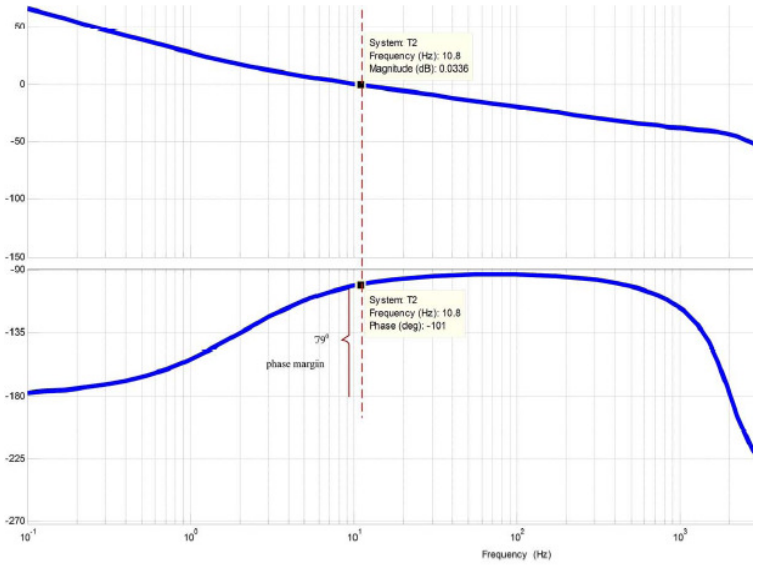

Figure 4.10: Bode response to SC converter.

4.4 Conclusions

It has been proposed a scheme of control, which allows to operate the power conditioner with FC/SC as a source of energy. The main function of this control structure is to regulate I_{FC}, I_{SC} currents as well as the voltages V_0 and V_{SC} respectively. The method used in this thesis corresponds to an assignment of poles to obtain the coefficients of the inner controllers in this case PI_I_{FC} and PI_I_{SC}, the outer controllers have been found by heuristic methods of adjustment and error through the observation of the temporal response of the system to certain slogans PI_V_{SC} and PI_V_O.

Chapter 5

Simulation

5.1 Simulation

In this section the proposed control to operate a hybrid converter has been simulated in MATLAB-Simulink with the objective to study their response in a closed loop. The specifications of the converters are shown in Table 5.1 and 5.2.

Table 5.1: Specifications to operate the FC converter.

FC converter	
$V_{FC} = 33 - 26\ V$	$\Delta I_{L_1} = 0.8\ A$
$L_1 = 1\ mH$	$f_s = 20\ kHz$
$V_{SC}* = 25\ V$	$P_0 = 500\ W$

Table 5.2: Specifications to operate the SC converter.

SC converter	
$V_{SC} = 30\ V$	$L_2 = 3.4\ mH$
$V_0* = 80\ V$	$\Delta I_{L_1} = 0.2\ A$
$P_0 = 500\ W$	$f_s = 20\ kHz$

Below are presented the cases to analyse:

Case 1.- **Test with variable load and SC fully charged.** The SC was fully charged at 30 V, with graphs obtained from variable voltage, current and power energy.
Case 2.- **Test with variable load and SC fully discharged.**
Case 3.- **Test with cut off FC energy and SC fully charged.** In this section, the hybrid system had a constant load, which was made with a cut

off power by the FC, in order to observe the response from the back-up system.

5.1.1 Test with variable load and SC fully charged

For this test it has been considered that the SC was fully charged at 30 V. The graphs obtained from voltage, current and power for this test are shown in Figures 5.1 and 5.2.

Voltage waveforms

Figure 5.1 shows the V_0 regulation where the value is 50 V. This value remains constant with changes in load power. It can also be seen that the value V_{SC} remains constant. Some changes are observed in V_{FC} synchronized with changes in load power.

Current waveforms

Figure 5.1 also shows the evolution of I_{FC}, I_{SC} and I_0 load. It can be seen that I_{SC} helps I_{FC} because intrinsically the dynamic response of FC is slow and therefore, requires an auxiliary device to help delivering the energy required in the load with a rapid response.

Power waveforms

Figure 5.2 shows the evolution of the power, starting with the fuel cell, the supercapacitor and the load. It can be seen that with these variations in the load power, the backup system is able to help the fuel cell when there are load variations. Also, the structure of the hybrid converter is capable of recharging the supercapacitor when the power demand is lower than the previous one.

Efficiency waveforms

The efficiency of the fuel cell is directly related to the energy demanded by the load, so when there is less power demand, it is more greater efficiency from the fuel cell and when there is higher energy demand in the load there is less efficiency as shown in Figure 5.2.

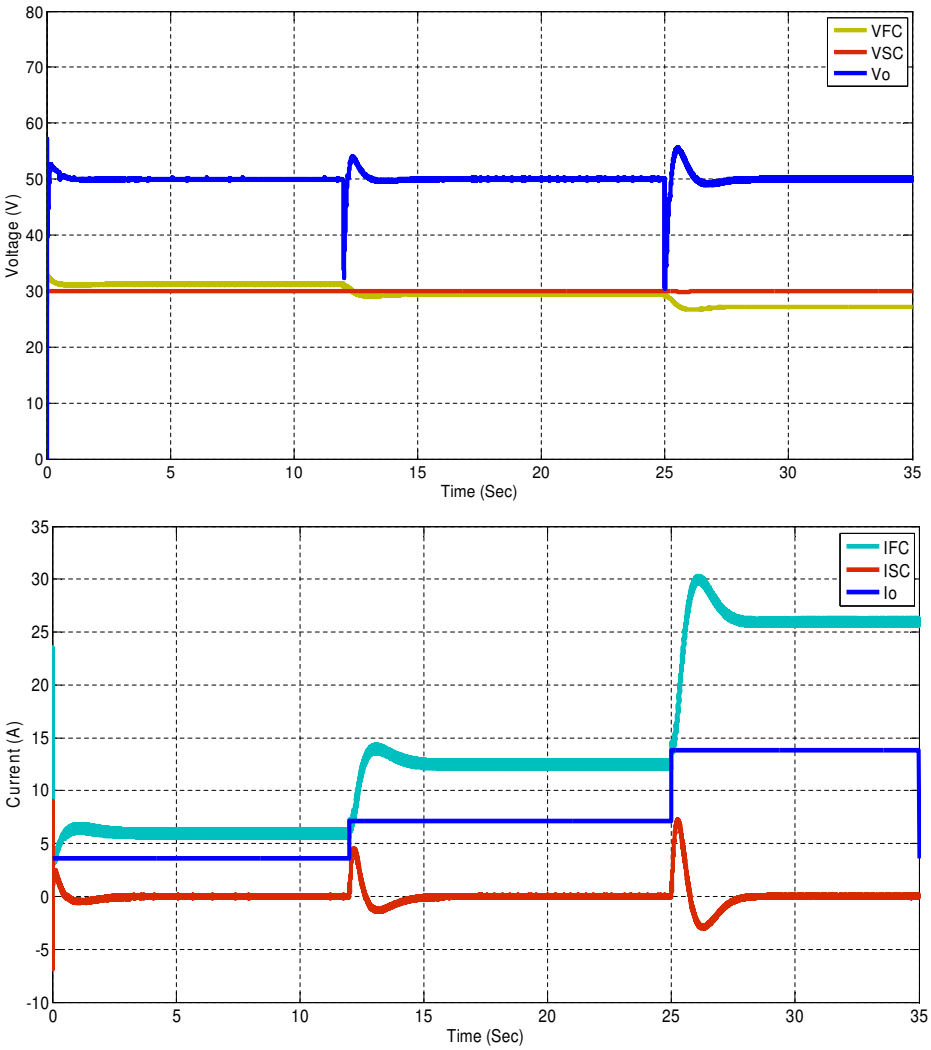

Figure 5.1: Voltage and current measurements case 1.

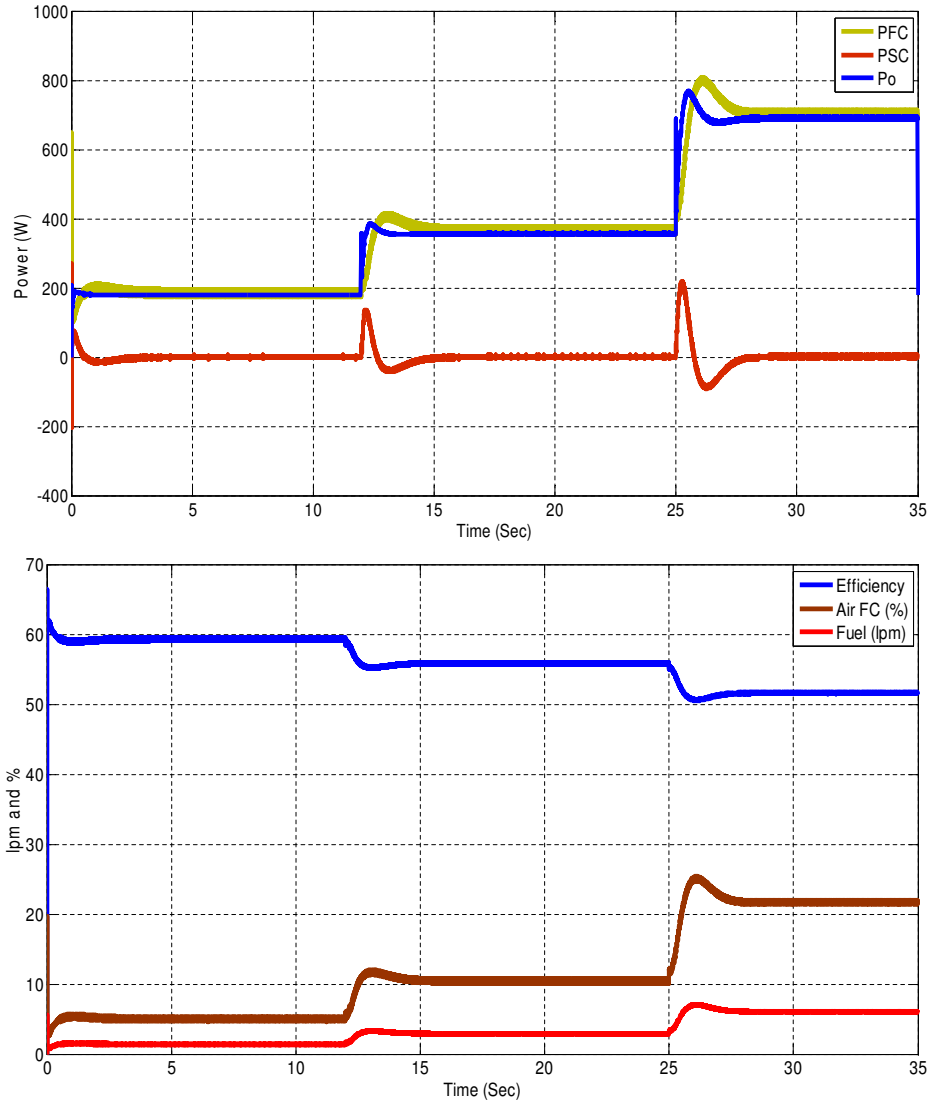

Figure 5.2: Power and efficiency measurements case 1.

5.1.2 Test with variable load and SC fully discharged

Supercapacitor voltage waveforms

In Figure 5.3, it is possible to see the evolution of the V_{SC}, since its initial state is fully discharged (simulation time of 0 seconds). Afterwards this will be recharged up to a value of 30 V (on the interval of 0 to 420 s. Once the supercapacitor is recharged, it has been proposed a change of load with positive and negative current in order to appreciate the behavior of V_{SC}. It is possible to see that, when a change is made with negative current, V_{SC} increases its value which is limited by the maximum value of saturation and when you make a positive change in current, the V_{SC} decreases to the minimum limit value imposed by the system control.

Supercapacitor current waveforms

Figure 5.3 shows the evolution of current in the supecondensador I_{SC}. It has been proposed a quick recharge of the SC which is limited by the current to 55 A in the recharge, This Figure also shows the recharge current. In this case, a simulation interval from 0 to 420 s, it can also appreciate the change of current transitions in the supercapacitor due to the proposed changes in the load.

Output voltage waveforms

Figure 5.4 shows how the control is able to maintain the 80 V in the V_0 with different changes in the load either positive or negative.

Output current waveforms

In Figure 5.4, it can appreciate current values both positive and negative for case 2.

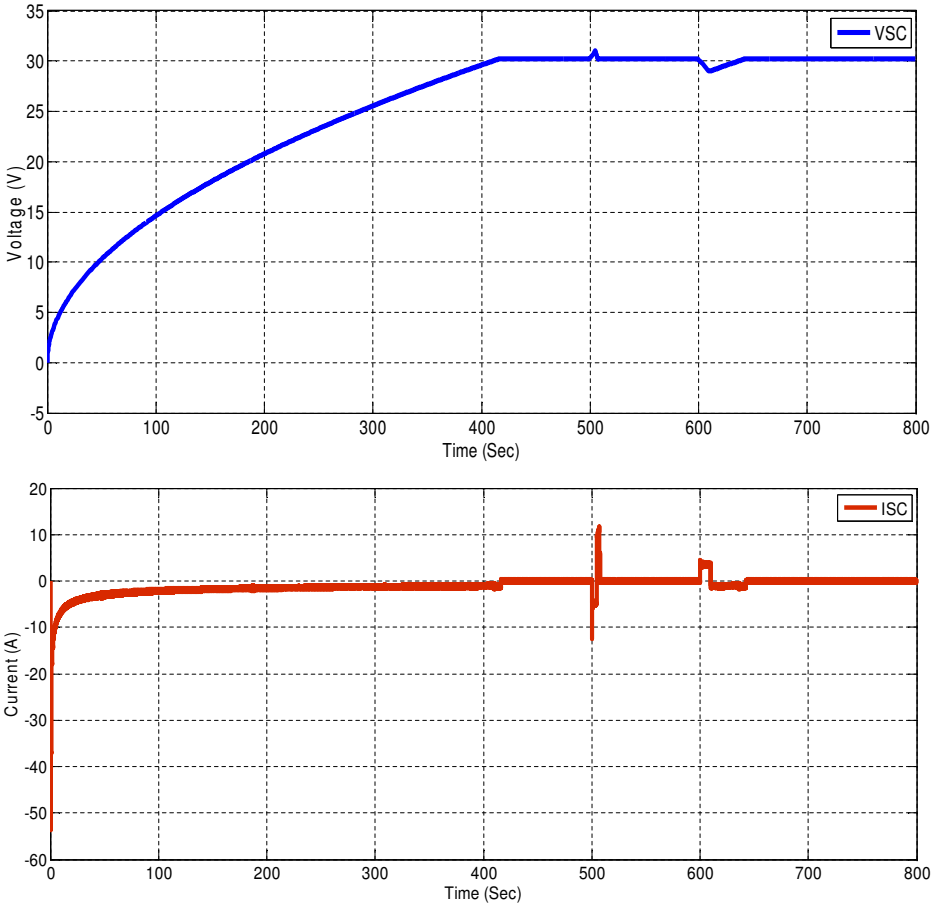

Figure 5.3: V_{SC} and I_{SC} measurements case 2.

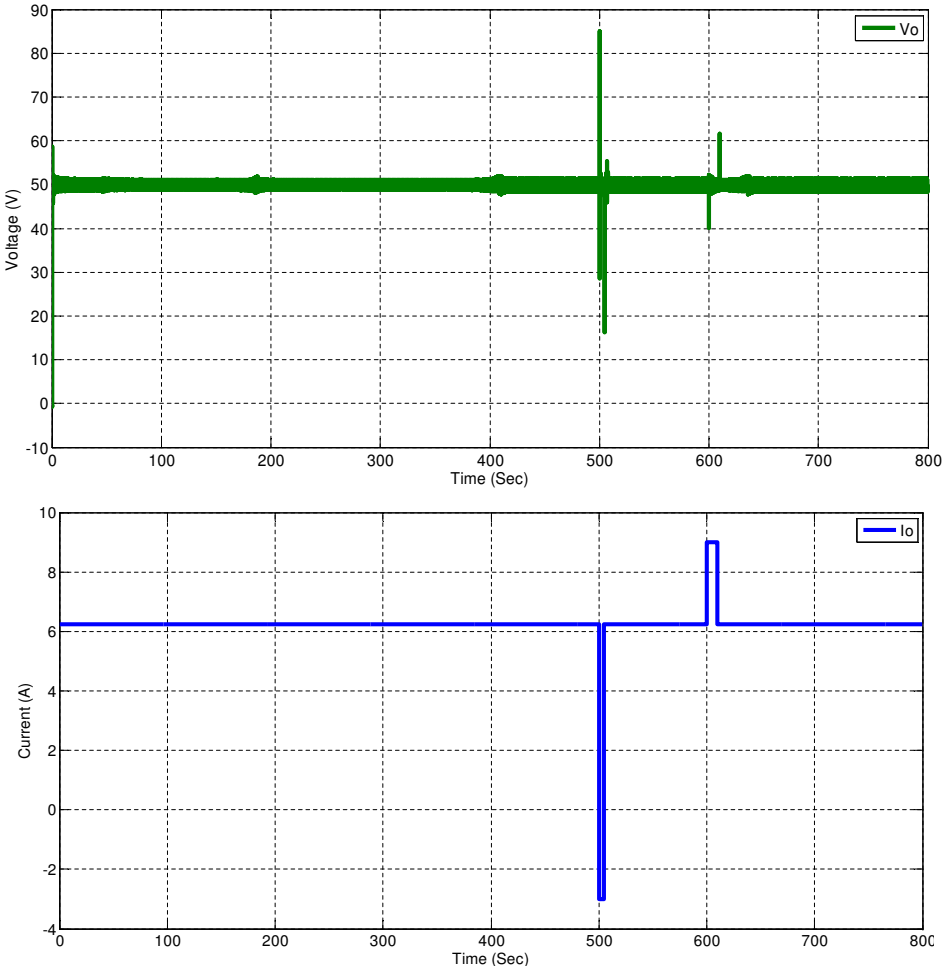

Figure 5.4: V_0 and I_0 measurements case 2.

Output Power Waveforms

On the top part of Figure 5.5 it is possible to see a power consign of 300 W load to recharge SC. After this, changes of power consign both positive and negative.

Supercapacitor power waveforms

At the bottom of Figure 5.5 it can be observed a negative power in the interval from 0 to 420 s due to the time of recharge of the SC. Afterwards it is observed a power of 0 W when the P_{SC} helps FC with a change of load. This happens when a positive change of load in P_0 is executed and when a negative power in P_0 is executed too, therefore energy is stored in the SC.

Fuel cell power waveform

Figure 5.6 shows the evolution of the P_{FC}, in the time interval from 0 to 420 s. In this interval, FC provides all the power to the system, because it is supplying as much load power as it is being demanded. After the 420 s of simulation, the SC is ready to help FC with changes that may exist in the load.

Fuel cell current waveform

The response shown in Figure 5.5 is very similar to the P_{FC} because I_{SC} helps existing I_{FC} to any change in load.

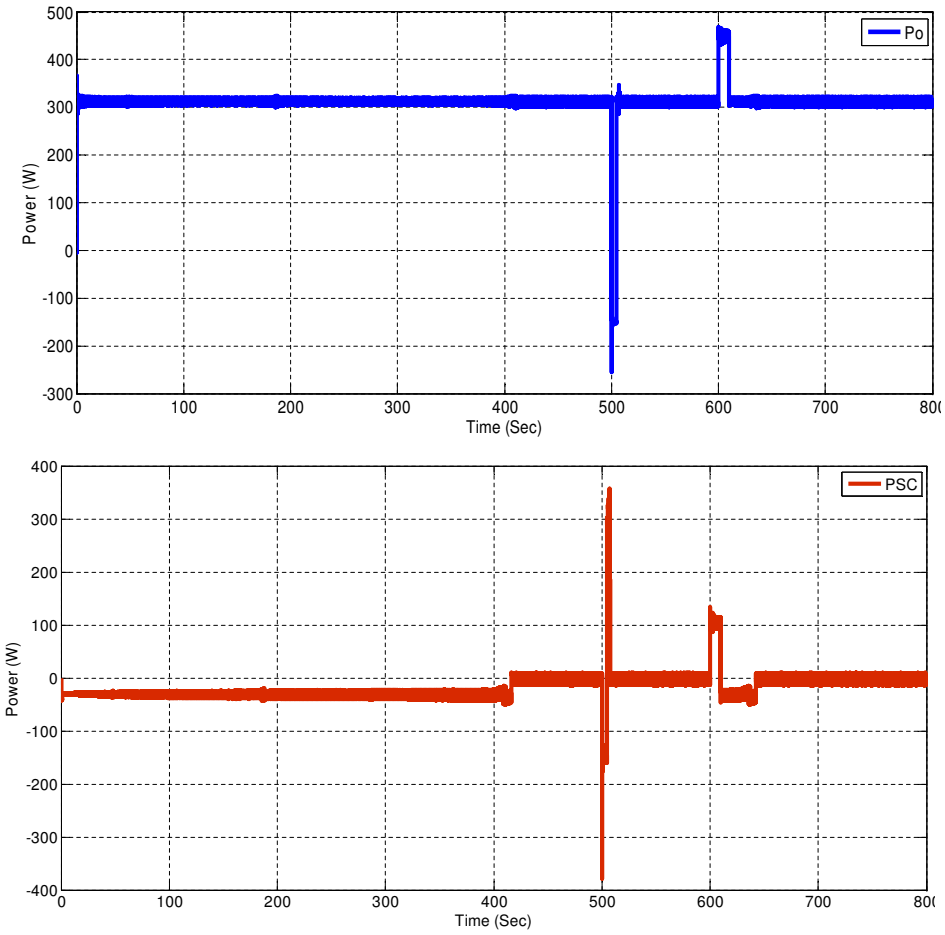

Figure 5.5: P_0 and P_{SC} measurements case 2.

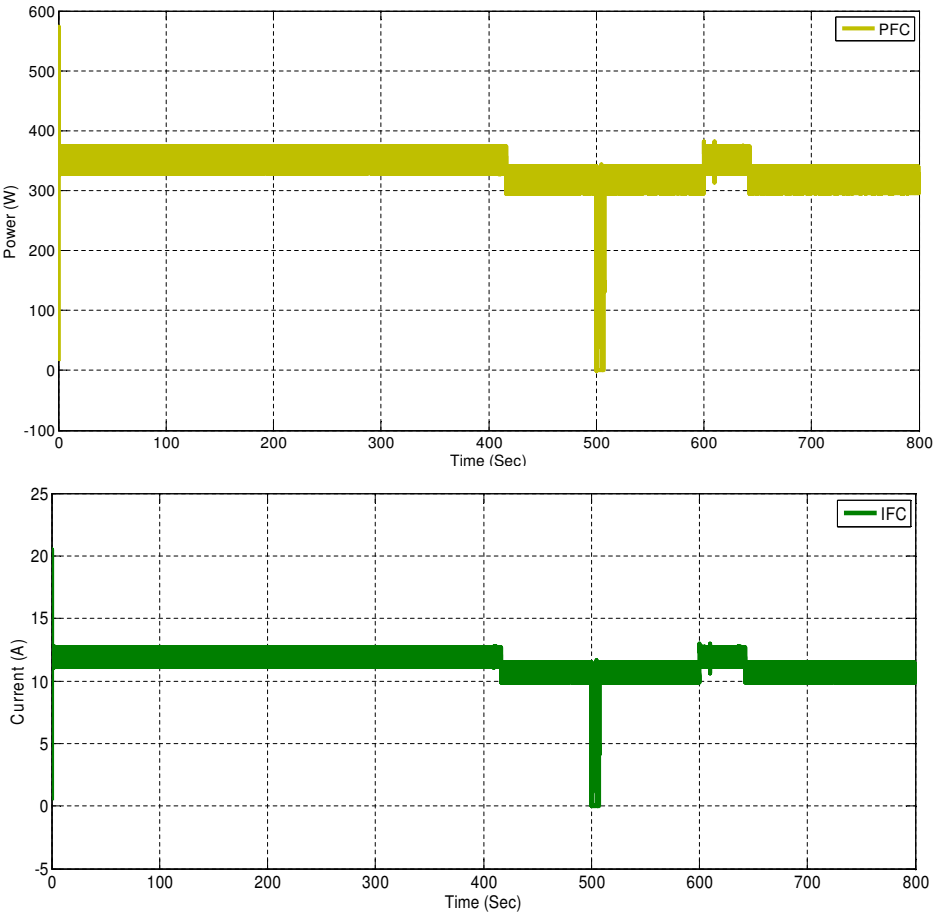

Figure 5.6: P_{FC} and I_{FC} measurements case 2.

5.1.3 Test with cut off FC energy

In this section, the hybrid system has a constant load, which has been made with a cut off power by the FC, in order to observe the response from the backup system.

Voltage waveforms

Figure 5.7 shows the time evolution of voltages V_{FC}, V_{SC} and V_0 load. A variation of V_0 load caused by the cut off of the FC may be seen in the simulation at the time of 1 s. However, the system is able to keep V_0 constant, while V_{SC} is transferring its power to the load.

Current waveforms

In Figure 5.7 it is shown the evolution of I_{FC}, I_{SC} and I_O load. In the interval from 0 to 1 second of simulation it can be seen that $I_{SC} = 0$, because in this interval I_{FC} FC is the only supply. When the cut off of the FC occurs $I_{FC} = 0$, and I_{SC} SC supplies all the power demanded by the load, while compensates the energy of the FC.

On the other hand I_0 Load stays always constant, therefore the good performance of the system of control is verified.

Power waveforms

Figure 5.8, shows the time evolution of P_{FC}, P_{SC} and P_0. A cut off of the FC is shown after 1 s of simulation. After this, the backup system is responsible for providing energy demanded by the load. This behavior describes a fast response by the control action which sends an immediate order to the supplies power backup system.

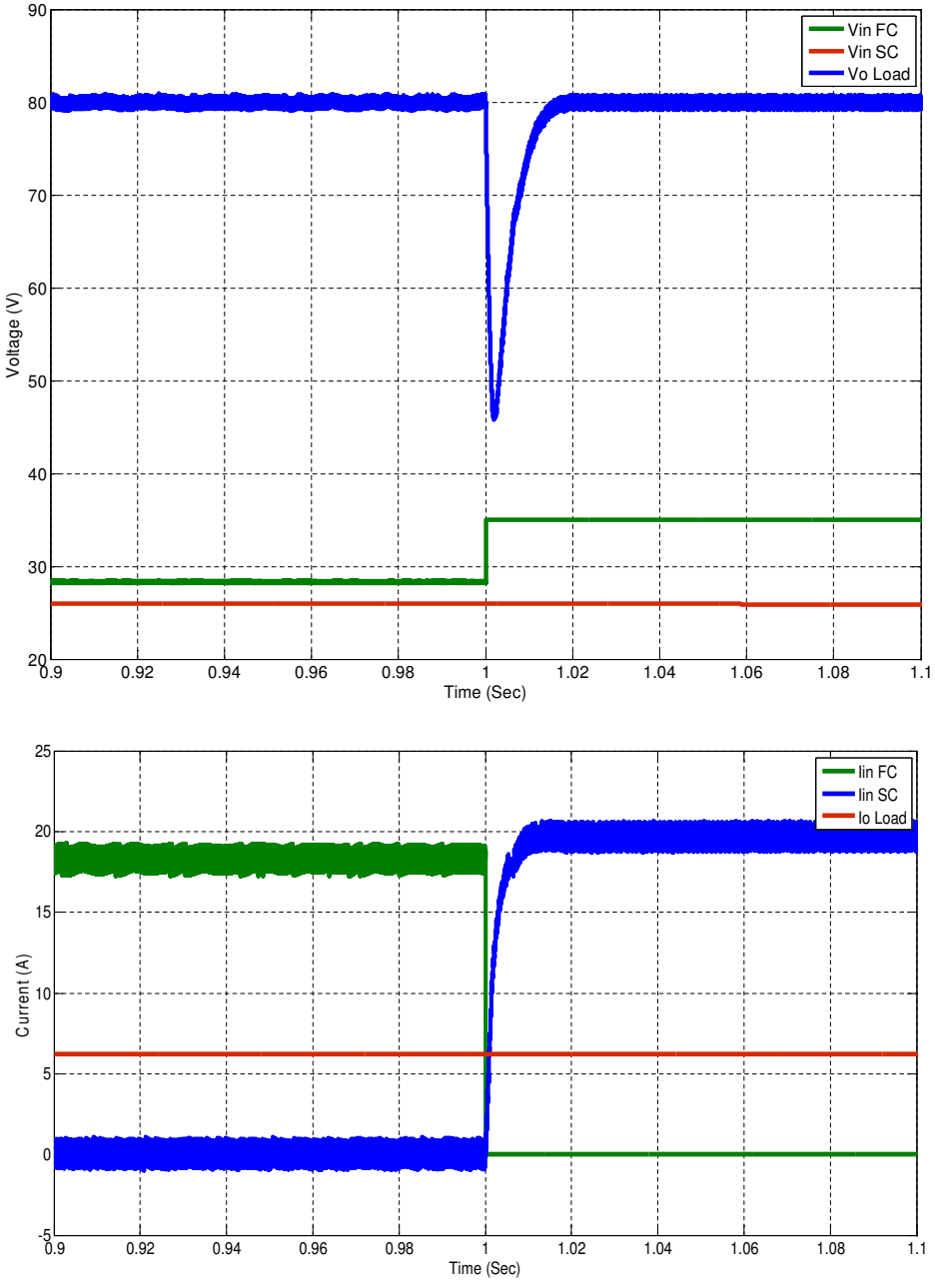

Figure 5.7: Voltage and current measurements case 3.

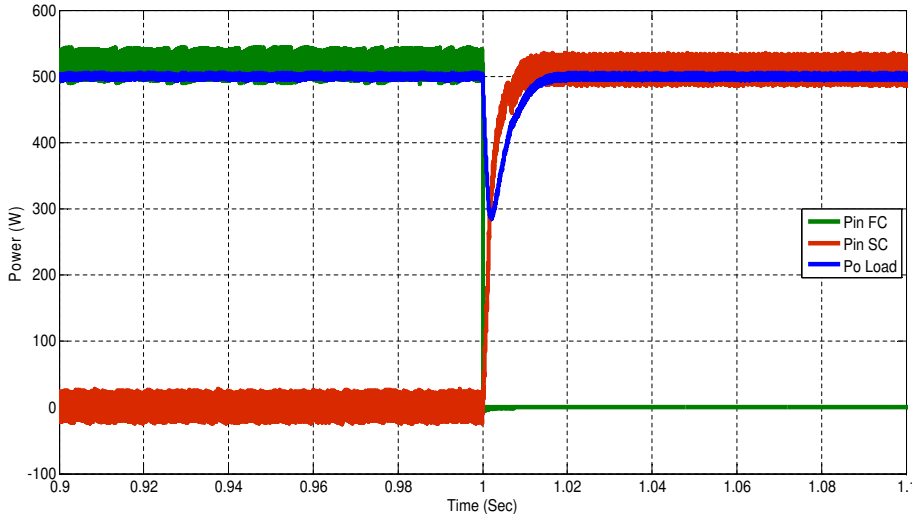

Figure 5.8: Power measurements case 3.

5.2 Conclusions

In this chapter, there is a hybrid converter that includes a primary converter called FC converter and an auxiliary converter called SC converter. The control system operates with four PIs controllers which were implemented in MATLAB-Simulink together with the hybrid converter of the FC/SC. According to the results, the control system gets an excellent performance because it is able to compensate V_0 and V_{SC} with changes of load and energy cut off. In this sense, the proposed control provides a good platform to design a control system suitable for power converter systems for FC/SC applications.

Chapter 6

Experimental validation

6.1 Electrical diagram of an hybrid converter to operate FC/SC

Figure 6.1 shows the proposed power conditioner and the proposed structure of control of the FC converter whose function is to control the SC voltage (V_{SC}) and the FC current through Proportional Integral (PI) controllers connected in cascade, PI_V_{SC} and PI_I_{FC}. The structure of control for the half-bridge converter has the function of controlling the V_0, as well as the current of the SC I_{SC} through the cascaded PI controllers PI_V_0 and PI_I_{SC}.

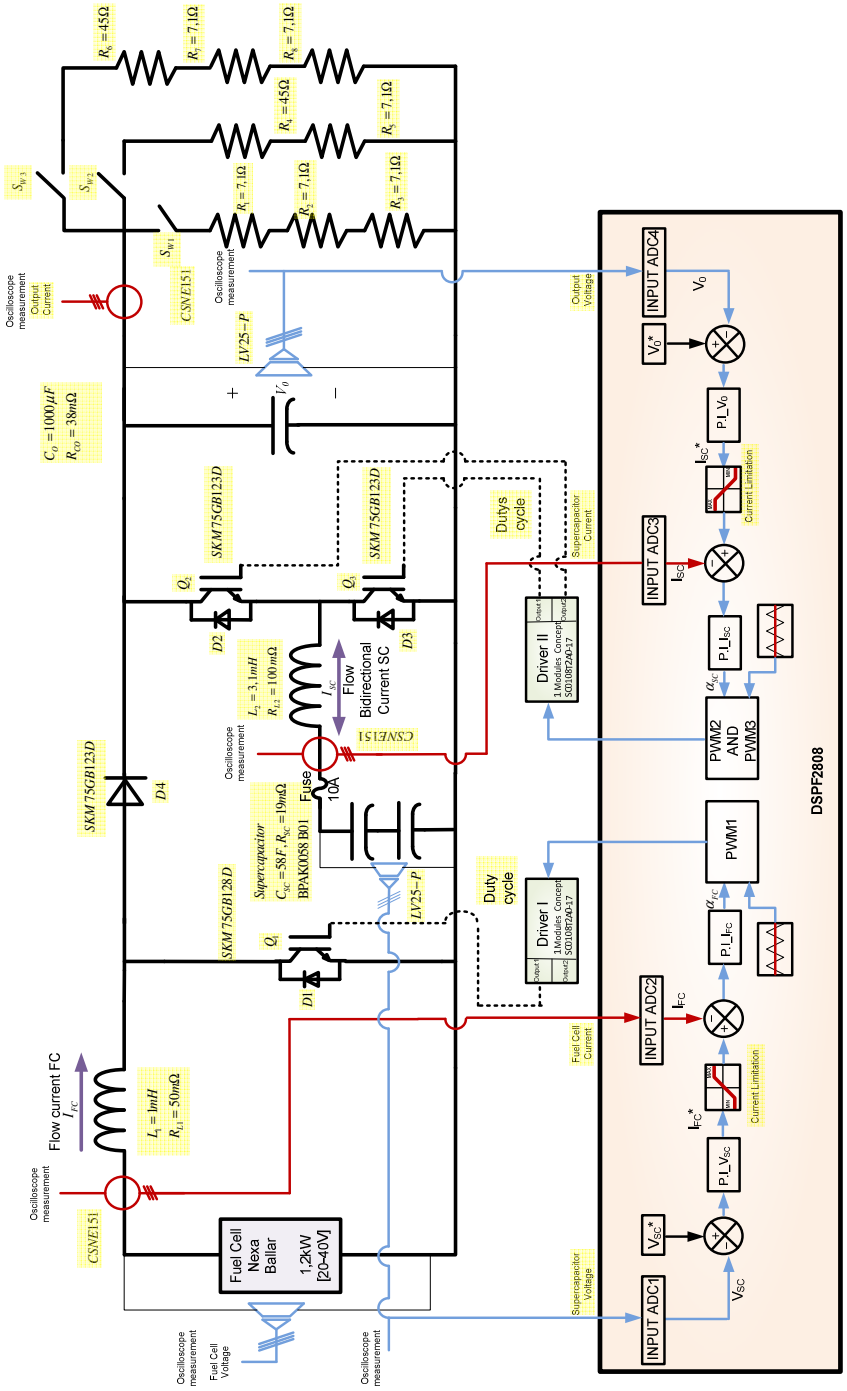

Figure 6.1: Proposed digital controller with DSP2808 for the FC/SC hybrid power source.

6.2 Test bench description

Figure 6.2 shows the connection of the $Nexa^{TM}$ power module, which has been installed in a chemistry lab, where the requirements of the fuel cell itself are very suitable for the operation. The $Nexa^{TM}$ PEMFC system (1.2 kW, 46 A, 26 V) was developed and commercialized by the Ballard Power Systems Inc. The FC provides a suitable supply of hydrogen connecting the fuel supply to the hydrogen connection, as shown in Figure 6.2.

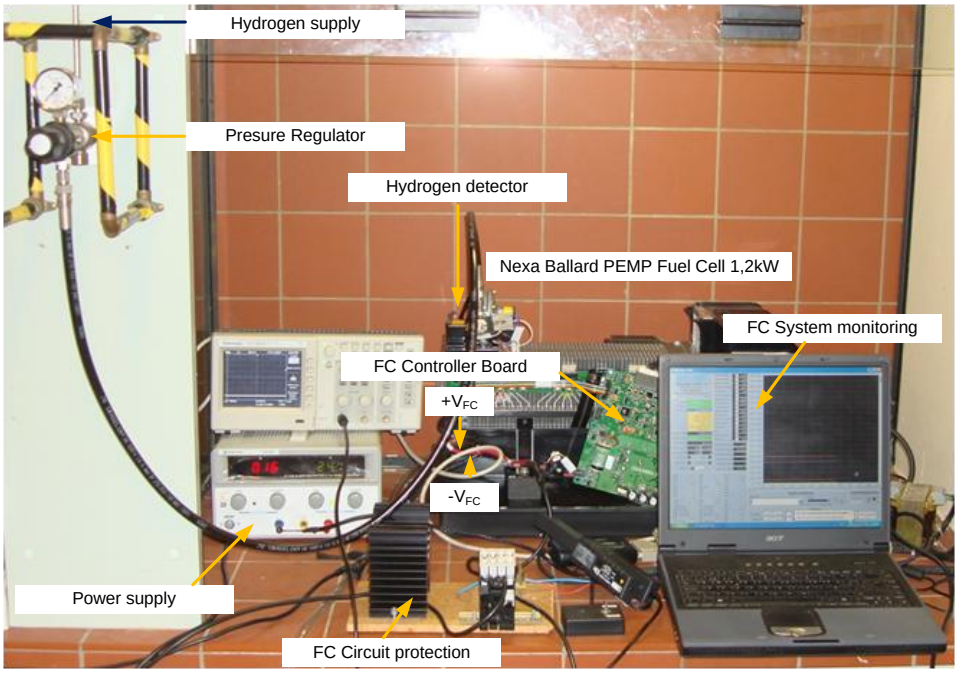

Figure 6.2: Photograph of a PEMFC stack.

FC requires an interface to communicate with the computer. Labview software has been used to monitor the $Nexa^{TM}$ module variables in real time.

FC needs a circuit protection, so therefore it is connected a blocking diode on the positive output terminal of the FC stack. To operate the FC it is necessary to connect a 24 V_{DC} power-supply to the $Nexa^{TM}$ control circuit. The experimental set-up of the hybrid FC/SC power source uses a Nexa BALLARD PEMFC stack as the main source. The auxiliary source

is obtained with a Maxwell SC module associating two modules in series: Maxwell BPAK0058 E015.

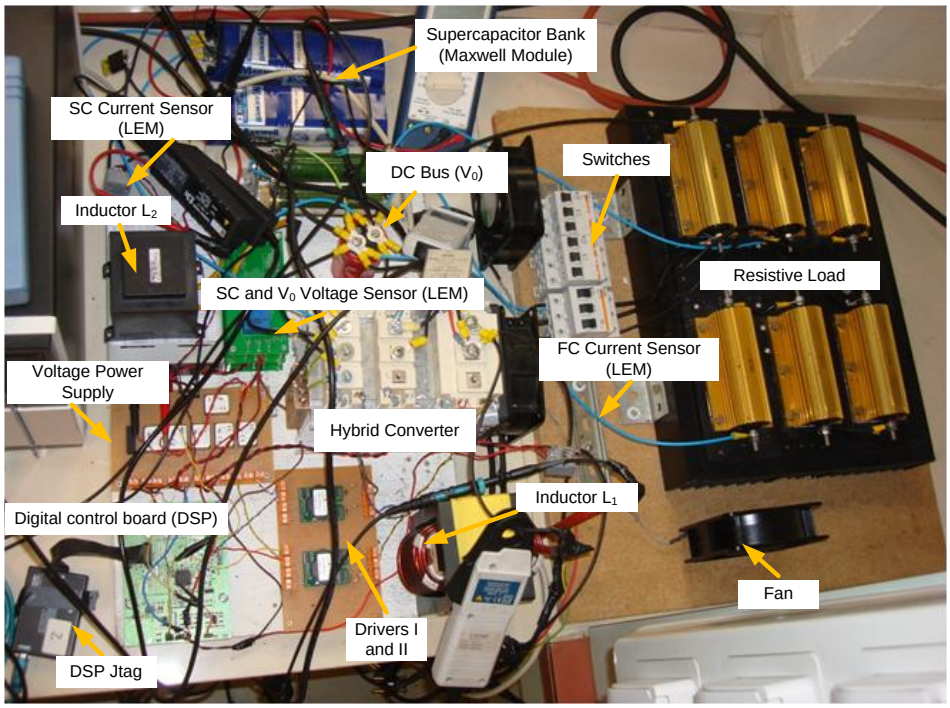

Figure 6.3: Photograph of a Fuel Cell/Supercapacitor converter.

The power converter DC/DC is made with standard IGBT modules SEMITRANS: SKM75GB128D and SKM75GB123D. A real-time Code Composer Estudio is used for programming the DSP 2808 of Texas Instruments to implement the energy management control strategy. The experimental environment is shown in Figure 6.3.

6.3 Test bench parameters

The Nexa BALLARD PEMFC stack has a nominal power of 1.2 kW related to a rated current of $Inom = 46\ A$ and rate output voltage of $Vnom = 26\ V$. Two Maxwell modules in series BPAK0058 E015 with the following characteristics: $C = 29\ F$, $V_{SCMAX} = 30\ V$,$V_{SCMIN} = 15\ V$, $I_{SC-PEAK-MAX} =$

Table 6.1: Resistive load combinations.

S_{W_1}	S_{W_2}	S_{W_3}	Power (P_0)
0	0	1	42.3 W
0	1	0	47.98 W
0	1	1	90 W
1	0	0	117.3 W
1	0	1	160.25 W
1	1	0	165.56 W
1	1	1	208.3 W

1500 A, $ES_{RSC} = 38\ m\Omega$ are connected. FC inductor has a value of 1 mH and SC inductor has a value of 3.4 mH. The bus capacitor has 1000 μF value connected in parallel with and DC link $V_0 = 50\ V$ for both sources. The modules of the drives used for switching the semiconductors ($IGBTs$) of FC and SC converters are two module concepts SC0108T2A0-17. The switching frequency of the Pulse-Width Modulation (PWM) for IGBTs of FC converter and SC converter are selected at 20 kHz.

6.4 Results

6.4.1 Experimental results

Table 6.1 shows load values for different combinations of demand power which the hybrid converter shall submit in its operation in closed loop for the following proposed tests.

Below is listed the cases to analyze:

Case 1.- It consists in observing the preload of the SC. Initially, the SC is completely discharged. The load power used for this test corresponds to 165.56 W.

Case 2.- This test is deemed to have preload SC. This test consists in making changes of load through S_{W_1}, S_{W_2} and S_{W_3} see Table (6.1).

Case 3.- Consists in making a step changes in the load based on load power of 42.3 W to 165 W and vice-versa.

Case 4.- This case involves subjecting the system to a higher load (208.3) W to the limit to which it has been set $I_{FC}*$.

Case 5.- It is caused a cut off energy in the FC.

Case 6.- Load changes are made between 42.3 W and 160 W in different intervals of time so the resulting load presents an oscillating component.

Case 7.- Consists of making changes in the slogan V_0*, operating the system with a resistive load of 42.1 W.

6.4.2 Case 1

In Figure 6.4, it can be observed a preload of the voltage of the SC from t_0 to t_1 with a time of 6.20 minutes starting from 0 V to 25 V, where 25 V is the reference proposed for the SC $V_{SC}*$.

In this Figure it can also be observed that during the interval of time from t_0 to t_1, V_0 is kept constant at the reference value of 50 V. Figure 6.4 shows the I_{FC} at the interval t_0 to its maximum value. Due to the demand of load power ($165.56W$) and the action of preload of the SC, the $I_{FC}*$ has been limited to its maximum value of 8 A. Figure 6.4 also shows a negative current flowing in the SC for its preload. After t_1, the $I_{SC} = 0$, as the SC is fully charged.

6.4.3 Case 2

Figure 6.5 shows that with the changes in load, V_0 does not present abrupt changes and it is kept at 50 V due to the rapid response of the action of the closed-loop control.

Similarly, V_{FC} is maintained with minimal variations and small oscillations while maintaining a voltage of 25 V. The V_{FC} is maintained with a voltage of 40 V. In Figure 6.5 it is possible to appreciate changes in I_0 0.85 to 1.8 A to 2.34 A and 3.3 A so the I_{SC} helps I_{FC} delivering energy demand to the load.

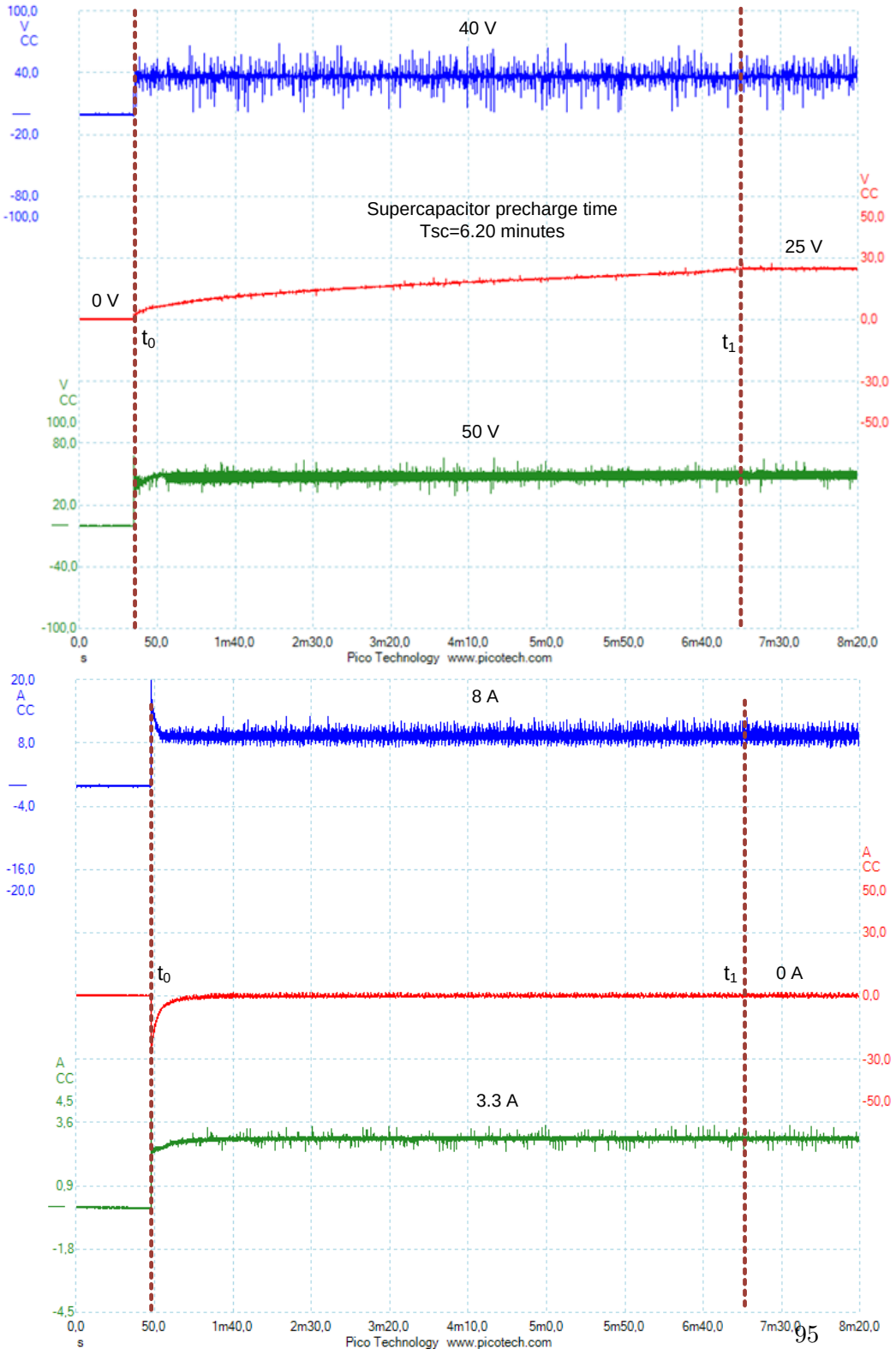

Figure 6.4: Voltage and current waveforms case 1.

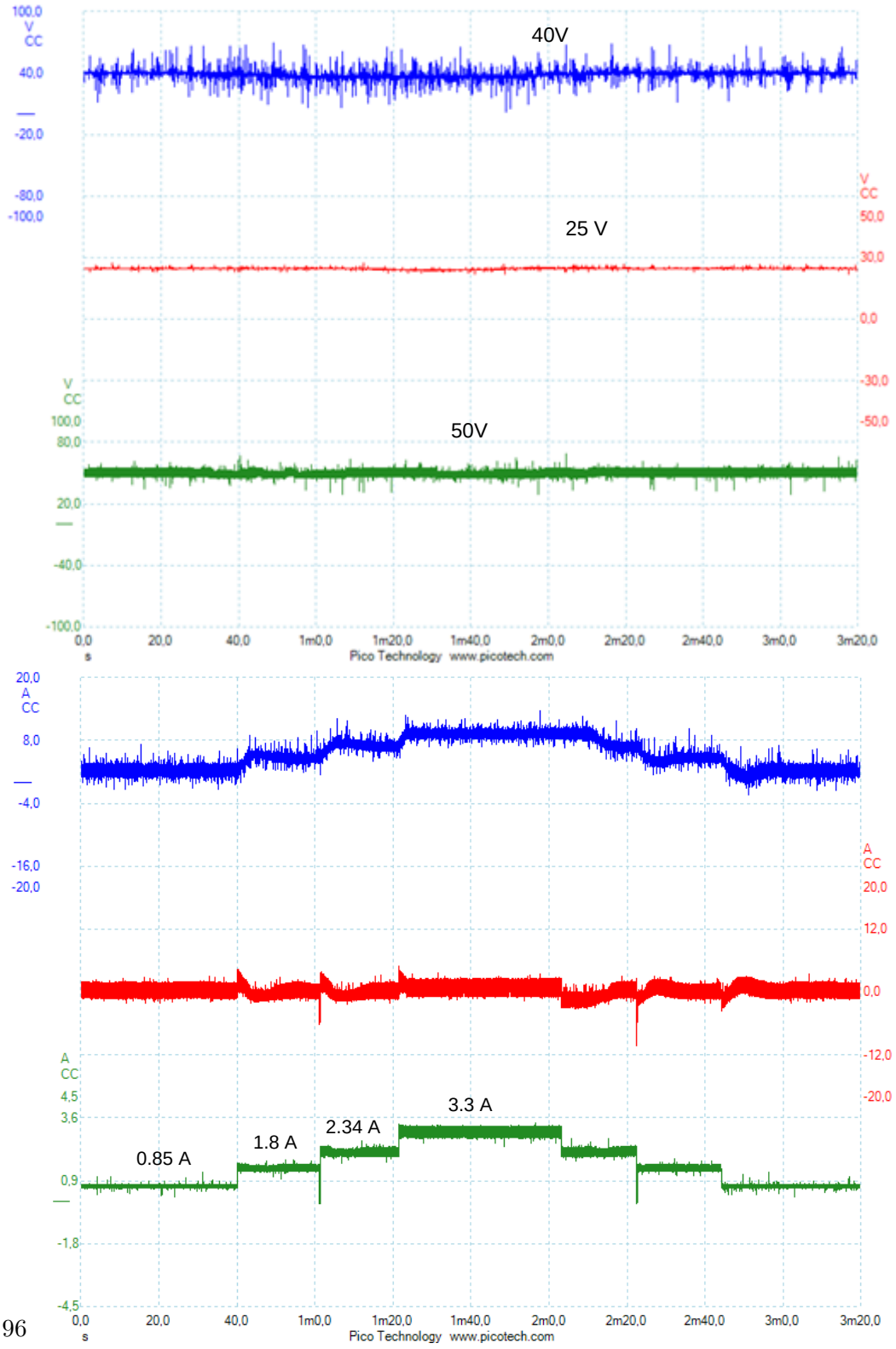

Figure 6.5: Voltage and current waveforms case 2.

6.4.4 Case 3

Figure 6.6 shows a constant V_0 of 50 V and V_{SC} shows a voltage of 25 V to such changes. Figure 6.6 also shows the response of I_{FC}, I_{SC} and I_O to the system flows. It is clear that to make the changes of load of 0.85 to a 3.3 A, I_{SC} often helps the changes demanded by the load.

6.4.5 Case 4

As seen in Figure 6.7 during the interval from t_0 to t_1, there is a discharged in V_{SC} because SC helps FC in delivering energy to the load. In the interval t_1 to t_2 a lower power (42.3) W is connected and therefore, FC is already able to delivery energy to the load and also to recharge the SC. In Figure 6.7 shows that V_0 is regulated to 50 V. The following things can be observed in interval time t_0 to t_1: the I_{SC} helping I_{FC} to deliver the I_0 demand due to the load, since at this time I_{FC} is limited.

In current waveforms it is observed that during the interval t_1 to t_2 and with a lower demand in load I_0, I_{FC} is able to deliver energy to the SC for recharging and it is also capable of delivering energy to the load. After this time the I_{SC} $t_2 = 0$ because it is fully recharged.

6.4.6 Case 5

Figure 6.8 shows the evolution of the V_{FC}, V_{SC} and V_0 voltages. At the time interval t_0 to t_1. $V_{FC} = 0$ due to the energy, the V_0 is maintained by regulating the consign value of 50 V and the V_{SC} begins to be discharged from 25 to 15 V because now SC provides all the energy transferred to the load and the controller V_{SC} is able to regulate even when $V_{SC} = 15$ V. At the time of t_1 to t_2 the following is observed: the adjustment range of the control system in SC when V_{SC} is less than 15 V, is not able to regulate and therefore V_0 begins to decrease its voltage until arriving to 0 V. The same happens when V_{SC} and $V_{FC} = 0$ V.
In current waveforms and at the time interval t_0 to t_1 the following happens: the value of $I_{FC} = 0$ A, now I_{SC} transfers its energy to the resistive load, the control system by the SC still presents regulation and I_0 remains constant delivering 2.34 A. For the time interval from t_1 to t_2 it is observed that I_{FC} = 0 and the I_{SC} value begins to decrease, while in this interval it is not able to regulate and therefore I_0 decreases to 0 A.

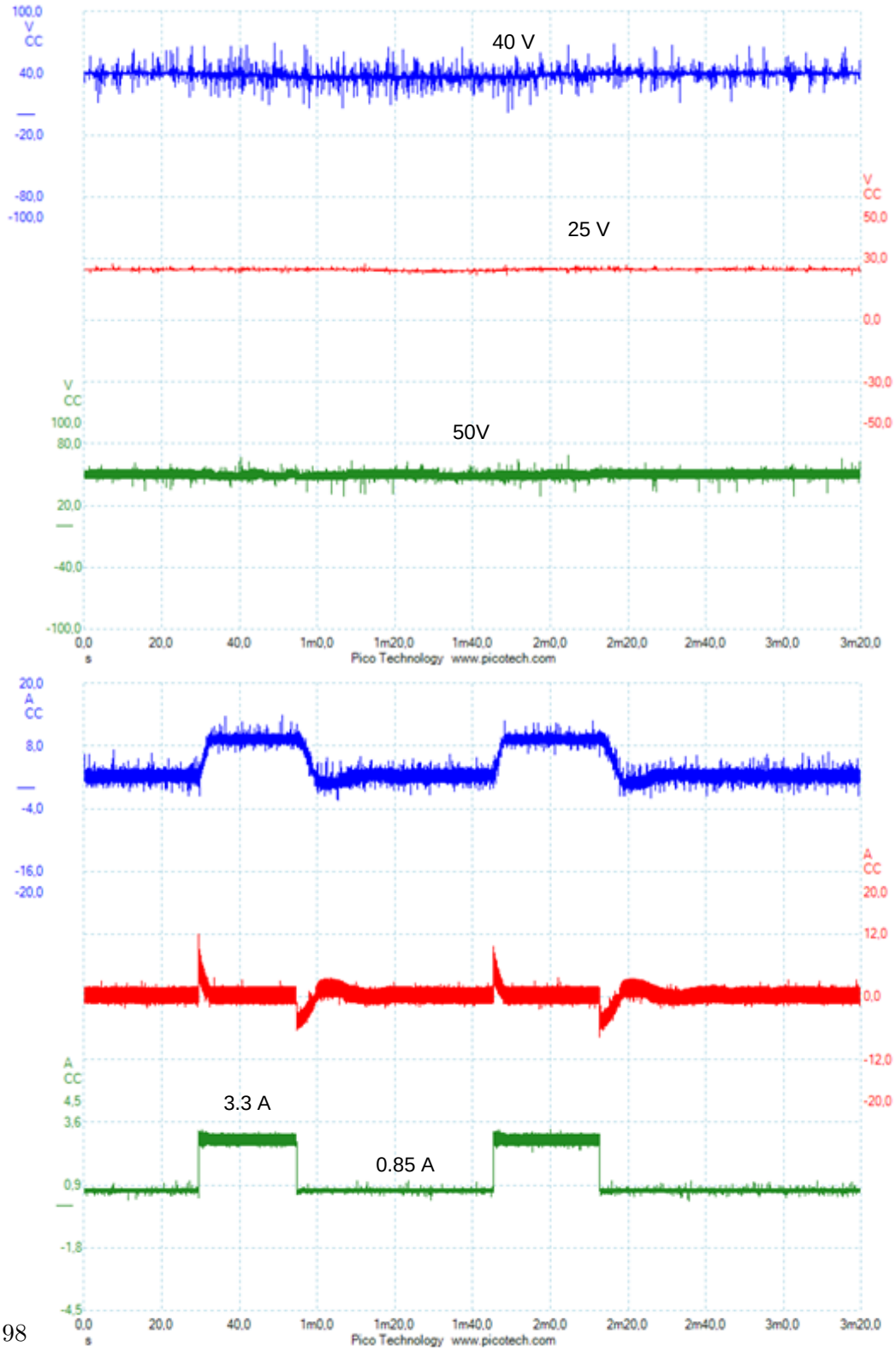

Figure 6.6: Voltage and current waveforms case 3.

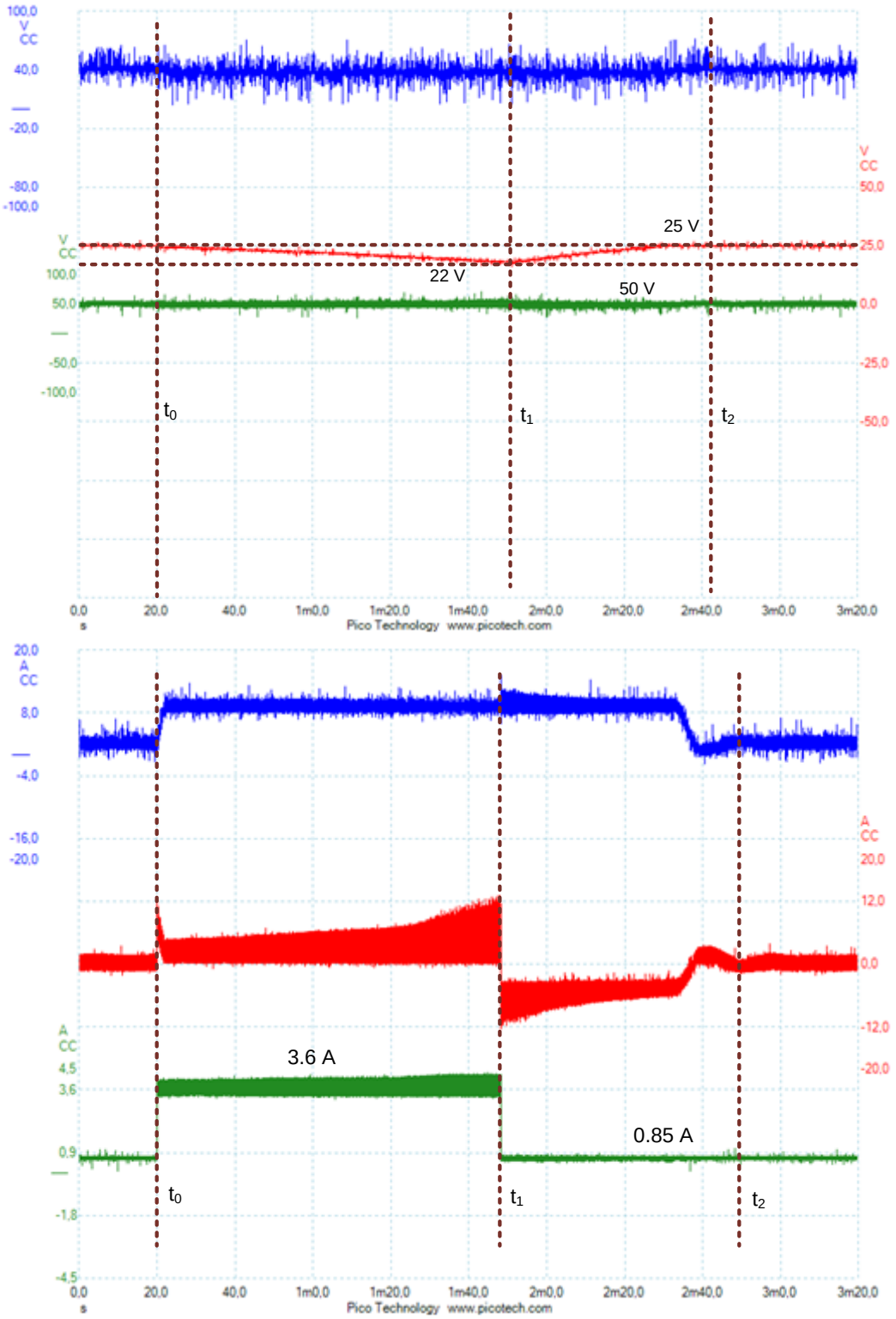

Figure 6.7: Voltage and current waveforms case 4.

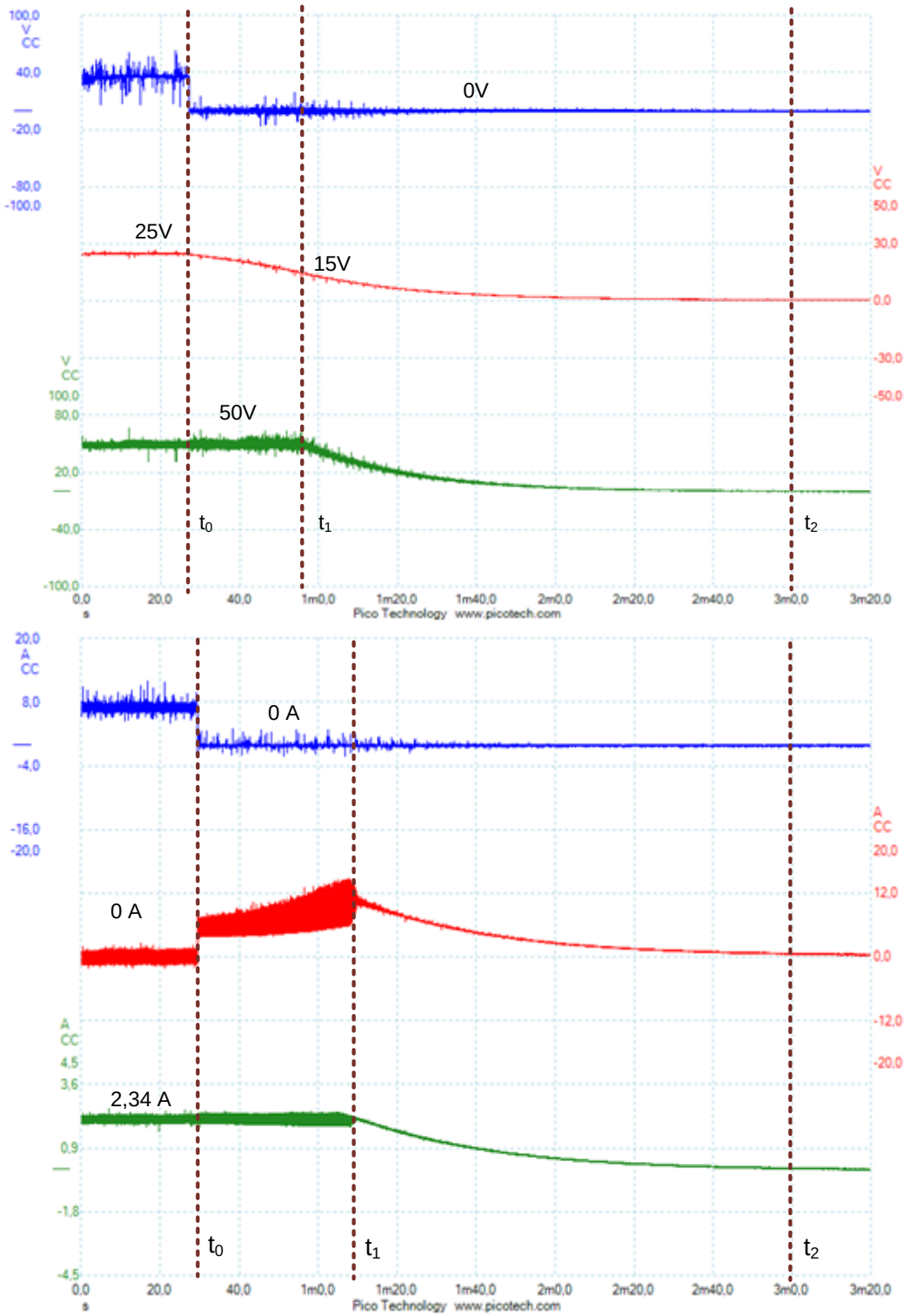

Figure 6.8: Voltage and current waveforms case 5.

6.4.7 Case 6

Figure 6.9 shows the evolution of the voltages V_{FC}, V_{SC} and V_0. The V_{FC} value presents small changes, V_{SC} very small variations and minimal changes in V_0 but still regulated to 50 V regulated to the proposed consign of 50 V.

Figure 6.9 shows the evolution of the current I_{FC}, I_{SC} and I_0. In I_{FC} it can see consecutive changes due to the regulated current in the load. In I_{SC} is helping I_{FC} to load changes I_0.

6.4.8 Case 7

Figure 6.10 shows the regulation of V_0 subjected to changes of consign V_0*. In this case it can be seen that at the interval time t_0 to t_1 there is a change of 50 to 80 V.

The current waveform shows the evolution of I_{FC}, I_{SC} and I_O. It has been observed that there are small changes in I_0 accordingly to V_0 consign changes V_0*. On the other hand, I_{FC} delivers energy demand by the load and I_{SC} helps FC to these changes.

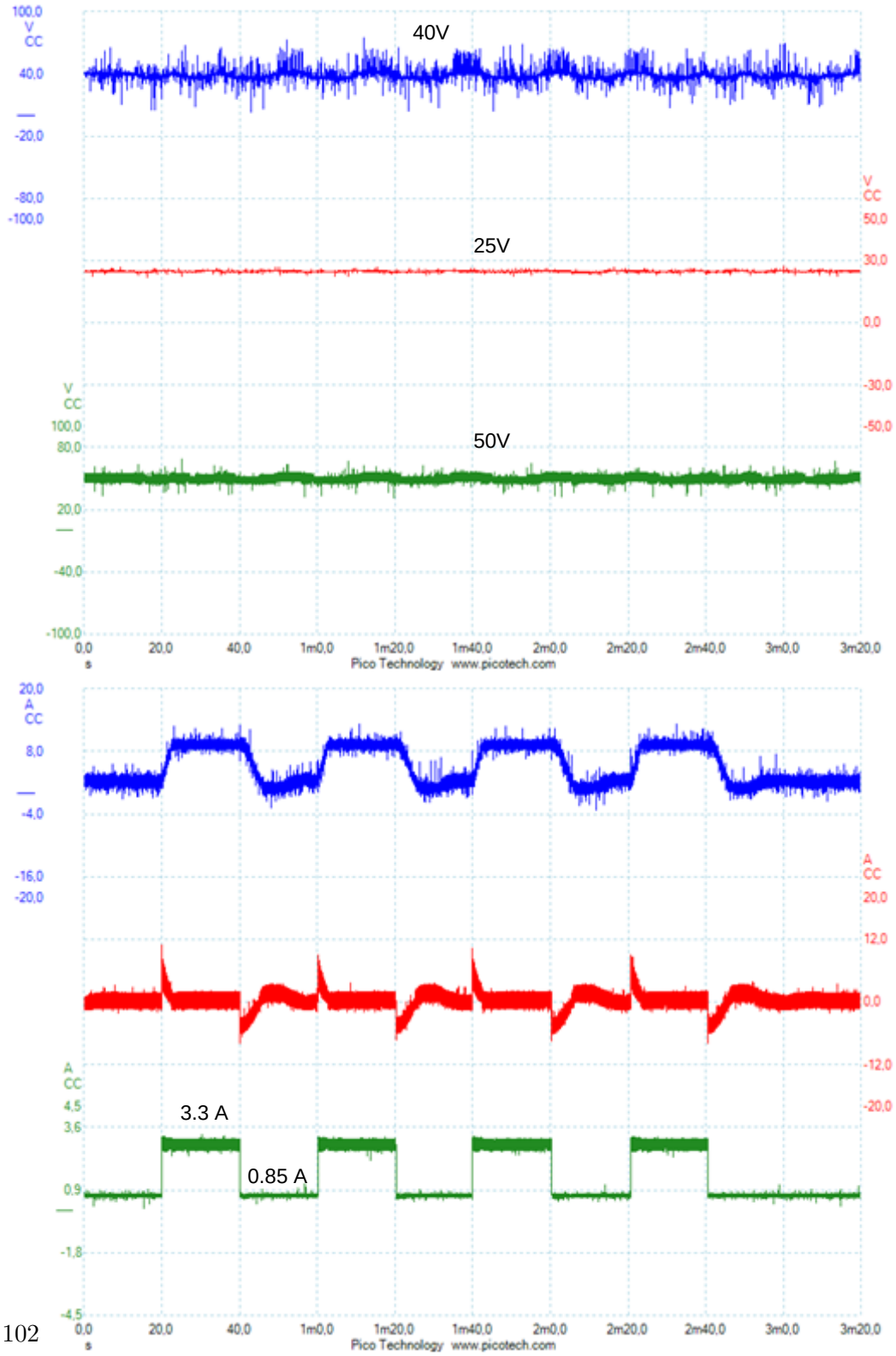

Figure 6.9: Voltage and current waveforms case 6.

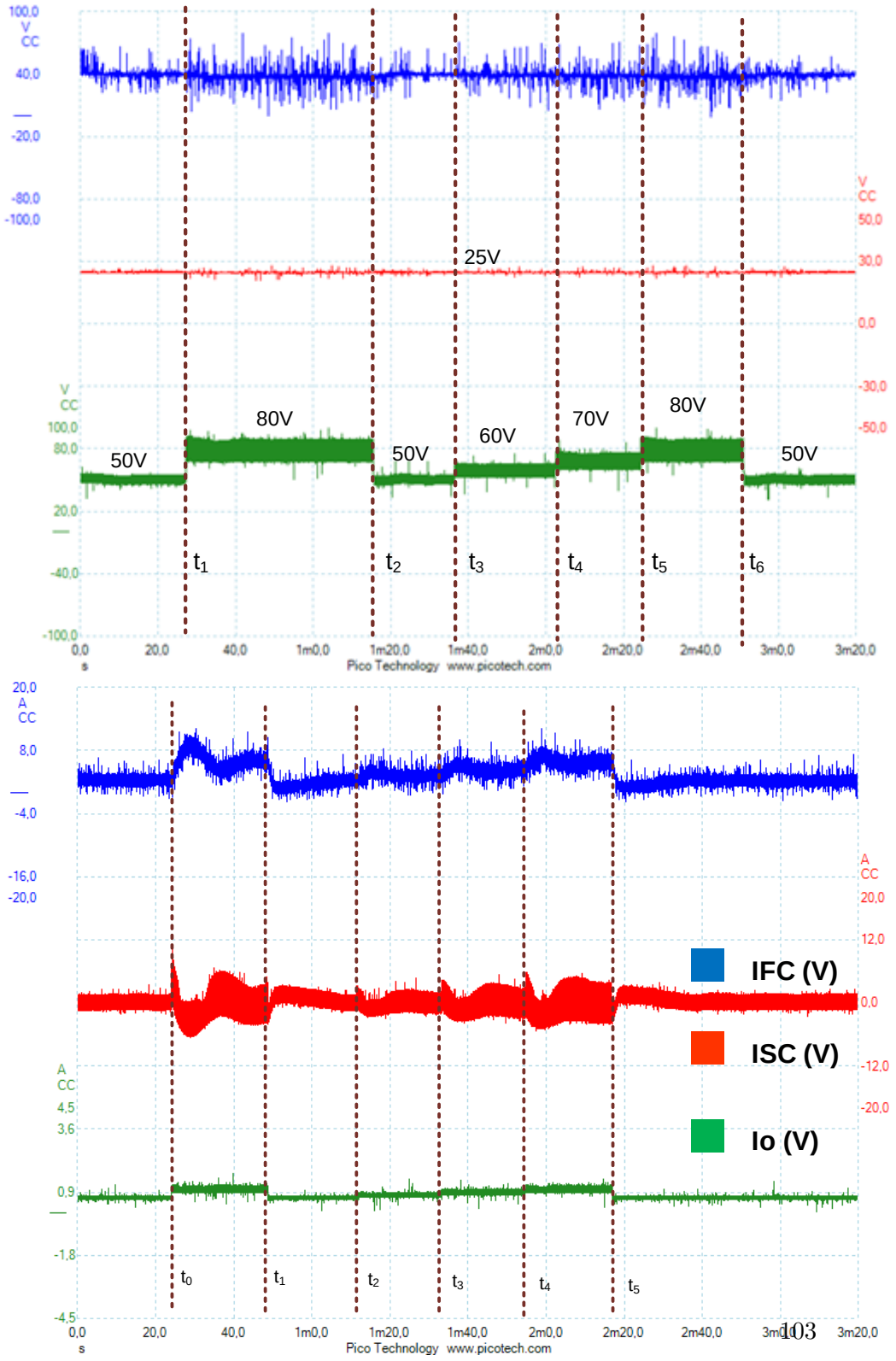

Figure 6.10: Voltage waveforms case 7.

6.5 Conclusions

Implemented in this thesis is a hybrid converter for the operation of a module of FC Nexa Ballard of 1.2 kW and a SC, with the proposal of a control system which has been implemented digitally using the Texas Instruments DSP2808 microcontroller. The proposed control scheme contains 4 loops of closed control for the operation of the system, which allows the control of the following variables: V_0, V_{SC}, I_{SC} and I_{FC}. The control is able to compensate the load changes as well as for the backup power system to respond quickly to slow start by the FC. The control of backup can also determine the charge and discharge of SC. Through the experimental tests exposed in this section the correct performance of the proposed structure of control has been validated. The digital control allows greater flexibility and simplicity in the control of complex processes in form versus analogy. The programming and the good signal conditioning simplifies the process and reduces its cost.

Chapter 7

Conclusions

7.1 General conclusions

Fuel cell and supercapacitor technologies have been studied in this thesis. The main problem of FC are: the slow response, the no regulated output voltage, difficult cold start, etc. Therefore it becomes necessary to study structures of power conditioners that can mitigate the disadvantages of FC. DC/DC converters have been studied for the integration of a power conditioner. According to this study, the boost converter presents a greater efficiency than any others converters in the operation of FC. This topology has a few components, low cost, simple design and control. However, FC needs a backup system with battery or supercapacitor which helps in the start and changes of power in load. Thus, using SCs together with FCs can improve performance and FC life by absorbing faster load changes and preventing fuel starvation of the FC. The SC requires a bidirectional converter in current (for the charge and discharge of the SC). The most used converter is the half-bridge.

A scheme of control has been proposed, which operates the power conditioner with FC/SC as a source of energy. The main function of this control structure is to regulate V_0 and V_{SC} voltages as well as the currents I_{FC}, I_{SC} respectively. The proposed control scheme contains four loops of closed control for the operation of the system. Two for the inner loop and two for the outer loop. The control system, operates with 4 controllers Proportional-Integral (PIs) which have been implemented in MATLAB-Simulink and digitally using the Texas Instruments DSP2808 microcontroller.

An experimental validation of the system implemented in the laboratory is provided. Several tests have been performed to verify that the system achieves an excellent output voltage (V_0) regulation and SC voltage control (V_{SC}), under disturbances from FC voltage, load voltage and other perturba-

tions. The digital control allows there to be greater flexibility and simplicity in the control of complex processes in form versus analogy. The programming and the good signal conditioning simplifies the process. The control system is able to compensate load changes as well and the backup power system responds quickly to slow start by the FC.

7.2 Future work

To optimize the design of the inductors L_1 and L_2 to operate FC and SC at full power 1.2 kW.

The design and implementation of a DC/AC inverter.

The design and implementation of a control algorithm for an inverter in digital form through DSP.

To do experimental tests of network integration.

To do experimental test using the load in AC motor.

Bibliography

[1] A. D. James Larminie, *Fuel Cell Systems Explained*, second, Ed. John Wiley & Sons Ltd, 2003. xiii, 9

[2] K. H. D. Mori, "Recent challenges of hydrogen storage technologies for fuel cell vehicles," *International journal of hydrogen energy*, pp. 1–6., 2008. 3

[3] S. Edition, Ed., *U.S. Department of Energy Office of Fossil Energy National Energy Technology Laboratory.* Fuel Cell Handbook, November 2004. 3

[4] V.-T. Liu, J.-W. Hong, and K.-C. Tseng, "Power converter design for a fuel cell electric vehicle," in *Proc. 5th IEEE Conf. Industrial Electronics and Applications (ICIEA)*, 2010, pp. 510–515. 3

[5] F. W. J.J. Hwanga, W.R. Chang, "Development of a small vehicular pem fuel cell system," *International Journal of Hydrogen Energy*, vol. 33, pp. 3801–3807, 2008. 3

[6] P. Thounthong, P. Sethakul, S. Rael, and B. Davat, "Control of fuel cell/battery/supercapacitor hybrid source for vehicle applications," in *Proc. IEEE Int. Conf. Industrial Technology ICIT 2009*, 2009, pp. 1–6. 3

[7] G. T. Samson, T. M. Undeland, O. Ulleberg, and P. J. S. Vie, "Optimal load sharing strategy in a hybrid power system based on pv/fuel cell/ battery/supercapacitor," in *Proc. Int Clean Electrical Power Conf*, 2009, pp. 141–146. 4

[8] O. Krykunov, "Comparison of the dc/dc-converters for fuel cell applications," *International Journal of Electrical, Computer, and Systems Engineering*, vol. 1, pp. 71–79, 2007. 4, 26

[9] X. Yu, M. R. Starke, L. M. Tolbert, and B. Ozpineci, "Fuel cell power conditioning for electric power applications: a summary," *IET Electric Power Applications*, vol. 1, no. 5, pp. 643–656, 2007. 4

[10] P. Thounthong and P. Sethakul, "Analysis of a fuel starvation phenomenon of a pem fuel cell," in *Proc. Power Conversion Conference - Nagoya PCC '07*, Apr. 2–5, 2007, pp. 731–738. 4

[11] P. Thounthong, S. Sikkabut, P. Sethakul, and B. Davat, "Control algorithm of renewable energy power plant supplied by fuel cell/solar cell/ supercapacitor power source," in *Proc. Int. Power Electronics Conf. (IPEC)*, 2010, pp. 1155–1162. 5

[12] A. Sanchez-Squella, R. Ortega, and S. Malo, "Dynamic energy router," *IEEE Control Systems*, vol. 30, pp. 72–80, 2010. 5

[13] M. Uzunoglu and M. S. Alam, "Modeling and analysis of an fc/uc hybrid vehicular power system using a novel-wavelet-based load sharing algorithm," *IEEE Trans. Energy Conversion*, vol. 23, no. 1, pp. 263–272, 2008. 5, 14

[14] E. A. Mohamed Ali and A. Abudhahir, "A survey of the relevance of control systems for pem fuel cells," in *Proc. Int Computer, Communication and Electrical Technology (ICCCET) Conf*, 2011, pp. 322–326. 5

[15] P. T. Bernard Davat, "Study of a multiphase interleaved step-up converter for fuel cell high power applications," *Energy Conversion and Management*, vol. 51, pp. 826–832, 2009. 5

[16] T. Azib, O. Bethoux, G. Remy, and C. Marchand, "Structure and control strategy for a parallel hybrid fuel cell/supercapacitors power source," in *Proc. IEEE Vehicle Power and Propulsion Conf. VPPC '09*, 2009, pp. 1858–1863. 5

[17] R. A. Kirubakaran, Shailendra Jain, "A review on fuel cell technologies and power electronic interface," *Renewable and Sustainable Energy Reviews*, vol. 13, pp. 2430–2440, 2009. 6

[18] Ole, "Comparison of the dc/dc converters for fuel cell applications," *International Journal of Electrical, Computer, and Systems Engineering*, vol. 1, pp. 71–78, 2007. 6

[19] F. Abdous, "Fuel cell / dc-dc converter control by sliding mode method," *World Academy of Science, Engineering and Technology*, vol. 49, pp. 1012–1016, 2009. 6

[20] Ballard, "Nexatm power module user's manual," Heliocentris, Tech. Rep., 2003. 7

[21] F. Bardir, "Pem fuel cells: Theory and practice," *Elsevier Academic Press*, 2005. 8

[22] J. Balakrishnan, "Fuel cell technology," in *Proc. Third Int. Conf. Information and Automation for Sustainability ICIAFS 2007*, 2007, pp. 159–164. 9

[23] V. Boscaino, R. Collura, G. Capponi, and F. Marino, "A fuel cell-battery hybrid power supply for portable applications," in *Proc. Int Power Electronics Electrical Drives Automation and Motion (SPEEDAM) Symp*, 2010, pp. 580–585. 11

[24] R. Romer, "Advantages of liquid fuel vs. hydrogen for backup power fuel cell systems in telecom," in *Proc. nd Int. Telecommunications Energy Conf. (INTELEC)*, 2010, pp. 1–2. 12

[25] Y. Y. Yao, D. L. Zhang, and D. G. Xu, "A study of supercapacitor parameters and characteri stics," in *Proc. Int. Conf. Power System Technology PowerCon 2006*, 2006, pp. 1–4. 13

[26] K. Xin and A. M. Khambadkone, "Dynamic modelling of fuel cell with power electronic current and performance analysis," in *Proc. Fifth International Conference on Power Electronics and Drive Systems PEDS 2003*, vol. 1, Nov. 17–20, 2003, pp. 607–612. 17

[27] S. J. A.Kirubakaran and R. Nema, "The pem fuel cell system with dc/dc boost converter: Design, modeling and simulation," *International Journal of Recent Trends in Engineering*, vol. 1, pp. 157–161, 2009. 18

[28] N. Frohleke, R. Mende, H. Grotstollen, B. Margaritis, and L. Vollmer, "Isolated boost full bridge topology suitable for high power and power factor correction," in *Proc. th Int Industrial Electronics, Control and Instrumentation IECON '94. Conf*, vol. 1, 1994, pp. 405–410. 19

[29] C. Liu, A. Johnson, and J.-S. Lai, "A novel three-phase high-power soft-switched dc/dc converter for low-voltage fuel cell applications," *IEEE Trans. Ind. Applicat.*, vol. 41, no. 6, pp. 1691–1697, 2005. 19

[30] J. Lee, J. Jo, S. Choi, and S.-B. Han, "A 10-kw sofc low-voltage battery hybrid power conditioning system for residential use," *IEEE Transaction on Energy Conversion*, vol. 21, no. 2, pp. 575–585, Jun. 2006. 20

[31] R. W. Ericson and D. Maksimovic, *Fundamentals of power electronics*, second, Ed., 1999. 22

[32] J. A. A. J. Jin Wang, Fang Z. Peng and R. Buffenbarger, "A new low cost inverter system for 5 kw fuel cell," *IEEE Power Electronics Society*, vol. 1, 2003. 26

[33] G. L. Yves Lembeye, Viet Dang Bang and Jean-Paul, "Novel half - bridge inductive dc/dc isolated converters for fuel cell applications," *IEEE Transaction on Energy Conversion*, vol. 24, pp. 203–210, 2009. 29

[34] P. Kornetzky, Z. Moussaoui, I. Batarseh, S. Hawasly, and C. Kennedy, "Modeling technique for dc to dc converters using weinberg topology," in *Proc. IEEE Southeastcon '96. 'Bringing Together Education, Science and Technology'*, 1996, pp. 551–556. 31

[35] M. Rugaju and P. H.C, "Full bridge dc-dc converter as input stage for fuel cell based inverter system," *IEEE Transaction on Energy Conversion*, vol. 1, 2008. 32

[36] A. K. Jin-Woo Jung, "Modeling and control of fuel cell based distributed generation systems in a standalone ac power supply," *Journal of Iranian Association of Electrical and Electronics Engineers*, vol. 1, pp. 10–23, 2005. 33

[37] T. Mishima, E. Hiraki, T. Tanaka, and M. Nakaoka, "A new soft-switched bidirectional dc-dc converter topology for automotive high voltage dc bus architectures," in *Proc. IEEE Vehicle Power and Propulsion Conf. VPPC '06*, 2006, pp. 1–6. 34

[38] W. Na and B. Gou, "Analysis and control of bidirectional dc/dc converter for pem fuel cell applications," in *Proc. IEEE Power and Energy Society General Meeting - Conversion and Delivery of Electrical Energy in the 21st Century*, Jul. 20–24, 2008, pp. 1–7. 35

[39] A. T. G. Kovacevic and R. Bojoi, "Advanced dc dc converter for power conditioning in hydrogen fuel cell systems," *International Journal of Hydrogen Energy*, vol. 33, pp. 3215–3219, 2008. 36

[40] L. Palma and P. Enjeti, "Analysis of common mode voltage in fuel cell power conditioners connected to electric utility," in *Proc. IEEE International Conference on Industrial Technology ICIT 2006*, Dec. 15–17, 2006, pp. 200–205. 36

[41] W. Choi, P. Enjeti, and J. W. Howze, "Fuel cell powered ups systems: design considerations," in *Proc. IEEE 34th Annual Power Electronics Specialist Conference PESC '03*, vol. 1, Jun. 15–19, 2003, pp. 385–390. 38

[42] V. Yakushev, V. Meleshin, and S. Fraidlin, "Full-bridge isolated current fed converter with active clamp," in *Proc. Fourteenth Annual Applied Power Electronics Conference and Exposition APEC '99*, vol. 1, Mar. 14–18, 1999, pp. 560–566. 38

[43] P. Thounthong, S. Rael, B. Davat, and I. Sadli, "A control strategy of fuel cell/battery hybrid power source for electric vehicle applications," in *Proc. 37th IEEE Power Electronics Specialists Conf. PESC '06*, 2006, pp. 1–7. 39

[44] P. Thounthong, S. Rael, and B. Davat, "Analysis of supercapacitor as second source based on fuel cell power generation," *IEEE Trans. Energy Conversion*, vol. 24, no. 1, pp. 247–255, 2009. 39

[45] U. Mohan and Robbins, *Power Electronics: Converters, Applications, and Design*, third edition, Ed., 2003. 46

[46] I. D. Oltean, A. M. Matoi, and E. Helerea, "A supercapacitor stack - design and characteristics," in *Proc. 12th Int Optimization of Electrical and Electronic Equipment (OPTIM) Conf*, 2010, pp. 214–219. 62

[47] N. Khan, N. Mariun, M. Zaki, and L. Dinesh, "Transient analysis of pulsed charging in supercapacitors," in *Proc. TENCON 2000*, vol. 3, 2000, pp. 193–199. 62

Appendix A

Appendix

A.1 Fuel cell installation

Figure A.1 shows the installation of a $Nexa^{TM}$ power module in the chemistry laboratory.

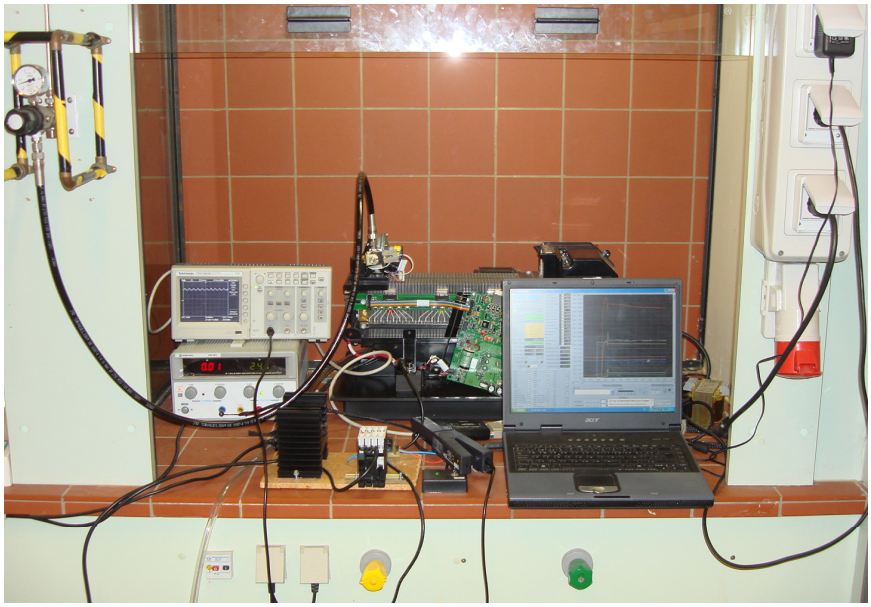

Figure A.1: Installation of the $Nexa^{TM}$ power module.

Follow the provided instructions to establish a laboratory test station for the $Nexa^{TM}$ power module.

- Install the NexaOEM software provided by the manufacturer $Nexa^{TM}$ 1.2 kW module on a computer.

- Connect the monitoring data to the fuel cell and the computer where it was installed the software.

- Run the application and activate NexaOEM receiving data.

- Connect the hose hydrogen fuel cell to hydrogen tank.

- Power the relay protection of the fuel cell through the signal cable that comes from the control board of the FC.

- Connect the data cable from the control board of the FC.

- Connect the protection relay and the diode to the positive terminal Ballard $Nexa^{TM}$.

- Connect the power cable from the control board to 24 V and make sure the FC start-up switch is in stop. When connecting the power cable two LEDs will light on the control board of the fuel cell, so you can verify that there is power at the control board.

- Open the supply of hydrogen fuel cell operating at a pressure range from 0.17 to 17 bar.

- Switch from "stop" to "run". You will hear the noise of the compressor of the stack and some clicks that correspond to the purge valves and relay protection. After approximately 30 seconds, the noise disappears and the voltage across the fuel cell will be approximately 42-43 V. This can be checked in the software.

- To explore the power polarization curve, it is possible connect a variable resistive load.